Adeno-Associated Virus Vectors for Gene Therapy: From Scalable Production Systems via Serotype-Specific Glycan Interaction Patterns to Gene Transfer Applications

Inaugural-Dissertation
to obtain the academic degree
Doctor rerum naturalium (Dr. rer. nat.)

Submitted to the Department of Biology, Chemistry and Pharmacy
of the Freie Universität Berlin

by

Mario Mietzsch

from Berlin, Germany

February 2014

The work presented in this doctoral thesis was carried out between July 2009 and February 2014 at the Institute of Virology of the Charité in Berlin under supervision of Prof. Dr. Regine Heilbronn.

1st Reviewer:	Prof. Dr. Regine Heilbronn Charité - Universitätsmedizin Berlin Institut für Virologie Campus Benjamin Franklin Hindenburgdamm 27 12203 Berlin
2nd Reviewer:	Prof. Dr. Rudolf Tauber Charité - Universitätsmedizin Berlin Institut für Laboratoriumsmedizin, Klinische Chemie und Pathobiochemie Campus Benjamin Franklin Hindenburgdamm 30 12200 Berlin
Date of defense:	10.07.2014

Acknowledgments

First and foremost, I would like to express my special appreciation and gratitude to my mentor Prof. Regine Heilbronn for giving me the opportunity to conduct my doctoral research study at the Institute of Virology of the Charité, her continuous support and guidance which led to the present thesis. As a part of my doctoral research study, she gave me the chance to join the lab of Dr. Sergei Zolotukhin at the University of Florida for six months. This exchange was not only of tremendous help for this thesis but also extended my scientific and personal experience. In this context, I would like to thank Sergei for sharing his knowledge of his vector production system but also for his hospitality and support during my stay at the University of Florida. Furthermore I thank the German Academic Exchange Service (DAAD) which partially funded travel and life expenses by the PROMOS program.

I am also very grateful for countless, very helpful discussions with Dr. Stefan Weger concerning the realization and evaluation of experiments.

In addition, I thank Catherine Zurawski, Sabrina Grasse, Dr. Antonette Bennett, Dr. Mavis Agbandje-McKenna, Felix Broecker, Anika Reinhardt, Prof. Peter H. Seeberger, Prof. Herbert Herzog and the staff of the Consortium for Functional Glycomics for their contribution to the research presented in this thesis.

Furthermore, I would like to thank my current and former colleagues in the group of Prof. Regine Heilbronn for their help, assistance and interesting scientific and non-scientific conversations: Eva-Maria Hammer, Kerstin Winter, Eva Guhl, Ruth Joncker, Catrin Stutika, Dr. Daniela Hüser, Kristina von Kietzell, Natalja Rutz, Melanie Heßler and Dr. Martin Alex.

Last not but least I would like to express my gratitude to my parents, who have supported, encouraged and motivated me through my entire life.

Foreword

This cumulative thesis is based on the following four peer-reviewed original publications:

Mario Mietzsch, Sabrina Grasse, Catherine Zurawski, Stefan Weger, Antonette Bennett, Mavis Agbandje-McKenna, Nicholas Muzyczka, Sergei Zolotukhin and Regine Heilbronn (2014) OneBac: Platform for Scalable and High-Titer Production of AAV Serotype 1-12 Vectors for Gene Therapy.
Human Gene Therapy, *in press*

Mario Mietzsch, Felix Broecker, Anika Reinhardt, Peter H. Seeberger and Regine Heilbronn (2014) Differential AAV Serotype-Specific Interaction Patterns with Synthetic Heparins and Other Glycans.
Journal of Virology 88; 2991-3003

Yan-Chuan Shi, Jackie Lau, Zhou Lin, Hui Zhang, Lei Zhai, Guenther Sperk, Regine Heilbronn, **Mario Mietzsch**, Stefan Weger, Xu-Feng Huang, Ronaldo F. Enriquez, Paul A. Baldock, Lei Zhang, Amanda Sainsbury, Herbert Herzog and Shu Lin (2013) Arcuate NPY Controls Sympathetic Output and BAT Function via a Relay of Tyrosine Hydroxylase Neurons in the PVN.
Cell Metabolism 17; 236-48

Martin Alex, Stefan Weger, **Mario Mietzsch**, Heiko Slanina, Toni Cathomen and Regine Heilbronn (2012) DNA-Binding Activity of Adeno-Associated Virus Rep Is Required for Inverted Terminal Repeat-Dependent Complex Formation with Herpes Simplex Virus ICP8.
Journal of Virology 86; 2859-63

List of Abbreviations

3V	third ventricle
AAP	assembly activating protein
AAV	adeno-associated virus
AcMNPV	*Autographa californica* multiple nucleopolyhedrovirus
Ad	adenovirus
AGRP	agouti-related peptide
ARC	arcuate nucleus
Bac	baculovirus
BAT	brown adipose tissue
Bsd	blasticidin S deaminase
CART	cocaine and amphetamine-regulated transcript
CBA	chicken beta actin
CFG	Consortium for Functional Glycomics
CMV	cytomegalovirus
CNS	central nervous system
ds	double-stranded
FACS	fluorescent-activated cell sorter
FCS	fetal calf serum
FL1-H	fluorescence channel 1 height
FLEX	flip-excision element
FSC-H	forward scatter height
GAD65	glutamic acid decarboxylase 65
GAG	glycosaminoglycan
GFP	green fluorescent protein
GlcA	glucoronic acid
GlcN	glucosamine
gp	genomic particles
GST	glutathione S-transferase
HEK	human embryonic kidney
HFD	high fat diet
h.p.i.	hours post infection
HPLC	high-pressure liquid chromatography
hr2	homologous region 2
HSPG	heparan sulfate proteoglycan

HSV	herpes simplex virus
ICP8	infected cell protein 8
IdoA	iduronic acid
IE	immediate-early
ITR	inverted terminal repeat
LC	locus coeruleus
mAb	monoclonal antibody
mE	monomer extended
mT	monomer turnaround
MOI	multiplicity of infection
MWCO	molecular weight cut-off
Neu5Ac	N-acetyl-neuraminic acid / sialic acid
NLS	nuclear localization signal
NPY	neuropeptide Y
NTS	nucleus tractus solitarii
ORF	open reading frame
PLA2	phospholipase A2
POMC	proopiomelanocortin
PVN	paraventricular nucleus
PYY	peptide YY
rAAV	recombinant adeno-associated virus
RBE / RBS	Rep-binding element / Rep-binding site
RER	respiratory exchange ratio
RFU	relative fluorescent unit
sc	self-complementary
SDS-PAGE	sodium dodecyl sulfate-polyacrylamide gel electrophoresis
SEM	standard error of the mean
Sf	*Spodoptera frugiperda*
SNS	sympathetic nervous system
ss	single-stranded
TH	tyrosine hydroxylase
trs	terminal resolution site
UCP1	uncoupling protein 1
VLM	ventrolateral medulla
WPRE	woodchuck post-transcriptional element
WT	wild type

Directory

1 Introduction

1.1 Adeno-Associated Virus

Adeno-associated viruses (AAVs) belong to the family Parvoviridae and are among the smallest known viruses. Their non-enveloped, icosahedral capsids of roughly 20 to 25 nm in diameter contain the linear, single-stranded DNA genome. AAVs were first identified as contaminations of adenovirus isolates [1,2]. The AAVs require coinfection with a helper virus for productive replication, and have therefore been assigned to the genus Dependovirus within the family Parvoviridae. In addition to adenoviruses [3] many herpesvirus strains [4,5] can act as helper viruses to support AAV replication. Currently, 13 human and primate AAV serotypes and many more variants thereof have been described. The capsids of the various AAV serotypes differ in their structure and mediate the interaction of the virus with different host cell receptors. The attachment to differential receptors leads to alternative cell or tissue tropism of the AAV serotypes. Despite the high seroprevalence of AAV (about 80%) in the human population [6] no diseases or pathogenic properties have been associated with AAV infection.

1.1.1 Genome Structure and Expression of the Viral Proteins

The genomes of the different AAV serotypes consist of linear, single-stranded DNA molecules with a length of approximately 4700 nucleotides. Generally, the genome structures are mostly identical for all AAV serotypes. However, most research was performed with AAV2, and it therefore serves as a prototype for the AAV family. Both ends of the AAV genome contain identical inverted terminal repeats (ITRs) of roughly 150 bp [7]. These ITRs form a hairpin-shaped secondary structure through internal base pairing (Fig. 1) and contain *cis*-elements required for AAV replication [8] and packaging of the genomes into AAV capsids [9]. The Rep-binding site (RBS) within the ITR allows binding of the large Rep proteins (Rep78 and Rep68) to the AAV genome. Rep78/68 also display endonuclease activity needed to specifically introduce a single-strand DNA nick at the nearby terminal resolution site (*trs*) [10]. The ITRs flank two large open reading frames (ORFs) which code for the families of Rep and Cap proteins including the assembly activating protein (AAP) (Fig. 1). The expression of the viral proteins is achieved from mRNAs initiated at either one of three AAV promoters named according to their relative positions in the AAV genome [11,12]. The open reading frame for the non-structural Rep proteins is transcribed from the p5 and p19 promoters, leading to the translation of four different Rep proteins. Transcripts from either promoter are generated in an unspliced and a single-spliced form. While the unspliced

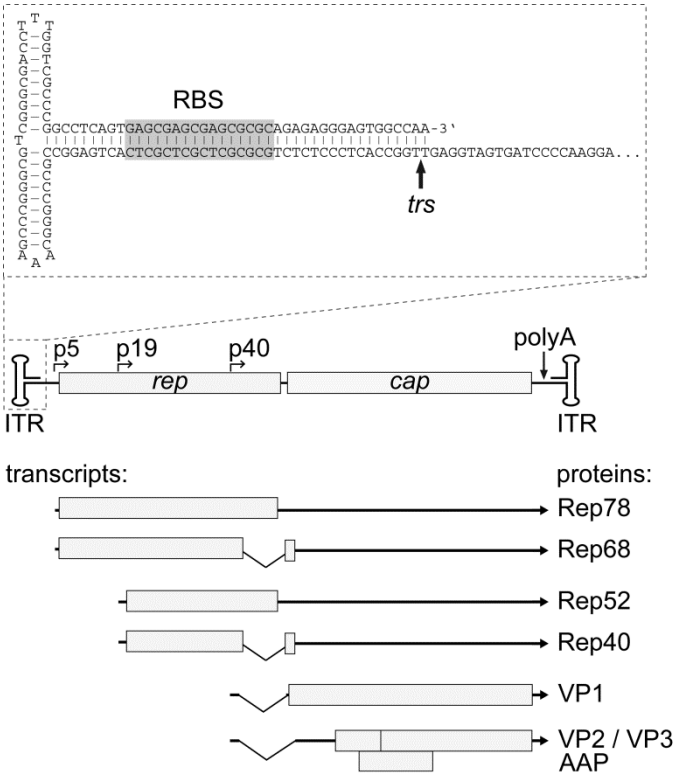

Fig. 1 Genome Structure of AAV: The lower part of the figure shows an overview of the AAV2 genome with the two open reading frames flanked by inverted terminal repeats (ITRs). The transcripts initiated at the p5, p19 or p40 promoters are depicted below along with their translation products. In the upper part the secondary structure of the left ITR is illustrated with the Rep-binding site (RBS) and the adjacent terminal resolution site (*trs*).

transcripts lead to the expression of Rep78 and Rep52, the corresponding C-terminally truncated variants Rep68 and Rep40, are translated from spliced mRNAs (Fig. 1). Since the site-specific DNA-binding and the endonuclease domains are located within the N-terminus of the Rep78/68 proteins these protein characteristics are absent from Rep52/40. However, all Rep proteins possess a 3'-to-5' helicase activity. The structural proteins VP1 to -3 encoded by the second ORF are translated from mRNAs generated by the p40 promoter. For AAV2 the expression levels of the VP1, VP2 and VP3 proteins approximate to a 1:1:10 ratio [13]. This ratio is achieved by the usage of alternative start codons and by differential splicing. In contrast to the upstream promoters the majority of transcripts from the p40 promoter are spliced [14]. The splice donor site can be joined to two different splice acceptor sites which are used with varying frequencies. The major splice acceptor site is located downstream of the ATG start codon for VP1 with the consequence that only VP2 and VP3 can be translated from this mRNA variant. Usage of the minor splice acceptor site makes the VP1 start codon accessible to the translational machinery [15]. The difference of the expression levels of VP2 and VP3 is achieved by alternative start codons. While VP3 translation is initiated at a standard ATG start codon, VP2 translation is initiated further upstream at a weak ACG start codon. All of the three AAV capsid proteins reside in the same reading frame. VP1 and VP2 represent N-terminal extended variants of VP3 [16]. The recently identified AAP required for virus assembly (Fig. 1) is encoded in an alternative reading frame of the *cap* gene and translated from a non-conventional CTG start codon [17].

1.1.2 Life Cycle of AAV

Despite the fact that the AAVs are widely spread in the human population little is known about their natural infection cycle. The knowledge about the viral life cycle is mostly based on studies of infections conducted in cell culture since AAV only replicates in the presence of a suitable helper virus and no pathology has been associated with AAV infections in humans. In absence of a helper virus, AAV establishes a latent infection either by chromosomal integration [18] or by persistence in an extrachromosomal state [19]. Either coinfection with helpervirus or helpervirus superinfection of latently AAV infected cells results in a productive replication of AAV.

1.1.2.1 Latency

In the absence of a suitable helper virus initial limited Rep expression leads to *trans* repression of all AAV promoters [20]. For AAV it was long believed that integration into the host cell genome represents an integral part of its life cycle. However, studies on human tissue samples have shown that AAV also persists in episomal forms [19]. Integration into the host cell genome is mediated by the Rep proteins [21]. The most frequent integration site is called AAVS1 and is located on the human chromosome 19 [18]. Within the AAVS1 region GAGC repeats are present that resemble the RBS on the AAV genome (Fig. 1). More recently, numerous, alternative genomic integration sites have been described in open chromatin regions in the vicinity of consensus GAGC repeats [22].

1.1.2.2 Helper Functions

Productive AAV replication is initiated by helper viruses. For adenovirus the responsible set of viral helper functions has been defined. The isolated adenoviral gene products E1A, E1B, E2A, E4ORF6 and the VA-RNA are sufficient to support productive AAV replication. E1A acts as transcription factor for the activation of the AAV promoters [23], E2A acts as ssDNA-binding protein that colocalizes to Rep in nuclear replication centers [24,25], the VA-RNA enhances the expression of the AAV proteins at the ribosomes [26] and the E1B/E4ORF6 complex promotes AAV replication [27]. The fact that these isolated adenoviral early functions are sufficient for the helper effect is exploited for AAV productions. Cotransfection of plasmids for the AAV genome and others for the set of adenovirus helper genes leads to high titer AAV production [28].
The minimal set of helper functions provided by herpes simplex virus (HSV) for productive AAV replication consists of the proteins encoded by UL5, UL8, UL29 and UL52. The HSV proteins UL30, UL42 and ICP0 further enhance AAV replication [29,30]. In contrast to adenovirus, the HSV helper factors represent HSV DNA replication functions, all of which are directly involved in

AAV DNA replication. The UL5, UL8 and UL52 proteins constitute the HSV helicase-primase complex which is indispensible for AAV DNA replication. UL30 and UL42 form the two-component HSV DNA polymerase which further enhances AAV DNA replication. Similar to the adenoviral E2A protein, UL29 (ICP8) acts as ssDNA binding protein which recruits the single-stranded AAV DNA genome to the HSV replication centers [31]. The immediate-early protein ICP0 transactivates the AAV promoters in a similar fashion as the adenoviral E1A protein.

1.1.2.3 Productive Replication

Infection of a latently infected cell with a helper virus leads to productive replication of AAV. Initially, the helper viruses activate the AAV promoters leading to expression of Rep. In case of a latently infected cell, harboring integrated AAV copies, the AAV genome is rescued by Rep [32], which marks the onset for the transition from the latent to the productive phase of the replication cycle. AAV replication is initiated, which requires DNA binding, helicase and endonuclease activity of the large Rep proteins [33]. The self-annealing and self-priming abilities of the ITRs play an important role during replication of the AAV genome. After binding to the non-replicated ITR of the monomer turnaround (mT) replication intermediate (Fig. 2), Rep helps to unwind the DNA with its helicase activity and introduces a single-strand-specific nick at the *trs*, which provides a 3'-OH group for reinitiation of DNA synthesis [34]. At that stage HSV ICP8 ssDNA-binding proteins have been shown to colocalize with Rep proteins [31], stabilize the replication fork [35] and support the

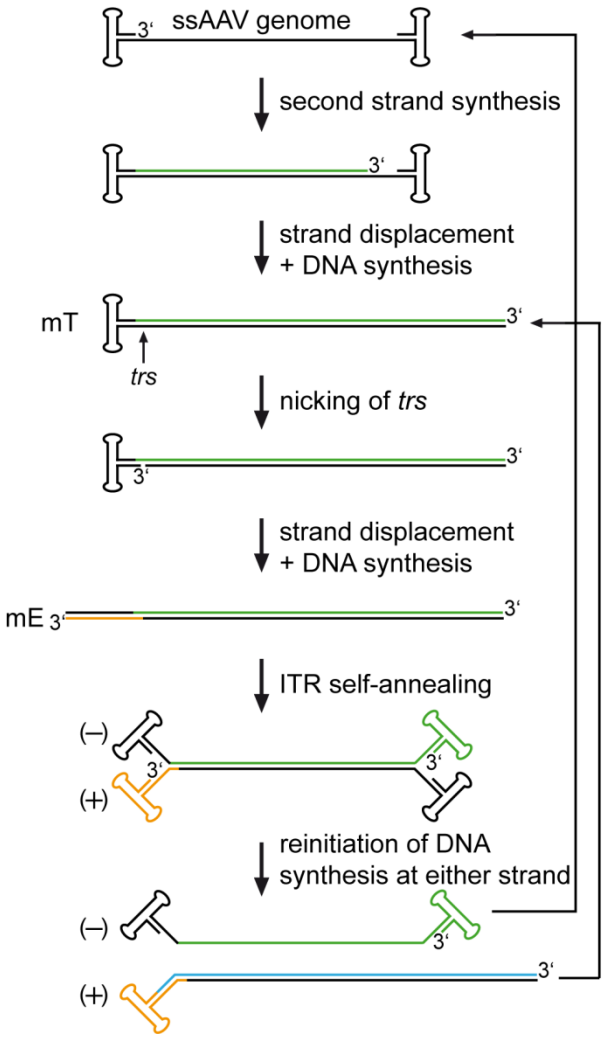

Fig. 2 AAV Genome Replication: Simplified model of the replication of single stranded (ss) AAV genomes, which lead to the generation of multiple copies of genomic DNA. mT = monomer turnaround, mE = monomer extended, *trs* = terminal resolution site

recruitment of the HSV helicase-primase complex (UL5, UL8, UL52), the HSV DNA-polymerase (UL30, UL42) and additional cellular proteins [36-38]. Synthesis of the complementary ITR sequence by strand displacement leads to the monomer extended (mE) form. Self-annealing of the ITRs at both ends generate new 3'-OH groups which are used for further replication of the AAV genome resulting in the generation of a full-length single-stranded (ss) genome and a new mT-replication intermediate. Whereas the displaced ssDNA can be packaged into the viral progeny particles, the mT-form reenters the replication cycle by nicking at the *trs*-site, elongation and reinitiation (Fig. 2). Reinitiation of DNA synthesis can also take place at the mT-genome without prior nicking at the *trs* by self-annealing of the ITR at the opposite genome end. In this process dimers or even higher replication forms are generated. This property is exploited for the production of self-complementary AAV vectors by deleting the *trs* in one of the ITRs (chapter 1.2.1) [39]. Expression of the capsid proteins leads to the assembly of empty particles in the nucleus assisted by the AAP protein which targets the individual capsid subunits to the nucleolus, where the capsid morphogenesis takes place [17]. Replication of the AAV genome generates genome copies of positive and negative polarity (Fig. 2). These are packaged as single-stranded DNA with equal efficiency into preformed empty AAV capsids. Encapsidation requires the helicase activity of the small Rep proteins Rep52 and Rep40 [9].

1.1.3 Capsid Structure

The icosahedral AAV capsids are composed of 60 subunits of the three capsid proteins VP1 (87 kDa), VP2 (73 kDa) and VP3 (61 kDa) in a 1:1:10 ratio [13,40]. AAV particles display diameters of roughly 20 to 25 nm. They show characteristic structures at the symmetry axes which are common to all AAV serotypes analyzed by electron microscopy so far [41]. Depressions at the 2-fold symmetry axis are flanked at both sides by protrusions of the 3-fold axis. These protrusions of the 3-fold symmetry axis are the most prominent feature of the AAV capsid [42]. Another characteristic feature is a cylindrical channel at the 5-fold symmetry axis, which is surrounded by depressions (Fig. 3 A). The basic structures of the individual capsid subunits show high similarities between the AAV serotypes. Each subunit is composed of eight antiparallel β-barrel motifs (βB-βI) which face the inside of the capsid (Fig. 3 B) and are highly conserved among all AAV serotypes [43]. The β-barrel strands are interrupted by loops which form the surface of the AAV capsids and show extensive variations between the different AAV serotypes. The loops are named according to the strands they connect. With more than 200 amino acids, the loop between the β-strands G and H represents the most extensive domain in the AAV capsid (Fig. 3 B).

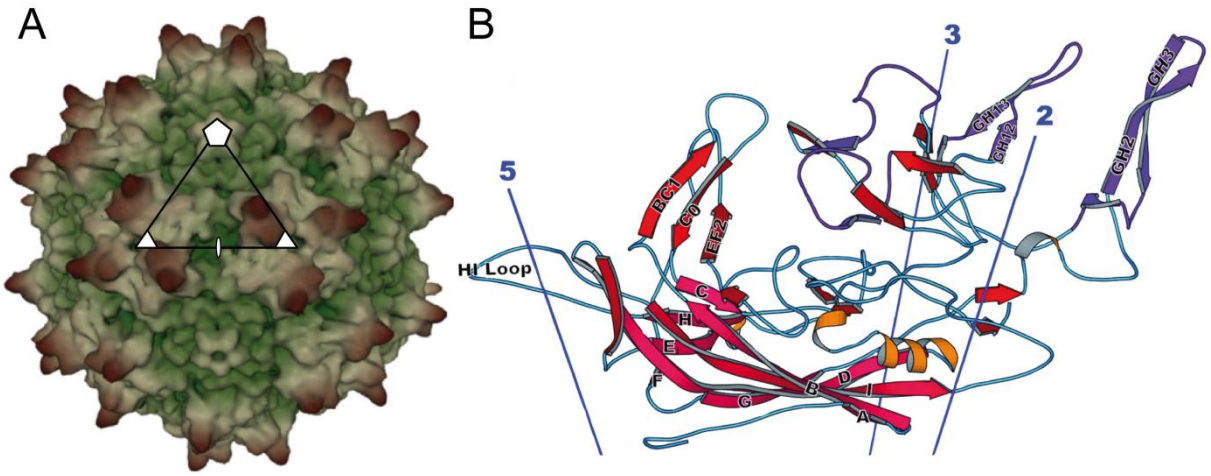

Fig. 3 AAV Capsid Structure: (A) 3D electron microscope reconstruction of an AAV2 particle. The large triangle shows a schematic representation of one of the 60 capsid subunits. The symmetry axes of the icosahedral capsid are depicted as a pentagon (5-fold), a small triangle (3-fold) and a slim oval (2-fold). Illustration adapted from [42] **(B)** Ribbon drawing of a VP3 subunit (AAV2). The eight antiparallel β-barrels (B-I) are located on the inner surface of the capsid. The loops on the outer surface of the capsid are named according to their flanking β-strands (e.g HI loop). The positions of the symmetry axes are shown. Illustration taken from [43].

Most of the GH-loop is located at the 3-fold symmetry axis and is associated with receptor binding [41,42,44] or binding of neutralizing antibodies [45]. The N-termini of the VP1 and VP2 capsid proteins reside at the inside of the capsid and are exposed during infection in the presence of a low pH in the endosomes [46]. The N-terminus of VP1 is highly conserved among the AAV serotypes. It contains a catalytic phospholipase A2 (PLA_2) domain [47] and three basic clusters that act as nuclear localization signals (NLS) [48].

1.1.4 Capsid Functions during Adsorption and Intracellular Trafficking

The first step of the replication cycle comprises the attachment of the AAV capsid to the primary receptor on the surface of the host cell (Fig. 4 A). All currently identified primary receptors of AAV are glycans that are conjugated to proteins or lipids in the cell membrane. The presence of a specific surface glycan thus determines whether a cell can be infected by AAV. Additionally, co-receptors have been described that play a role for the internalization of the AAV particle (Fig. 4 B) [49-53]. After binding of the respective receptors, AAV enters the cell via endocytosis (Fig. 4 C). The nature of the endocytosis is still not fully resolved. Studies indicated that AAVs can be internalized through clathrin-mediated endocytosis, assisted by dynamin [54] or by a clathrin-independent carrier (CLIC) through a GPI-anchored-protein enriched endosomal compartment (GEEC) [55].

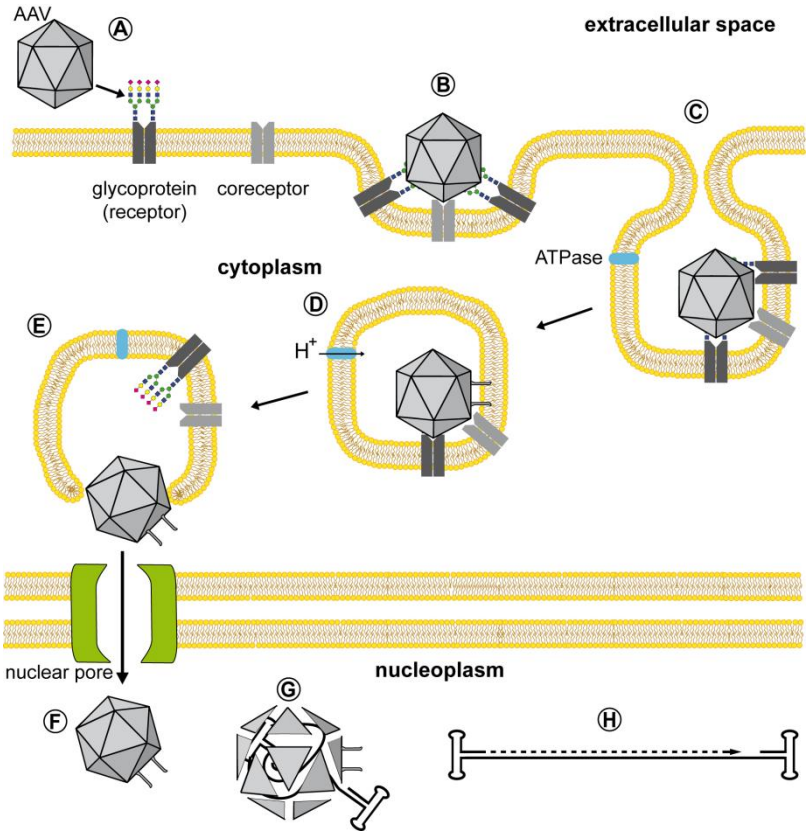

Fig. 4 Entry and Intracellular Trafficking of AAV: Schematic representation of the early steps of the AAV life cycle. Depicted is the binding of the capsid to the cellular receptor (A), invagination of the cell membrane through clustering by binding to multiple receptors and coreceptors (B), the internalization by endocytosis (C), the intracellular trafficking including acidification of the endosome (D), the release of the AAV particle from the endosome (E) and the translocation of the AAV particle into the nucleus (F), where the capsid is degraded (G) and second-strand synthesis of the AAV genome occurs (H).

Following endocytosis the formed vesicles are transported to the nucleus by the microtubule network [56]. Acidification of the vesicles leads to conformational changes in the capsid structure [57] which expose the N-termini of the VP1 and VP2 proteins (Fig. 4 D) [46]. The catalytic PLA_2 domain at the N-terminus of the VP1 protein is assumed to play a role for the release of the AAV particle from the endosomes (Fig. 4 E) [58]. Subsequently, the NLS of the VP1 and VP2 proteins are recognized by the cell nuclear import machinery, which leads to the transport of the capsids into the nucleus [59] (Fig. 4 F). Inside the nucleus the AAV genome is released from the capsid by degradation of the capsid (Fig. 4 G). In the presence of host cell polymerases the complementary strand of the single stranded genome is synthesized (Fig. 4 H).

1.1.5 AAV Serotypes and their Receptors

After the identification of AAV as contaminants in adenovirus preparations in the 1960s, antibodies were used to eliminate AAV from the preparations [2]. However, the antibodies were only able to exclude AAV from some, but not all adenovirus stocks. Soon it was realized that AAV exists in different serotypes. Currently, 13 AAV serotypes have been described, isolated from human cell lines (AAV2, -3, -5 and 6) or from non-human primate cell lines (AAV1, -4 and -7 to -13). The

major differences between the existing AAV serotypes are found in the surface exposed regions of the capsids which are responsible for the binding to cell surface receptors.

1.1.5.1 AAV Serotype 1

Infection with AAV1 was initially shown to require the binding of α2-3 or α2-6-linked sialic acids on the surface of the host cell. These sialic acids are an integral part of a glycan which is attached to asparagines (N-glycan) of yet unknown membrane proteins. Pretreatment of the cells with neuraminidases inhibits the internalization of the virus into the cell. On glycan arrays, AAV1 interacts with a synthetic glycan with a terminal α2-3 N-acetylneuraminic acid conjugated to N-acetylgalactosamine which is β1-4 linked to N-acetylglucosamine [60]. The crystal structure of the capsid has been determined at a resolution of 2.5 Å [61]. However, the amino acids responsible for the binding of the receptor have not been identified so far. Local *in vivo* delivery of AAV1 to different tissues of rodents has been shown to efficiently infect skeletal muscle, retina, pancreatic and neuronal cells [62].

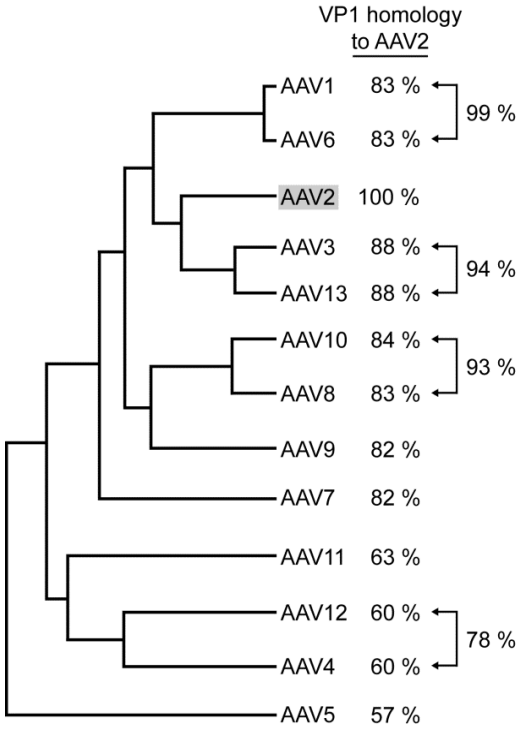

Fig. 5: Phylogenetic Tree of the Family of AAV Serotypes. The relationships of the AAV serotypes are displayed based on the amino acid sequence of the VP1 capsid protein. Next to the AAV serotype (right) the identity of the capsid is given (in percentage, compared to the prototype AAV2, highlighted in gray). Additionally, the homology of the closest related AAV serotypes is shown.

1.1.5.2 AAV Serotype 2

AAV2 represents the best-studied serotype so far. The capsids of this serotype are known to use heparan sulfate proteoglycan (HSPG) as primary receptor [63]. Infection of AAV2 can be inhibited either by soluble heparins or by pretreatment of the cells with heparinases. Furthermore, coreceptors have been described which support the internalization of AAV2, e.g. the fibroblast growth factor receptor 1 [53], the hepatocyte growth factor receptor [49], integrins [51] or laminin [52]. On the capsid basic amino acids (R585 and R588) have been identified which participate in heparin binding [64,65]. These are located at the GH12-GH13 loop (Fig. 3B) on the side, close to

the top of the 3-fold symmetry axis [41]. Local *in vivo* delivery of AAV2 to different tissues of rodents has been shown to efficiently infect kidney tubular epithelial, neuronal, vascular smooth muscle and skeletal muscle cells. After intravenous injection AAV2 has also been shown to efficiently infect liver cells [62].

1.1.5.3 AAV Serotype 3

For AAV3 two different isolates exist (AAV3A [66] and AAV3B [67]) which differ by six amino acids based on the amino acid sequence of the VP1 protein. Most studies for the characterization of this serotype have been performed with the isolate AAV3B which is therefore conveniently designated as AAV3. Similar to AAV2, AAV3 uses HSPG as primary receptor [68]. For the binding of heparin R594 is necessary on the capsids [69]. This amino acid is located at the center of the 3-fold symmetry axis in a cluster with the corresponding amino acid residues from two neighboring capsid subunits. The fibroblast growth factor receptor [70] and laminin [52] have been described as coreceptors for AAV3. Local *in vivo* delivery of AAV3 to mice has been shown to efficiently infect skeletal muscle cells [71]. Furthermore, in cell culture AAV3 was demonstrated to infect hepatocarcinoma cells much more efficiently than any other AAV serotype [72].

1.1.5.4 AAV Serotype 4

Infection with AAV4, which was isolated from primate cell lines, requires the binding of α2-3-linked sialic acids on the surface of mammalian host cells [73]. These are integral parts of glycans attached to serines or threonines (O-glycans) of yet unknown membrane proteins. The specific amino acids responsible for receptor binding have not been identified so far. However, the replacement of positively charged lysines located at the 3-fold symmetry axis of the capsids by negatively charged glutamic acids has been shown to dramatically reduce AAV4 infectivity [74]. *In vivo* injections of AAV4 to the central nervous system of mice have been shown to lead to ependyma-specific infection [75]. Furthermore, AAV4 was demonstrated to efficiently infect retinal pigmented epithelium in rat, dog, and nonhuman primates after subretinal delivery [76].

1.1.5.5 AAV Serotype 5

AAV5 represents the evolutionary most divergent member of the AAV family (Fig. 5) with major differences in the genome [77] and capsid structure [78]. AAV5 infection requires the binding to glycans with α2-3-linked sialic acids on the surface of the host cell that are attached to asparagines of membrane proteins [73]. The platelet-derived growth factor receptor was described as co-

receptor for the infection of AAV5 [50]. Local *in vivo* delivery of AAV5 to different tissues of rodents has been shown to efficiently infect skeletal muscle, retina, lung epithelial and neuronal cells [62].

1.1.5.6 AAV Serotype 6

AAV6 is closely related to the serotype 1 (Fig. 5). The capsids of either serotype differ in six amino acids based on the amino acid sequence of the VP1 protein [67] leading to variant cell tropism [79]. In contrast to AAV1, AAV6 can infect cells in the spinal cord, epithelial lung cells and the myocardium but also skeletal muscle cells [62,80]. Similar to AAV1, AAV6 infection requires the binding of N-glycans with α2-3 or α2-6-linked sialic acids that are attached to unknown membrane proteins of the host cell [60]. Additionally, AAV6 also binds to HSPGs [81]. The amino acid K531 is involved in heparin binding which is located at the base of the protrusions at the 3-fold symmetry axis [82]. In contrast to AAV2 and AAV3, soluble heparins cannot be used to inhibit the internalization of the virus [83].

1.1.5.7 AAV Serotypes 7, 8 and 10-12

A primary glycan receptor for the infection with AAV7, AAV8, AAV10, AAV11 and AAV12 has not been identified so far. Pretreatment of the cells with neuraminidases or addition of soluble heparins does not inhibit the internalization of these viruses into the cell [84-86]. Laminin was described as coreceptor for the AAV8 infection [52]. In comparative analyses of local *in vivo* delivery of various AAV serotypes to rodents, AAV7 and AAV8 have been shown to efficiently infect skeletal muscle, retina and neuronal cells [62]. Additionally, AAV8 efficiently infects liver cells *in vivo* [87]. AAV10 and AAVrh.10 are closely related differing by 12 amino acids based on the amino acid sequence of the VP1 capsid protein [84,88].

1.1.5.8 AAV Serotype 9

Infection with AAV9 requires the binding to glycans with terminal galactoses attached to asparagines of membrane glycoproteins [89]. Also on glycan arrays AAV9 capsids bound synthetic glycans with terminal galactoses [86]. Similar to AAV8, laminin has been described as coreceptor for AAV9 infection [52]. Local *in vivo* delivery of AAV9 to different tissues of rodents has been shown to efficiently infect liver, pancreatic and lung epithelial cells. After intravenous injection AAV9 has also been shown to efficiently infect the myocardium, skeletal muscle and kidney cells

[62]. Furthermore AAV9 has been shown to cross the blood-brain barrier to infect astrocytes in the central nervous system after intravenous injection in mice [90].

1.1.5.9 AAV Serotype 13

Similar to AAV serotypes 2 and 3, AAV13 requires HSPGs for infection [91]. Soluble heparins inhibit the internalization of the virus. For heparin binding activity the importance of the amino acid K528 of the capsid protein has been demonstrated. This lysine residue is located at the base of the protrusions at the 3-fold symmetry axis similar to K531 of the capsid of AAV serotype 6 [91].

1.2 AAV Vectors

Gene therapy with vectors based on adeno-associated viruses has developed in recent years into one of the most successful tools for the treatment of monogenetic diseases. In human clinical trials AAV vectors showed impressive therapeutic long-term successes, e.g. for the treatment of congenital blindness and hemophilia [92,93]. Recently, an AAV vector for the expression of lipoprotein lipase to treat congenital lipoprotein lipase deficiency became the first human gene therapy commercially available in the European Union [94]. The major advantage of AAV vectors is their long-term persistence and transgene expression in post-mitotic cells. The combination of site-specific application with the selection of appropriate AAV serotypes allows precise transduction of foreign genes to the tissue or cell type of choice. Additional advantages of AAV vectors include their low pathogenicity, the limited immune response and the high chemical and physical stability of the capsids [95]. In contrast to gene therapy with retroviral vectors the AAV vector genomes persist as free nuclear episomes [96]. Since the *rep* gene is deleted in AAV vectors, genomic integration only occurs rarely [97] and insertional mutagenesis which represents the major risk in retroviral gene therapy is virtually non-existent. Although the packaging capacity of AAV vectors is limited to 5 kb, this size is sufficient for many cDNAs or small genes. For larger genes, the AAV split vector technology exists, which is based on the distribution of a transgene on two or more AAV vectors and formation of full-length transcripts by splicing after recombination of mixed concatamers following transduction [95].

1.2.1 Construction of Recombinant AAV Vectors

Recombinant AAV (rAAV) vectors are constructed by replacement of the entire viral *rep* and *cap* gene sequences. From the wild type AAV backbone only the flanking *cis*-active ITRs are retained. These represent the only elements required in *cis* for rAAV replication and packaging. This leaves

sufficient space (up to 5 kb) for a foreign gene of choice including a promoter and a polyA site (Fig. 6). AAV vectors can be generated for protein expression or for non-coding RNAs (e.g. siRNAs, miRNAs) aiming at targeted gene knockdown [98]. The deleted AAV Rep and Cap proteins together with helper virus functions have to be delivered *in trans* in the producer cells. In their presence rAAV genomes are replicated similar to wild type AAV (Fig. 2). The Rep proteins of AAV2 are also required for packaging of AAV2-ITR flanked vector genomes as single-stranded DNA. The AAV2-derived vector backbone can be packaged not only into the homologous AAV2 capsids, but in capsids of any variant AAV serotype identified so far [99].

Upon nuclear entry of rAAVs the single-stranded genome requires the synthesis of the complementary DNA strand to generate a transcription-competent double-stranded DNA template. This step is dependent on the host cell DNA replication machinery. However, most target cells are post-mitotic and the DNA replication machinery is largely inactive. This leads to a delayed onset of transgene expression. To circumvent this problem, self-complementary AAV (scAAV) vectors have been developed which contain a double-stranded transgene cassette (Fig. 6) formed through hybridization of the self-complementary sequences after back-folding of the ITR sequence. These self-complementary genomes provide a suitable template for immediate transcription of the transgene in dividing as in quiescent cells [39].

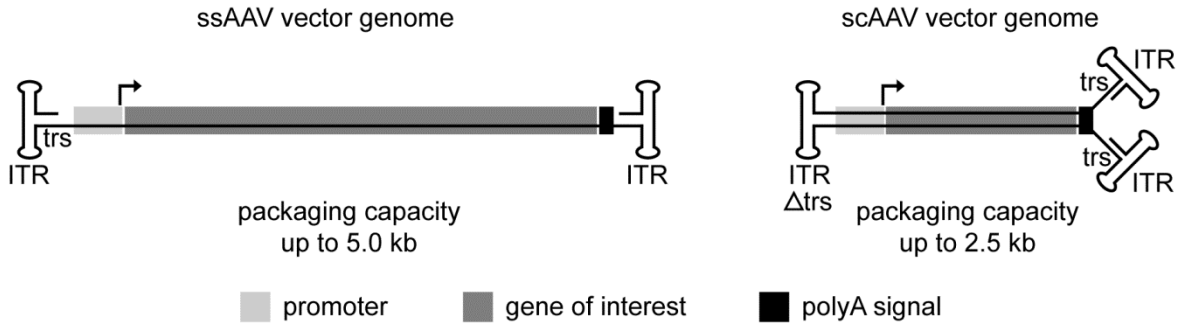

Fig. 6 Recombinant ssAAV vs. scAAV Vector Genome: Schematic representation of the structure of a single-stranded, ssAAV and a self-complementary, scAAV vector genome, respectively. ITR: inverted terminal repeat, Δ*trs*: deleted terminal resolution site

For the generation of scAAV vectors the *trs* in one of the ITRs has been deleted. During the replication of the vector genome nicking of the DNA and reinitiation of the DNA synthesis (Fig. 2) is prevented at the mutated ITR leading to the formation of a vector genome with partially double-stranded, complementary DNA connected by an internal ITR (Fig. 6). Since this strategy reduces the maximum packaging capacity of AAV vectors to approximately 50% these vectors are ideal for the expression of small cDNAs, e.g. neuropeptides, or for regulatory RNAs.

1.2.2 Production of rAAV Vectors in HEK 293 Cells

The most widely used protocol for laboratory-scale rAAV production represents plasmid cotransfection of adherent HEK 293 cells with a combination of plasmids, one for rAAV genome and one or two for AAV *rep* and *cap* and for the adenoviral helper functions E2A, E4ORF6 and VA-RNA [28,99]. The adenoviral helper functions E1A and E1B are constitutively expressed by HEK 293 cells (Fig. 7). The plasmid cotransfection system enables easy and rapid production of AAV vectors of any AAV serotypes at laboratory scale. When large quantities of AAV vectors are required, as is the case for most clinical applications, this system is limited in scalability.

1.2.3 Production of rAAV Vectors in *Sf*9 Insect Cells

Insect cells are frequently used for the expression of heterologous proteins. For that purpose recombinant baculoviruses are required, which deliver the transgene into insect cells. *Sf*9 cells, which are derived from ovary cells of *Spodoptera frugiperda*, can be easily grown in suspension culture allowing convenient and scalable production of heterologous proteins. *Sf*9 cell infection with recombinant baculoviruses expressing AAV *cap* leads to high titers of properly assembled, empty AAV capsids [100]. The system was further developed for the production of genome-containing rAAV vectors. Coinfection of *Sf*9 cells with three independent baculoviruses strains Bac-*rep*, Bac-*cap* and Bac-rAAV harboring the AAV-ITR-flanked transgene cassette leads to high titer production of rAAV vectors [101]. Combination of AAV *rep* and *cap* on one baculovirus reduced the number of Bacs, which had to be coinfected leading to a facilitated and enhanced rAAV production [102]. The reduction of the number of required baculovirus has proven advantageous since the genetic instability of recombinant baculovirus limit their propagation over multiple successive passages. The development of stable *rep*/*cap* *Sf*9 cell lines further reduced the number of recombinant baculovirus strains needed for the production of rAAV down to one (Fig. 7) [103]. In these cells Rep and Cap expression is induced upon infection with any baculovirus. This rAAV production system has been described for the production of rAAV1 and rAAV2 and was shown to generate superior vector titers as compared to the three- or two-Bac system [103].

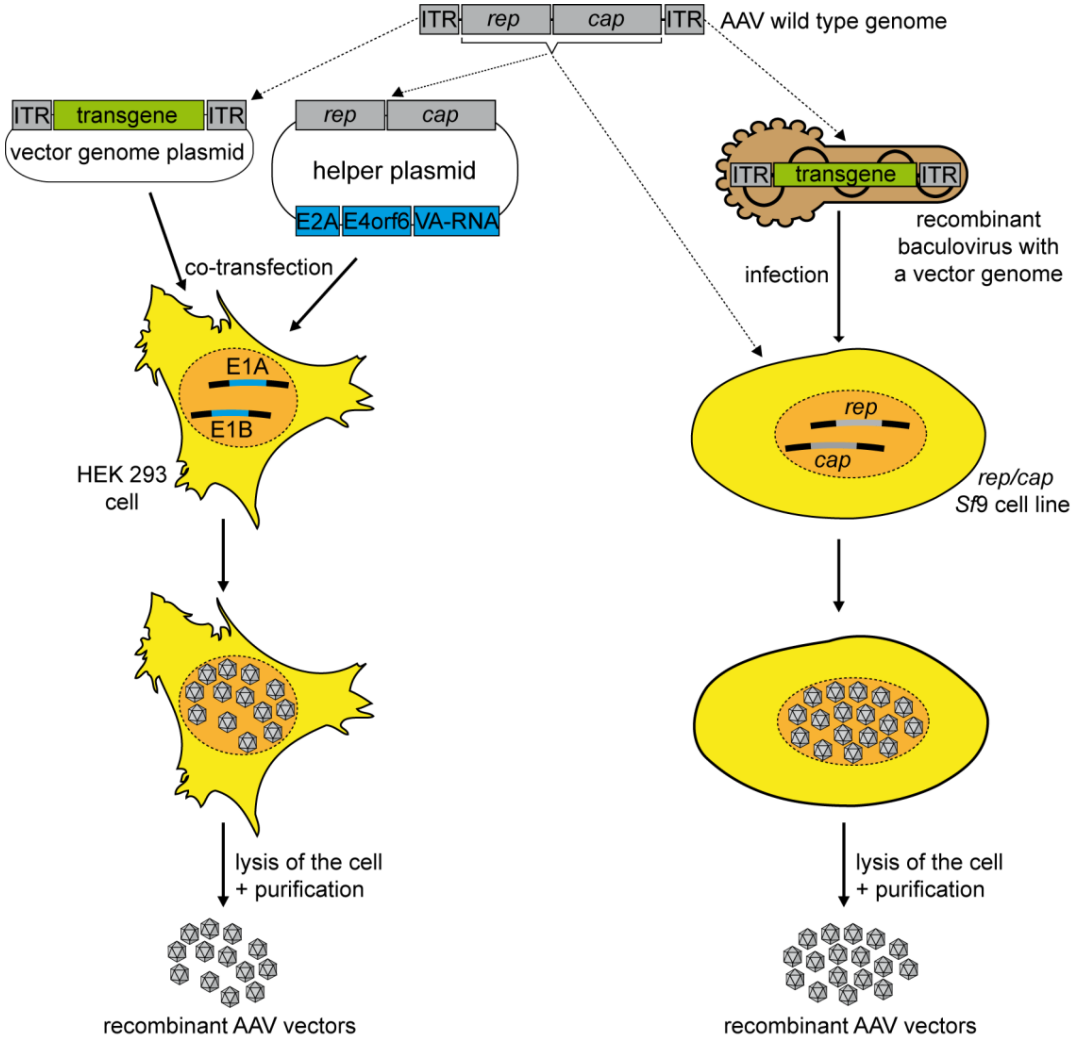

Fig. 7 Production of rAAV Vectors in HEK 293 Cells and in *Sf*9 Cell Lines: left: schematic representation of the rAAV production by transient transfection of HEK 293 cells, right: schematic representation of the rAAV production in *rep*/*cap* *Sf*9-cell lines by infection of recombinant baculoviruses harboring the vector genome.

1.3 Glycans

Carbohydrates represent one of the four major classes of biological macromolecules. Glycans belong to a subclass of carbohydrates, which comprise polysaccharides and oligosaccharides conjugated to lipids or proteins [104]. Glycans display a high variety of structures involved with various biological processes.

1.3.1 Glycan Structures

Monosaccharides represent the basic structural components of glycans. Despite their high diversity only ten different monosaccharides have been described in mammalian glycan structures so far

[105]. The individual monosaccharide units are joined by O-glycosidic bonds at the anomeric carbon atoms. These glycosidic linkages can occur in two configurations, called α- or β-glycosidic bonds, leading to the formation of different glycan stereoisomers. For the nomenclature of the glycans the linked carbon atoms of two monosaccharides are stated with the glycosidic bond (e.g. α2-3, β1-4) [106]. The diversity of glycan biopolymers is further increased by branching of the carbohydrate chains, variable modifications of monosaccharides (e.g. sulfation or phosphorylation) [107] or by conjugation of the glycan to different proteins (glycoproteins, proteoglycans) or lipids (glycosphingolipids) (Fig. 8). Virtually all membrane proteins are glycosylated, but their glycosylation patterns differ in different tissues [108]. Cytoplasmic and nuclear proteins can also be glycosylated [109]. Glycans are either attached to asparagines (N-glycans) or to serines and threonines (O-glycans) within membrane proteins (Fig. 8). Proteoglycans represent a special group of glycoproteins, where the proportion of polysaccharides and oligosaccharides markedly outweighs the protein part. In proteoglycans multiple glycans, especially glycosaminoglycans (GAG), are conjugated to a core protein. GAGs are composed of linear, long-chained polysaccharides with repetitive disaccharide units. Members of this group are heparan sulfate, heparin, dermatan sulfate, chondroitin sulfate, keratan sulfate and hyaluronic acid [110].

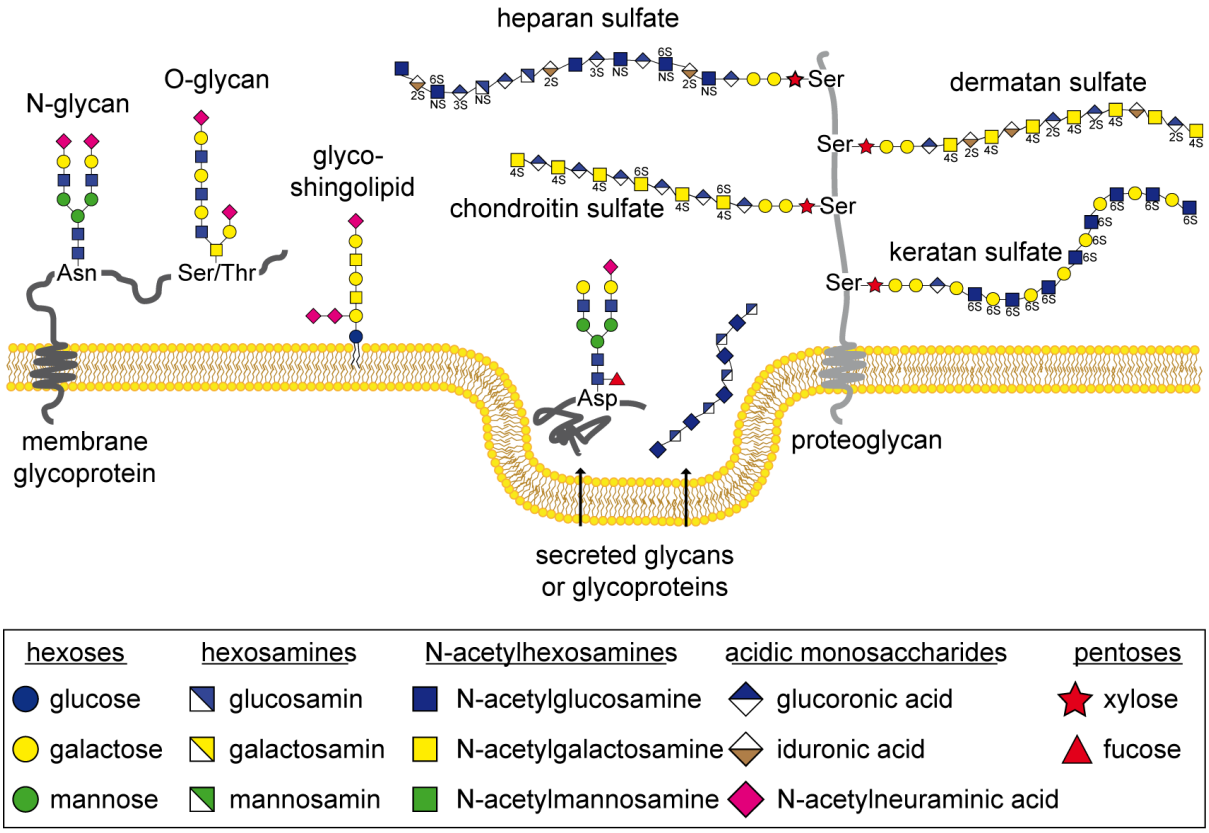

Fig. 8 Glycans at the Cell Membrane: Schematic representation of different glycan structures at the cell membrane. Bottom: Overview of monosaccharides and their symbol nomenclature [111]

1.3.2 Biological Functions of Glycans

Revealing the biological role of glycans has been the subject of intensive research. However, due to the lack of appropriate methods and the high diversity of glycan structures specific functions have as yet only been assigned to a small number of these structures. The functions identified so far can be divided into two groups: (I) glycans with structural or modulatory functions and (II) glycans recognized by proteins [112].

Glycans with structural functions include GAGs in the extracellular matrix [110]. Other glycans are involved in protein-folding [113] or play a role in signal transductions [114]. Furthermore, glycans are important for cell-cell interactions including symbiotic or host-pathogen interactions [112]. Surface exposed glycans are recognized as host cell receptors by divergent virus genera, e.g. influenza virus, picornavirus, polyomavirus, herpesvirus and parvovirus [115,116].

1.3.3 Sialic Acids, Heparan Sulfate and Heparin

Sialic acids represent N- or O-substituted derivatives of neuraminic acid, a 9-carbon monosaccharide. Since N-acetylneuraminic acid (Neu5Ac) is the most common sialic acid, both terms are often used synonymously. Sialic acid-containing glycans are present in all vertebrates and are ubiquitously distributed in all tissues [117]. These are mostly located at the terminating branches of N-glycans, O-glycans or glycosphingolipids (Fig. 8). Due to the high number of sialic acids on the surface of the cells they provide a negative charge to the membrane. Furthermore, they are involved in ion exchange processes, protect the cell from proteases and serve as receptors for various signaling pathways [118].

Similar to sialic acid-containing glycans, heparan sulfate has been found on the surface of most cells. Heparan sulfate is present as proteoglycan (HSPG) (Fig. 8) and a component of the extracellular matrix. The related heparin is synthesized by mast cells and stored in vesicles until its induced release. Both GAGs share a similar structure. These linear polysaccharides are composed of alternate units of glucosamine (GlcN) and uronic acid, either a glucoronic acid (GlcA) or iduronic acid (IdoA), with the two units linked by α/β-1-4-glycosidic bonds. The individual monosaccharides can be variably modified by sulfates or acetyl groups. Heparin displays a higher degree of sulfation than HSPGs [110,119]. In addition to the structural function, HSPGs are important for cell migration, cell proliferation and cell differentiation. Furthermore, they are bound by growth factors and involved in signal transductions [120]. Mast cell-released heparin is involved in pathogen defense, especially against bacteria [121].

1.3.4 Glycomics

The term glycomics is used for the research on the repertoire of glycans of an organism, the glycome, and the interactions of glycans with proteins. The analysis of the glycome has been proven difficult since glycosylation patterns differ in different cell types. Furthermore, the glycome is sensitive to exogenous nutrient levels that may change the composition of the glycans [122]. For the determination of the glycome mass spectrometry is often used. For functional analysis microarrays with several hundred immobilized glycans have been developed, to allow comparisons of glycan binding patterns of proteins or other biomolecules (Fig. 9) [123].

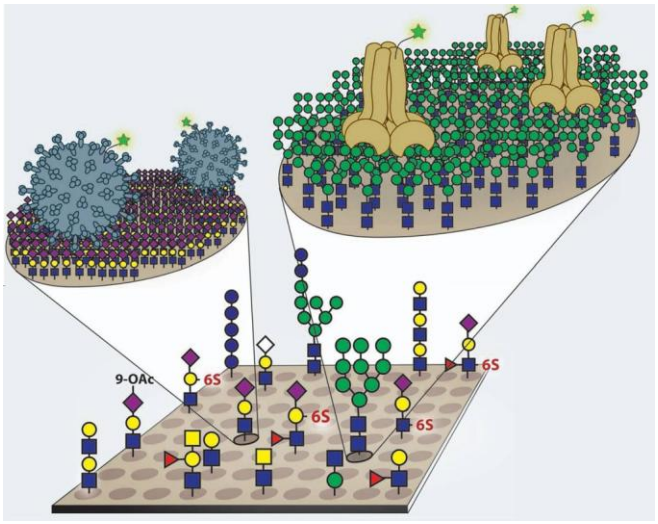

Fig. 9 Glycan Microarray Analysis: Schematic representation of a glycan microarray with different immobilized glycans. Fluorescence-labeled proteins or viral capsids interact with specific glycans on the array. Illustration taken from [123].

1.4 Aims of the Thesis

Adeno-associated virus (AAV) vectors are becoming increasingly promising for human gene therapy of genetic disorders and for the more sophisticated determination of gene functions in animal studies. The initial objective of this thesis was the determination of the receptor glycan binding characteristics of AAV capsids from variant serotypes, which determine the cell tropism for AAV gene transfer. For this purpose highly-purified and concentrated AAV vector particles of the full range of AAV serotypes needed to be produced in sufficient amounts to allow labeling of the capsids with a fluorescent dye. AAV vector production with the most widely used laboratory-scale protocol, namely plasmid transfection of HEK 293 cells, was found to be insufficient to achieve the required titers in the range of more than $1x10^{13}$ genomic particles per ml. To achieve higher AAV yields, the scalable insect cell based rAAV production protocol described for AAV1 and -2 by Aslanidi *et al.* [103], seemed suitable. The aim was to establish and further develop the system for the production of the full range of AAV serotypes 1-12. The novel AAV production platform, named OneBac, facilitated high-titer production of AAV vectors as required for binding studies on glycan microarrays with hundreds of synthetic glycan structures or on specialized heparin microarrays. Furthermore, to be acknowledged as an AAV vector production system suitable for gene therapy applications, OneBac-derived AAV vectors needed to be characterized

with respect to virus integrity, AAV burst sizes per cell and infectivity in direct comparison with the existing plasmid transfection-based production protocol in HEK 293 cells.

As part of an ongoing cooperation a side project was pursued. Self-complementary AAV vectors for the expression of neuropeptide Y (NPY) in neurons were constructed to determine the role of NPY in the CNS for the development of obesity. Highly concentrated and purified AAV vectors were prepared for stereotactic injections in the hypothalamus of wild type and NPY knock-out mice.

To complement an ongoing study on the mechanism of AAV replication in the presence of its helper virus herpes simplex virus (HSV) the *in vitro* interaction of AAV Rep protein mutants with the HSV single-stranded DNA binding protein, ICP8 was analyzed on AAV ssDNA. Through complementary experiments the proposed model for the initiation of AAV DNA replication was further validated as required for publication.

2 Publications

2.1 OneBac: Platform for Scalable and High-Titer Production of AAV Serotype 1-12 Vectors for Gene Therapy

Authors: Mario Mietzsch, Sabrina Grasse, Catherine Zurawski, Stefan Weger, Antonette Bennett, Mavis Agbandje-McKenna, Nicholas Muzyczka, Sergei Zolotukhin and Regine Heilbronn

Year: 2014

Journal: Human Gene Therapy, in press

2.1.1 Contribution to the Publication

The generation of the set of novel AAV3-12 *rep/cap* expressing stable *Sf*9 cell lines described in this study was initiated as part of my doctoral research. The previously described AAV1 and AAV2 cell lines [103] were kindly provided by Dr. Sergei Zolotukhin, University of Florida, where I spent 6 months during my thesis to initiate the study. The cell lines for production of AAV8 and AAV9, AAV11 and AAV12 were developed under my supervision by two master students, Sabrina Grasse and Catherine Zurawski. Their generation is described in their master's thesis: "Verbesserte Produktion von rekombinanten AAV Vektoren der Serotypen 8 und 9" and "Etablierung von *Spodoptera frugiperda*-basierten Verpackungszelllinien für die Produktion von AAV-Vektoren der Serotypen 11 und 12", both submitted to the department of Biology, Chemistry, and Pharmacy at the Freie Universität Berlin in 2012. The characterization of the set of cell lines was designed by me and my mentor, Prof. Regine Heilbronn. I performed all displayed experiments with the exception of the electron microscopy analysis shown in Fig. 3C, which was provided by Dr. Antonette Bennett in the lab of Dr. Mavis Agbandje-McKenna at the University of Florida, USA.
The manuscript was written together with my mentor Prof. Regine Heilbronn.

http://dx.doi.org/10.1089/hum.2013.184

HUMAN GENE THERAPY 25:212–222 (March 2014)
Mary Ann Liebert, Inc.
DOI: 10.1089/hum.2013.184

OneBac: Platform for Scalable and High-Titer Production of Adeno-Associated Virus Serotype 1–12 Vectors for Gene Therapy

Mario Mietzsch,[1] Sabrina Grasse,[1] Catherine Zurawski,[1] Stefan Weger,[1] Antonette Bennett,[2,3] Mavis Agbandje-McKenna,[2,3] Nicholas Muzyczka,[4,5] Sergei Zolotukhin,[6] and Regine Heilbronn[1]

Abstract

Scalable and genetically stable recombinant adeno-associated virus (rAAV) production systems combined with facile adaptability for an extended repertoire of AAV serotypes are required to keep pace with the rapidly increasing clinical demand. For scalable high-titer production of the full range of rAAV serotypes 1–12, we developed OneBac, consisting of stable insect *Sf9* cell lines harboring silent copies of AAV1–12 *rep* and *cap* genes induced upon infection with a single baculovirus that also carries the rAAV genome. rAAV burst sizes reach up to 5×10^5 benzonase-resistant, highly infectious genomic particles per cell, exceeding typical yields of current rAAV production systems. In contrast to recombinant *rep/cap* baculovirus strains currently employed for large-scale rAAV production, the *Sf9rep/cap* cell lines are genetically stable, leading to undiminished rAAV burst sizes over serial passages. Thus, OneBac combines full AAV serotype options with the capacity for stable scale-up production, the current bottleneck for the transition of AAV from gene therapy trials to routine clinical treatment.

Introduction

Gene therapy with adeno-associated virus (AAV) vectors has witnessed enormous clinical progress in recent years. Exiting improvements in the treatment of diverse genetic diseases, including congenital blindness and hemophilia (Mingozzi and High, 2011; Nathwani *et al*., 2011), have been made possible by recombinant AAV (rAAV)-mediated gene delivery. Recently, Glybera, an AAV vector expressing lipoprotein lipase to treat metabolic lipid disorders, was approved as the first human gene therapy to become commercially available (Kastelein *et al*., 2013). The increasing request for clinical application requires robust and scalable production methods for an increasing range of AAV serotypes. At present, 12 major AAV serotypes have been isolated from humans and nonhuman primates, not counting the numerous engineered variants thereof. The AAV serotypes have distinct capsids, which interact with specific cell surface receptors. Whereas AAV2 or AAV1 have mostly been used in clinical trials so far, the extended cell- and tissue-specific transduction patterns of alternative AAV serotypes are being increasingly translated into clinical gene therapy (Mingozzi and High, 2011; Nathwani *et al*., 2011).

rAAV vectors are constructed as gene-deleted AAVs comprising the gene of interest flanked the AAV-ITRs, the only *cis* elements required for rAAV replication and packaging. The AAV gene *rep* codes for the regulatory proteins Rep78/68 and Rep52/40, while *cap* codes for the capsid proteins VP1, VP2, and VP3. For rAAV production, *rep* and *cap* have to be provided *in trans* together with the required helper virus genes. Plasmid cotransfection of the rAAV genome, AAV*rep/cap*, and adenovirus helper genes in 293 cells represents the most widely used protocol for rAAV production (Grimm *et al*., 1998, 2003; Xiao *et al*., 1998). However, inherent problems in growing and transfecting 293 cells in suspension culture limit the scalability of this system.

To develop a scalable rAAV production system, Urabe *et al.* (2002) exploited *Sf9* insect cells that produced rAAV2 upon coinfection with three recombinant baculovirus (Bac)

[1]Institute of Virology, Campus Benjamin Franklin, Charité Universitätsmedizin Berlin, 12203 Berlin, Germany.
[2]Department of Biochemistry and Molecular Biology; [3]Center for Structural Biology; [4]Department of Molecular Genetics and Microbiology; [5]Powell Gene Therapy Center; [6]Department of Pediatrics; University of Florida College of Medicine, Gainesville, FL 32610.

vectors, encoding the *rep* gene, the *cap* gene, and the rAAV genome, respectively. Production of three Bac-mediated rAAVs was subsequently scaled up to bioreactor size (Cecchini *et al*., 2011), and *rep* and *cap* were combined to reduce the number of coinfecting Bacs (Smith *et al*., 2009). Unfortunately, Bac instability, especially of Bac-Rep, limits rAAV yields after few successive passages (Kohlbrenner *et al*., 2005). Rep78 expression has long been known for its cell toxicity, a feature that has notoriously hampered efforts to generate stable Rep-expressing cell lines (Zolotukhin, 2005).

To circumvent the above problems, Aslanidi *et al.* (2009) did the next step and developed a two-component rAAV production system consisting of a stable *Sf9* cell line with integrated but silent copies of AAV *rep* and *cap*, each controlled by the Bac-derived polyhedrin promoter polh and the *cis*-acting element hr2-0.9. Expression of AAV *rep* and *cap* is induced upon Bac infection by immediate-early (*IE-1*) gene-mediated transactivation of the hr2-0.9 enhancer. The Bac also harbors the rAAV genome as described before (Urabe *et al*., 2002; Aslanidi *et al*., 2009). Once expressed, Rep78 initiates a feed-forward loop that amplifies the integrated *rep* and *cap* genes by interaction with the incorporated cognate AAV Rep-binding site (RBE). This leads to rAAV2 burst sizes per cell exceeding those of the three-Bac infection system (Aslanidi *et al*., 2009).

In the present study, we have further developed this system to OneBac: *Sf*9 *rep*/*cap* producer cell lines for the entire range of rAAV1–12 serotypes produced upon infection with a single Bac (Bac-rAAV). rAAV production efficiencies were quantified in comparison to the 293-cell cotransfection protocol, the only other system offering easy access to an extended range of rAAV serotypes. High rAAV burst sizes per cell persist over successive cell passages surpassing the efficiency and stability of current rAAV production systems. OneBac can easily be adapted to production of novel serotypes by selection of additional *Sf9* cell lines, as described here for rAAV serotypes 1–12. Taken together, OneBac is ideally suited for scale-up production of the rAAV serotype of choice as required for clinical application.

Materials and Methods

Plasmids and cloning

Plasmids pIR-VP-hr2-RBE and pIR-rep78-hr2-RBE were described previously (Aslanidi *et al*., 2009). AAV2 *cap* of pIR-VP-hr2-RBE was replaced by *cap* from other serotypes with the VP1 start codon mutated to ACG (Grimm *et al*., 1998, 2003; Gao *et al*., 2002, 2003; Mori *et al*., 2004; Schmidt *et al*., 2008). AAV2 *rep* of pIR-rep78-hr2-RBE was replaced by *rep* of AAV4 or by *rep* of AAV12 (Grimm *et al*., 2003; Schmidt *et al*., 2008). See Supplementary Table S1 (Supplementary Data are available online at www.liebertpub.com/hum) for details on polymerase chain reaction (PCR) amplification.

Cell culture

HEK 293 and HeLa-derived C12 cells (Clark *et al*., 1996) were cultivated as adherent monolayers as described (Winter *et al*., 2012). *Sf9* cells and cell lines derived thereof were maintained either as adherent monolayers or in suspension culture at 27°C under constant agitation in serum-free Spodopan medium (Pan-Biotech) supplemented with 200 μg/ml streptomycin, 200 U/ml penicillin, and 250 ng/ml amphotericin B (Invitrogen).

Construction of stable Sf9 cell lines

Adherent *Sf9* cells in 6-cm-diameter dishes were transfected with Cellfectin II Reagent (Invitrogen) at a confluency of 70%. A total of 15 μg of pIR-Rep-hr2-RBE and pIR-VP-hr2-RBE as needed for the AAV serotype of choice was transfected at a molar ratio of 1:2.5. For selection and isolation of single-cell clones, transfected cells were replated on 6-cm-diameter dishes at 48 hr posttransfection in Spodopan medium with 10% fetal calf serum (FCS) and 25 μg/ml Blasticidin S (Invitrogen) at dilutions from 1:20 to 1:500. After 1 week, the medium was replaced to remove dead cells. Single-cell colonies become visible after 2–3 weeks. Up to 50 cell clones were picked and expanded on cell culture dishes of stepwise increasing diameters. rAAV production efficiency was screened by infection with Bac-rAAV-GFP (multiplicity of infection [MOI] = 3). Increasing GFP expression in infected *Sf9* cells leads to green coloration of the suspension culture, the extent of which served as rough estimate of rAAV replication efficiency. Genomic rAAV titers (genomic particles [gp]/ml) of the most promising cell clones were determined as outlined below.

Recombinant Bac

Recombinant Bac carrying the rAAV cassette for GFP expression under the control of the chicken β-actin-CMV hybrid (CBA) promoter (Bac-rAAV-GFP) was generated by the MultiBac system (Berger *et al*., 2004). Recombinant Bac replication was identified by GFP expression combined with detachment of *Sf*9 cells. Bac stocks were prepared and titers were quantified by plaque assays on monolayer *Sf9* cells as described (Kohlbrenner *et al*., 2005). For short-term storage, stocks were kept at 4°C in the dark. For long-term storage, Bac-infected *Sf*9 cells were frozen 24 hr postinfection (p.i.), and stored in liquid nitrogen.

rAAV production in 293 cells

HEK 293 cells were seeded at 25–33% confluency. Cells were transfected 24 hr later using the calcium phosphate cotransfection method as described (Winter *et al*., 2012). AAV vectors were produced using plasmids for AAV *rep*, *cap*, Ad5 helper genes, and the rAAV cassette expressing GFP under the control of the CBA promoter (pTR-UF26) by two- or three-plasmid transfection as described (Grimm *et al*., 1998, 2003; Xiao *et al*., 1998; Gao *et al*., 2002; Mori *et al*., 2004) For the production of rAAV12, vector transfection of four plasmids, pTR-UF26, pAAV12-Rep, pAAV12-Cap, and pHelper, was required (Schmidt *et al*., 2008). The medium was replaced 12 hr later by a medium with 2% FCS. Cultures were harvested 72 hr after transfection by three freeze–thaw cycles of cell lysis. Crude lysates were digested with 250 U/ml benzonase (Merck) at 37°C for 1 hr to degrade input and unpackaged AAV DNA until centrifugation at 8,000 × *g* for 30 min to pellet cell debris.

rAAV purification

rAAV vectors of the serotypes 1, 2, 3, 4, 5, 6, 7, 8, and rh.10 and 12 were purified from benzonase-treated, cleared freeze–thaw supernatants by one-step AVB sepharose affinity chromatography using 1 ml prepacked HiTrap columns on an ACTA purifier (GE Healthcare) as follows: Freeze–thaw supernatants were diluted 1:1 in 1× phosphate-buffered saline (PBS) supplemented with 1 m*M* $MgCl_2$ and 2.5 m*M* KCl (1× PBS-MK) before sample loading on the column at 0.5 ml/min. The column was washed with 20 ml of 1× PBS-MK at a rate of 1 ml/min. AAV vectors were eluted with 0.1 *M* sodium acetate and 0.5 *M* NaCl pH 2.5 at a rate of 1 ml/min and neutralized immediately with 1/10 volume of 1 *M* Tris-HCl pH 10. rAAV9 and rAAV11 vectors were purified by two-step ultracentrifugation through a 20% (w/v) sucrose cushion followed by a sucrose-step gradient [5–40% (w/v)] at 150,000 × *g* for 3 hr at 4°C as described (Mitchell *et al*., 2009). The AAV band at 25–30% sucrose was removed with a syringe. All rAAV preparations were dialyzed against 1× PBS-MK using Slide-A-Lyzer dialysis cassettes (10,000 MWCO; Thermo Scientific).

Quantification of rAAV vector preparations

Highly purified rAAV vector preparations or benzonase-treated rAAV freeze–thaw supernatants were spiked with 1 μg pBluescript carrier plasmid and digested with Proteinase K for 2 hr at 56°C. DNA was purified by repeated extractions with phenol and chloroform and precipitated with ethanol. Varying dilutions of capsid-released AAV genomes were analyzed by quantitative Light-Cycler PCR, using the Fast Start DNA Master SYBR Green kit (Roche). PCR primers were specific for the bovine growth hormone gene-derived polyA site of the vector backbone (5′-CTAGAGCTCGCTGATCAGCC-3′ and 5′-TGTCTTCCCAATCCTCCCCC-3′). Nonvector AAV *rep-cap* packaging was detected by primers specific for AAV2 *rep* and serotype-specific *cap* (Supplementary Table S1).

Southern blot analysis

Southern blot analysis of vector genomes packaged in AAV capsids was performed with AVB sepharose-purified AAV preparations. Capsid-released AAV genomes were quantified by Light-Cycler PCR, and 1×10^7 gp were loaded per lane of a 0.8% agarose gel. AAV vector genomes were hybridized for 48 hr with a 0.7 kb GFP-specific probe labeled with biotin-11-dUTP according to the manual of the DecaLabel DNA Labeling Kit (Fermentas), incubated for 20 min with horseradish-peroxidase-conjugated streptavidin (1:10,000), and detected by ECL (Pierce) (Winter *et al*., 2012).

Protein analysis

Western blot analysis was performed as described (Winter *et al*., 2012) using 1:10 dilutions of hybridoma supernatants monoclonal antibody (mAb) B1 (anti-VP1–3), mAb A1 (anti-VP1), or mAb 303.9 antibody (anti-Rep) (Wistuba *et al*., 1995, 1997). For quantitative Western blot analysis, near-infrared dye-labeled antimouse secondary antibodies were used. Signals were quantified with an Odyssey imager (Licor). For silver-staining gels, purified rAAV preparations, corresponding to 10^{10} gp, were lysed and gel-separated as described (Winter *et al*., 2012).

Native immuno-dot blot

Dilutions ranging from 10^{10} gp down to 10^8 gp of purified rAAVs of serotypes 1–12 were spotted onto nitrocellulose membranes and fixed in a dot-blot apparatus. The membranes were probed with antibodies specific for conformational epitopes on intact AAV particles of particular serotypes as described (Wistuba *et al*., 1997; Kuck *et al*., 2007; Sonntag *et al*., 2010, 2011). Hybridoma supernatants were used at the following dilutions: ADK1a (1:200), A20 (1:10), ADK4 (1:10), ADK5a (1:50), ADK6 (1:10), ADK8 (1:10), and ADK9 (1:10). Polyclonal rabbit antibody VP51 was used at a 1:200 dilution (Kuck *et al*., 2007; Sonntag *et al*., 2011). The membranes were incubated with an antimouse IgG horseradish-peroxidase-linked secondary antibody (1:2,500) and visualized by ECL (PromoKine).

Electron microscopy

High-performance liquid chromatography (HPLC)-purified rAAVs (5 μl) of serotype 1, 2, 5, or 8, were loaded onto carbon-coated copper EM grids (Ted Pella Inc.; cat. no. 01754-f) for 2 min, blotted with filter paper, and negatively stained with 5 μl of 2% uranyl acetate for 20 sec. The grids were air-dried and examined in an FEI-Spirit transmission electron microscope, operating at an accelerating voltage of 120 kV, at a magnification of 90,000.

Evaluation of transduction efficiency using fluorescence-activated cell sorting analysis

HeLa C12 cells were transduced by rAAV-GFP at MOI = 1,000 (gp) and superinfected with adenovirus type 2 at MOI = 10 (infectious titer). Cells were harvested at 48 hr posttransduction, washed with PBS, and fixed with 4% formaldehyde in PBS. For fluorescence-activated cell sorting (FACS) analysis, 100,000 cells per sample were counted. The proportion of GFP-positive cells was determined according to the manufacturer's protocol (Becton & Dickinson; FACS Calibur). Cells exceeding the cutoff of 30 in the FL1-H channel were counted as positive.

Results

Generation of Sf9 cell lines carrying integrated AAV rep *and* cap *genes*

To extend the production range of rAAV serotypes, *Sf9* cell lines were generated that carry integrated copies of AAV serotype *cap* genes combined with either AAV2 *rep,* or AAV4 *rep* or -12 *rep* in the case of rAAV4 or -12 production, as shown before for rAAV production by plasmid transfection in 293 cells (Grimm *et al*., 2003; Schmidt *et al*., 2008) (Fig. 1A). The start codon for VP1 was mutated to ACG to allow sufficient expression of VP2 and VP3 from the downstream start codons ACG (VP2) and ATG (VP3), a strategy proven useful for AAV2 and -1 *cap* expression (Urabe *et al*., 2002; Aslanidi *et al*., 2009). For selection of *rep/cap*-expressing cell clones, up to 50 single-cell clones per AAV serotype were isolated from transfected *Sf9* cells grown in blasticidin and screened for Bac-induced rAAV production using Bac-rAAV-GFP. rAAV titers were quantified in cleared supernatants as benzonase-resistant gp per

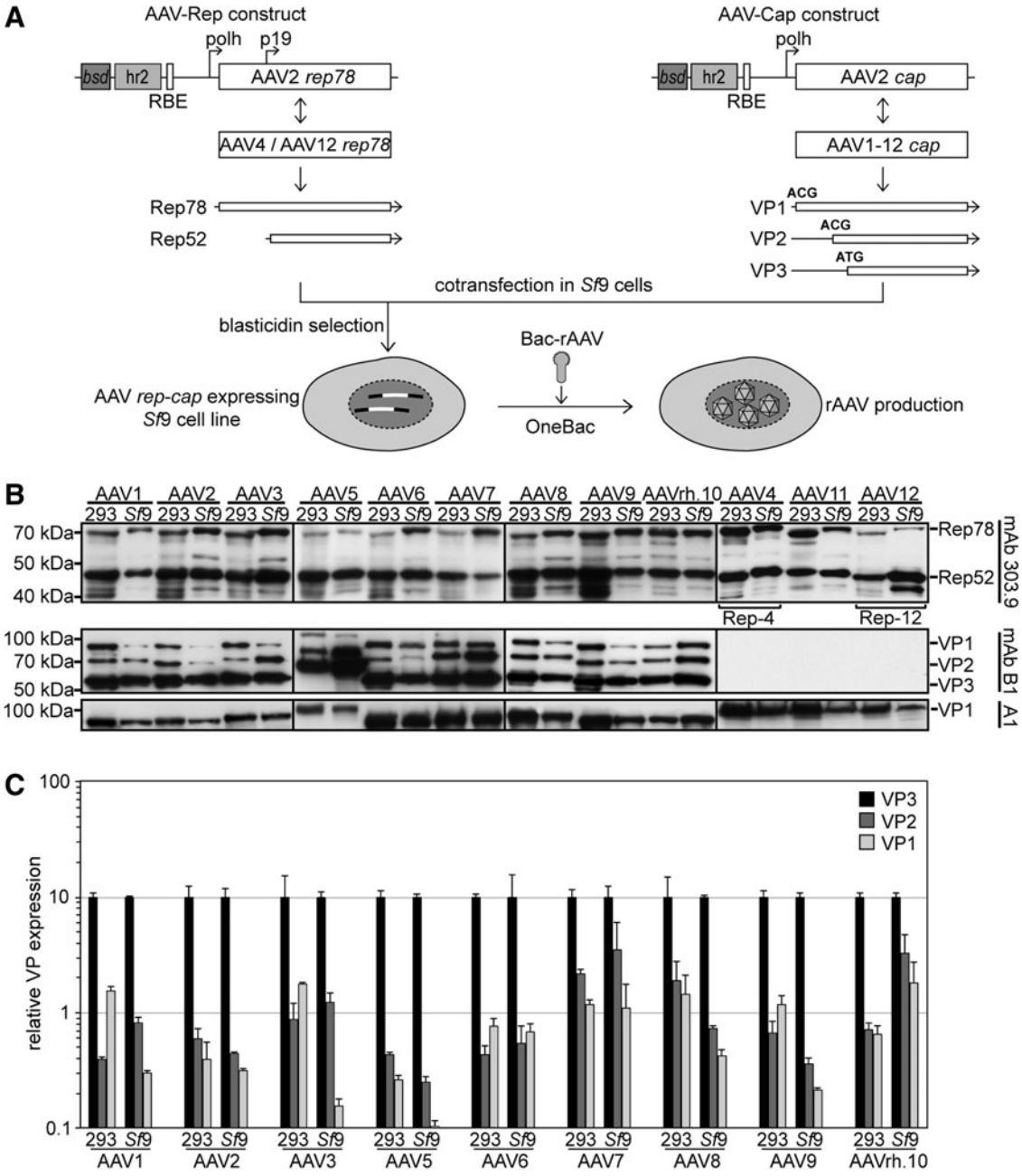

FIG. 1. Generation of OneBac: AAV1–12 *rep/cap* carrying *Sf9* cell lines and their baculovirus-induced expression profiles. **(A)** Plasmid pIR-rep78-hr2-RBE expressing *rep* of AAV2 (AAV-Rep construct) and the derivatives for AAV4 or AAV12 *rep* are depicted with the expressed proteins Rep78 and Rep52. Plasmid pIR-VP-hr2-RBE expressing *cap* of AAV2 (AAV-Cap construct) and the derived plasmids for *cap* of AAV serotypes 1–12 are depicted. The expressed proteins VP1 and VP2 start with an ACG codon and VP3 starts from an internal ATG. AcMNPVhr2, *Autographa californica* multiple nuclear polyhedrosis virus homologous region 2; bsd, blasticidin S deaminase; polh, baculovirus polyhedrin promoter; RBE, Rep-binding element (AAV2). **(B)** AAV serotype-dependent Rep- and Cap expression was analyzed by Western blot analysis of cell extracts harvested in parallel to rAAV production. Cell extracts from 293 cells were analyzed 72 hr posttransfection of the packaging plasmids. Equivalents of 5×10^4 293 cells were loaded per well. Cell extracts from *rep/cap*-expressing *Sf*9 cells were prepared 72 hr p.i. with the recombinant Bac-rAAV at an MOI = 5. For *Sf*9 cells, an equivalent of $1–2 \times 10^4$ cells were loaded per well. Rep proteins were detected by mAb 303.9, initially generated for AAV2 Rep, but also detecting Rep of AAV4 and AAV12. VP proteins expressed from AAV serotype-specific *cap* genes were reacted with mAb B1, which detects all three capsid proteins of most AAV serotypes with the exception of AAV4, -11, and -12. mAb A1 binds to VP1 of all serotypes. **(C)** Cell extracts from three independent rAAV preparations for each serotype were analyzed by quantitative Western blot analysis to compare the ratios of VP1, VP2, and VP3 expressed in 293 or *Sf*9 cells, respectively. VP proteins expressed in either cell type were analyzed by mAb B1 and a secondary antibody emitting near-infrared fluorescence as quantified by an Odyssey imager (Licor). Expression levels of VP3 were arbitrarily set to 10, and expression levels of VP2 and VP1 were calculated as relative values thereof. The results of three experiments are given as mean ± standard deviation. Please note the logarithmic scale of the *y*-axis. AAV, adeno-associated virus; mAb, monoclonal antibody; MOI, multiplicity of infection; p.i., postinfection; rAAV, recombinant AAV.

cell. The most efficient producer cell lines for each serotype were expanded for further testing.

AAV rep *and* cap *expression in Sf9 cell lines compared with plasmid-transfected 293 cells*

To compare Bac-induced rAAV *rep* and *cap* expression patterns in *Sf9* cell clones with those of plasmid-transfected 293 cells, the most widely used method for laboratory-scale rAAV production, cell extracts were analyzed side by side on Western blots (Fig. 1B). Rep showed comparable expression of Rep78 and Rep52 in Bac-infected *Sf9* cell lines and plasmid-transfected 293 cells as detected by mAb 303.9 (Fig. 1B, upper panel). *Sf9* cells were designed to express Rep78 and Rep52, but most of them appeared to also express small amounts of Rep68 and/or Rep40 similar to 293 cells. Expression patterns of *cap* analyzed by mAb B1 (VP1–3) (Wistuba *et al*., 1995) and mAb A1 (VP1) (Wistuba *et al*., 1997) were comparable among different serotypes and also between insect cells and 293 cells. This includes previously described variations in mobility, as in the case of AAV5 (Fig. 1B, mAb B1; A1) (Kohlbrenner *et al*., 2005). For wild-type AAV2, the ratio of VP1:VP2:VP3 was originally described as 1:1:10 (Becerra *et al*., 1988). VP1 is critical, since it comprises a phospholipase domain, which is required for AAV infectivity (Sonntag *et al*., 2006). Fluorescence intensity of the respective bands was quantified with near-infrared spectrometry. As depicted in Fig. 1C, most AAV serotypes expressed VP1:VP2:VP3 close to the prototypic 1:1:10 ratio.

AAV vector yield in Sf9 cells compared with 293 cells

The major advantage of rAAV production in *Sf9* cells is that the cells can grow in suspension culture to high densities and thus allow scale-up for rAAV production in bioreactors as required for clinical-scale production. Without extensive efforts to optimize growth conditions, rAAV preparations could be scaled up to 1-liter suspensions with rAAV yields of up to 2×10^{14} gp/liter. Using small-scale culture formats, the burst sizes (rAAV yields per cell) were compared in triplicate 30 ml cultures of *Sf9* cells and plasmid-transfected 293 cells (6 cm dishes). rAAV titers were quantified as gp per cell in benzonase-treated, cleared freeze–thaw supernatants of cells and medium (Fig. 2A). At this point, neither *Sf9*- nor 293 cell-based AAV production protocols were optimized as commonly done for large-scale, clinical-grade production (Lock *et al*., 2010). For the majority of AAV serotypes, vector yields per cell in *Sf*9 cells exceeded those of 293 cells, ranging from almost similar yields in case of AAV2 and AAV11 to up to 100-fold higher yields in the case of AAV3 and AAVrh.10. Only *Sf9* cells producing AAV12 yielded lower titers compared with those in 293 cells. The previously described *Sf*9 cell lines for AAV2 and AAV1 reproduced the reported high rAAV yields after numerous cell passages over several years without selection (Aslanidi *et al*., 2009). rAAV production stability of the newly generated *Sf9*-AAV8 and *Sf9*-AAV9 cell lines was therefore also tested after serial passages at high dilutions of 1:10 for 10 successive passages, with or without blasticidin selection. After passage 10, rAAV yields (gp) per cell were determined and compared with the starting rAAV yields (passage 0). As can be seen in Fig. 2B, rAAV yields remained stable, even in the absence of selection. This further underscores the stability of the *Sf9* producer cells, a prerequisite for successive scale-up. Comparative analysis of the integrity of packaged vector genomes from AVB sepharose-purified vector preparations by Southern blot hybridization showed intact AAV ssDNA and reassociated dsDNA genomes for *Sf*9- and 293-cell derived AAV vectors (Fig. 2C). To evaluate whether potentially replication-competent AAVwt was generated during the production process, quantitative PCR of packaged genomes was performed with primers spanning the *rep/cap* gene region (Supplementary Table S1). As displayed in Fig. 2D, purified rAAV1, -2, or -8 prepared from *Sf*9 cells displayed significantly reduced levels of packaged *rep/cap* sequences compared with vectors prepared in 293 cells. Comparable or higher percentages of packaged AAV2 *rep* or *cap* genes had been reported before (Nony *et al*., 2003; Martin *et al*., 2013). It is well established that AAV preparations also contain variable, low proportions of host cell or plasmid-derived DNA sequences (Hüser *et al*., 2003; Chadeuf *et al*., 2005). In summary, most *Sf9* cell-derived AAVs show higher burst sizes and improved purity of packaged rAAV genomes, when compared with AAVs from 293 cells.

Integrity of AAV capsids produced in Sf9 cells

To analyze the capsid composition and integrity of AAV vectors prepared from *Sf*9 cells, large-scale rAAV preparations from 1 liter of *Sf9* cell suspensions were highly purified by HPLC using AVB sepharose chromatography for all serotypes except for AAV9 and AAV11. These were refractory to HPLC purification and were therefore purified by sucrose gradient centrifugation (Mitchell *et al*., 2009). rAAV titers of the peak fractions exhibited genomic titers between 4×10^{12} and 7×10^{13} gp/ml. The resulting rAAVs of serotypes 1–12 were analyzed with a series of antibodies specific for conformational epitopes present on the surfaces of intact AAV capsids as described for rAAVs purified from transfected 293 cells (Wistuba *et al*., 1997; Kuck *et al*., 2007; Sonntag *et al*., 2010) (Fig. 3A). Since the proportions of genome-containing (gp) to physical (empty) particles are expected to vary among serotypes, equal amounts of gp of the purified rAAV preparations were also separated on a polyacrylamide gel, and the VP1–3 bands visualized by silver staining (Fig. 3B). Intact, background-free VP1–3 bands were detected for all HPLC-purified AAVs. Sucrose-banded AAV-9 and AAV11 displayed more background, as expected. Furthermore, the morphologies of rAAVs prepared in Bac-infected *Sf9* and plasmid-transfected 293 cells were compared by transmission electron microscopy of highly purified AAV vector preparations of serotypes 1, 2, and 8. Clusters of uniform, icosahedral capsids with a diameter of $\sim$25 nm characteristic of AAV were observed (Fig. 3C). There were no discernible differences between the capsids produced in *Sf9* and 293 cells, respectively.

Transduction efficiencies of Sf9- and 293-derived AAV vectors

Functional validation of gene therapy vectors commonly scores the efficiency of gene transfer through analysis of successful expression of the gene of interest. Since capsids of variant AAV serotypes target specific cell types, the absolute transduction efficiencies vary markedly depending on

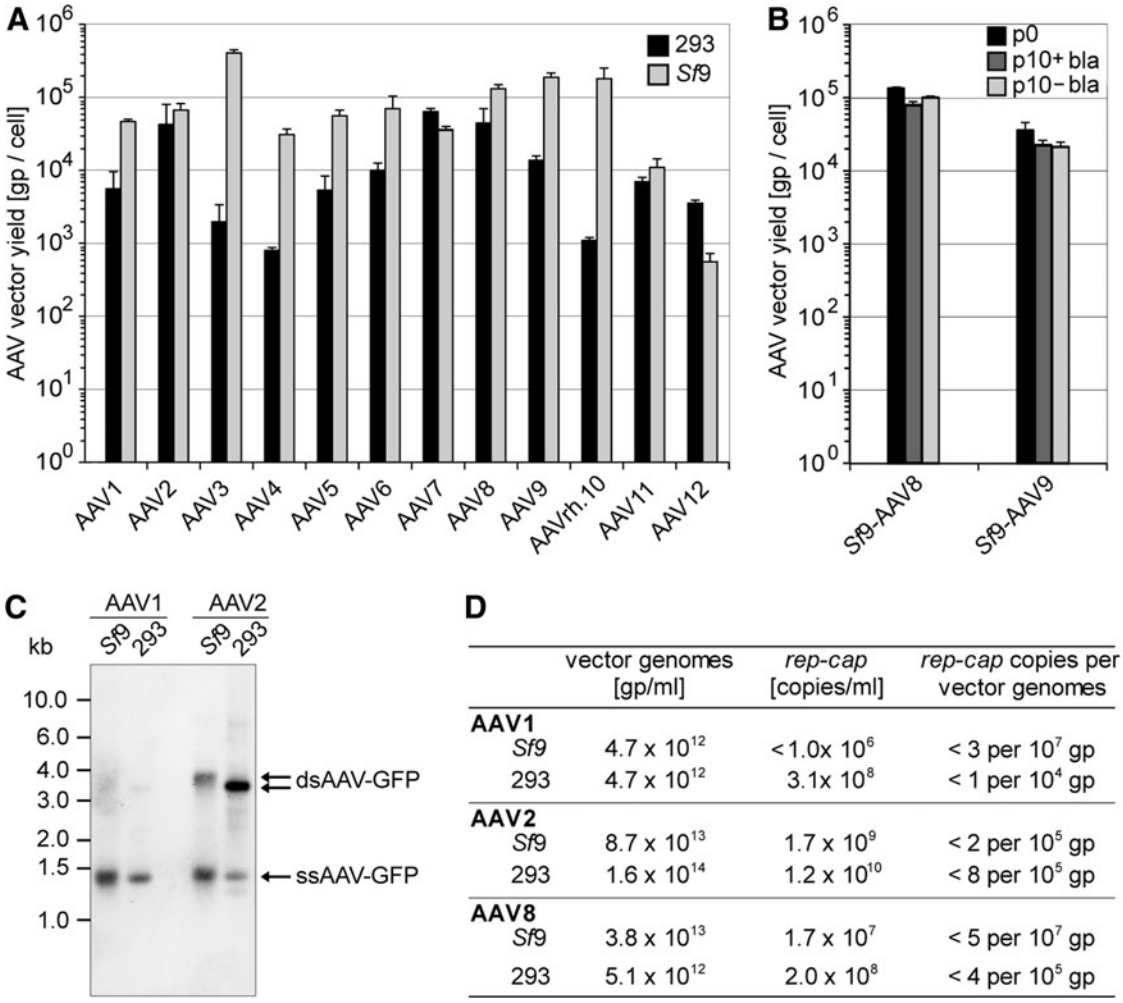

D

	vector genomes [gp/ml]	*rep-cap* [copies/ml]	*rep-cap* copies per vector genomes
AAV1			
*Sf*9	4.7×10^{12}	$< 1.0 \times 10^{6}$	< 3 per 10^7 gp
293	4.7×10^{12}	3.1×10^{8}	< 1 per 10^4 gp
AAV2			
*Sf*9	8.7×10^{13}	1.7×10^{9}	< 2 per 10^5 gp
293	1.6×10^{14}	1.2×10^{10}	< 8 per 10^5 gp
AAV8			
*Sf*9	3.8×10^{13}	1.7×10^{7}	< 5 per 10^7 gp
293	5.1×10^{12}	2.0×10^{8}	< 4 per 10^5 gp

FIG. 2. Burst sizes and integrity of AAV1–12 vectors produced in 293 cells compared with *Sf9* cells. **(A)** The yields of rAAV1–12 preparations were quantified as benzonase-resistant genomic particles (gp) per cell by LightCycler PCR using rAAV genome-specific primers. Benzonase-treated freeze–thaw supernatants were prepared 72 hr posttransfection of 293 cells or infection of *Sf*9 cells, respectively. rAAV burst sizes of three experiments are displayed as mean ± standard deviation. Please note the logarithmic scale of the *y*-axis. **(B)** Analysis performed similar to **(A)**. The burst sizes of rAAVs from AAV8 and -9 *Sf*9 producer cell lines after serial passages with or without blasticidin selection were quantified at passage 0 (p0) and passage 10 (p10 ± basticidin). **(C)** Southern blot analysis of vector genomes from AVB sepharose-purified AAV1 and -2 vector preparations. Vector genomes are detected by a biotin-labeled probe specific for GFP. The size of the packaged rAAV genomes varies between *Sf*9- (pTR-UF26: 3,794 bp) and 293-cell-derived (pTR-UF5: 3,388 bp) vectors. The arrows point to ssDNA and dsDNA AAV genomes that are detected because of partial reassociation of packaged (+) and (−) strand genomes. **(D)** Quantitative analysis of the AAV vector genomes (vg) and copackaged wild-type *rep/cap* sequences of AAV1, -2, and -8.

the target cell line. We therefore decided to compare only cell transduction of identical amounts of gp from the same AAV serotype produced in 293 and in *Sf9* cells. As target cells, we chose C12 cells (Clark *et al*., 1996), which express integrated AAV2*rep/cap* and replicate transduced rAAVs after Ad2 infection, thereby boosting expression of GFP levels even in the case of low transduction efficiency. Using FACS analysis as displayed in Fig. 4A, for each serotype, the percentage of GFP-positive cells after transduction of *Sf9*-derived rAAV-GFP was compared with that of 293 cell-derived rAAV-GFP. The transduction efficiencies of the latter were arbitrarily set to 1.0. The analysis was performed for rAAV preparations from cleared freeze–thaw supernatants (Fig. 4B), and also for a selection of AAV serotypes purified by HPLC-AVB column chromatography (Fig. 4C). Irrespective of the degree of purification, AAV transduction efficiencies of *Sf*9-derived vectors were mostly comparable with those of 293 cell-derived vectors, with minor 2–3-fold variance (Fig. 4B and C). *Sf*9-derived rAAV4 and rAAV5 transduced at a 10-fold reduced rate compared with vectors of the same serotype produced in 293 cells (Fig. 4B and C). This effect is compensated by more than 10-fold higher burst sizes in *Sf9* compared with 293 cells (Fig. 2A). In all cases where the analysis of vectors from cleared extracts was repeated with HPLC-purified preparations, that is, AAV1, -2, -5, and -8, the observed differences in transduction remained similar. Transduction efficiencies of rAAV1, -2, -3, -6, -8, -9, and -rh.10 were also analyzed in HEK 293 cells, confirming the above results (data not shown). In summary, AAV vectors prepared and purified from the majority of newly generated

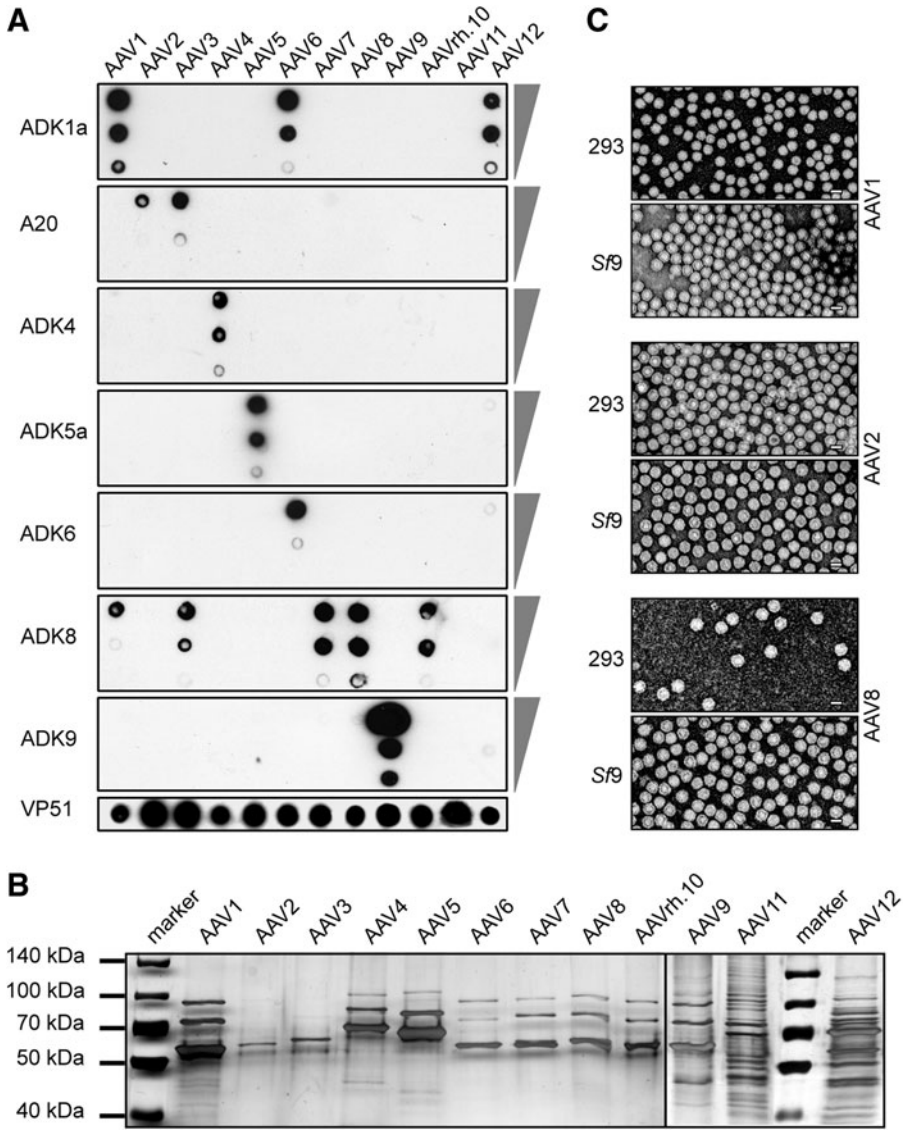

FIG. 3. Comparative capsid analysis of AAV serotypes 1–12 generated in 293 or *Sf9* cells. **(A)** Immuno-dot blot analysis of native rAAV capsids of the panel of AAV serotypes 1–12. All rAAV subtypes were purified by AVB chromatography except for rAAV9 and rAAV11, which were purified by sucrose gradient centrifugation. About 10^{10}, 10^{9}, and 10^{8} gp of serotype-specific rAAVs were spotted on a nitrocellulose membrane as indicated by the triangles to the right of the panels. The membranes were incubated with a panel of mAbs as depicted to the left of the membrane. Each mAb detects specific conformational epitopes on the surface of defined AAV capsids. Polyclonal antibody VP51 detects all AAV serotypes and served as an internal loading control for 10^{9} gp of each rAAV serotype. **(B)** Silver-staining gel analysis of the rAAV preparations used in **(A)** separated on 9% sodium dodecyl sulfate polyacrylamide gel electrophoresis with 10^{10} gp loaded per lane. **(C)** Electron microscopic analysis of negative-stained rAAV-GFP vectors of AAV serotypes 1, 2, and 8 generated from either transfected 293 cells or baculovirus-infected *Sf*9 cells. AAV vectors were highly purified by AVB chromatography. Titers ranged between 3×10^{12} and 4×10^{13} gp/ml. Scale bar = 25 nm.

Sf9 cell lines transduce comparably well as vectors produced in plasmid-transfected 293 cells.

Discussion

For bioreactor-size rAAV production, high-titer, scalable, and genetically stable systems are required to keep pace with the rapid increase of rAAV application in the clinic. The extended range of AAV serotypes currently being introduced for transduction of particular cell types or tissues requires the uncomplicated transfer of AAV production systems to novel AAV serotypes. Here we show the development of OneBac, a platform comprising a series of genetically stable insect *Sf9* cell lines that allow single Bac-induced, scalable production of the full range of AAV serotype 1–12 vectors. The described methods for cell line generation can be transferred to novel AAV serotypes to come. Moreover, existing Bac-rAAV recombinants developed for the three- or two-Bac infection system (Urabe *et al*., 2002; Smith *et al*., 2009) can be directly employed without modifications. The key features of OneBac are (i) high-titer, scalable production of an extended range of AAV serotypes; (ii) high infectivity-to-particle ratios of rAAVs produced in Bac-infected *Sf9* cell lines; (iii) high stability of *rep/cap*-carrying *Sf9* cell lines with undiminished Bac-induced rAAV burst sizes upon serial cell passage.

Composition and VP ratios of AAV capsids

Ever since rAAV production systems have been designed, obtaining the correct stoichiometry of VP1:VP2:VP3 has been a challenge. The strategy of wild-type AAV2 relies on the use of overlapping and partially spliced ORFs combined with the use of ACG as noncanonical start codon for VP2 translation. This is maintained in the pDG/pDP series (Grimm *et al*., 2003) of plasmids for AAV production in transfected 293 cells, but is difficult to mimic in insect cells. Because of the limited functionality of mammalian introns, the unmodified *cap* ORF would predominantly lead to VP1 expression. In wild-type AAV2, the ratio of VP1–3 proteins was originally determined as 1:1:10 (Becerra *et al*., 1988), which approximates to 3–6 VP1 molecules per capsid (Excoffon *et al*., 2009). To maintain the wild-type capsid composition, reduced but sufficient VP1 expression is critical, which was achieved

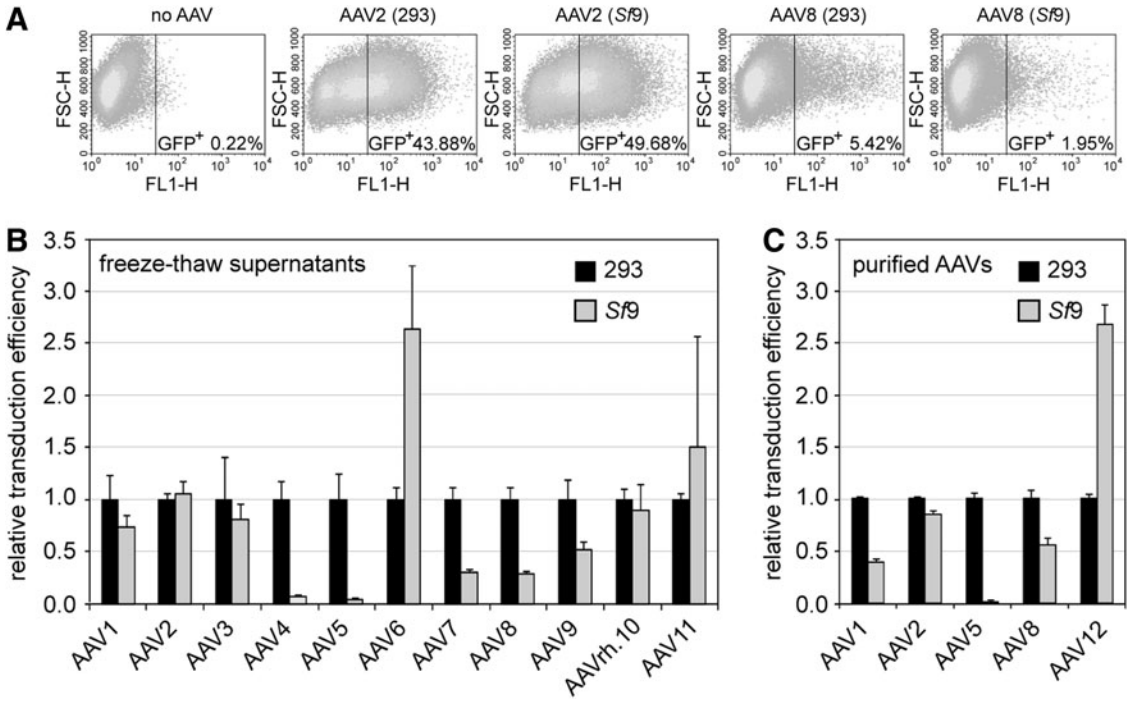

FIG. 4. Cell transduction efficiencies of rAAV serotype 1–12 vectors produced in 293 cells compared with *Sf9* cells. The transduction efficiencies of rAAV-GFP vectors of various serotypes derived from either 293 or *Sf*9 cells, respectively, were compared. AAV2 *rep/cap*-expressing HeLa C12 cells were transduced with 1,000 gp of rAAV-GFP vector of the chosen serotype. Cells were coinfected with adenovirus type 2 at an MOI of 10 (infectious titer). At 48 hr p.i., cells were harvested and the percentage of GFP-positive cells was determined by FACS analysis (GFP^+: FL1-H >30). **(A)** FACS read-outs displaying the transduction efficiencies for rAAV vectors of serotype 2 and produced either in 293 cells or in *Sf*9 cells. Control cells (designated ''no AAV'') were infected with adenovirus only. **(B)** Comparative analysis of the transduction efficiencies of rAAV vectors with serotype 1–11 capsids derived from freeze–thaw supernatants. The various AAV serotypes display variable absolute transduction efficiencies in C12 cells. To compare transduction efficiencies for each serotype, transduction of rAAVs prepared in 293 cells was set to 1.0. The transduction efficiency of rAAV vectors derived from *Sf*9 cells from the same serotype is displayed as percentage thereof. The experiments were performed in triplicates and are displayed as mean ± standard deviation ($n=3$). **(C)** Analysis of rAAV-1, -2, -5, -8, and -12 transduction as described in **(B)**, except that highly purified (AVB-column) rAAV vectors were used. FACS, fluorescence-activated cell sorting.

by mutating the VP1 ATG start codon to ACG (Aslanidi *et al*., 2009). The resulting capsid protein ratios are close to those seen for prototype AAV2. Burst sizes in *Sf9* cells are mostly higher than in 293 cells and correlate with infectivity. AAV5 produced in *Sf9* cells is an exception with calculated mean VP1 levels of one per capsid, which is obviously not sufficient for full infectivity. Insufficient VP1 levels resulting in reduced rAAV transduction rates have previously been described for AAV5 and AAV8 capsids generated from Bac-*cap* constructs that also used an ACG start codon for VP1 expression (Kohlbrenner *et al*., 2005; Urabe *et al*., 2006). Reduced AAV5 infectivity is compensated by increased burst sizes, making the *Sf9* cell line proficient for scale-up production. Alternative expression strategies for AAV5 *cap* may be considered to further improve *Sf9* AAV5 producer cells to decrease the ratio of noninfectious AAV5 vectors.

rAAV burst sizes and particle to infectivity ratios in Sf9 produced rAAV 1–12

The burst sizes for the majority of rAAV serotypes in *Sf9* cells are at least one log higher than those of 293 cells except for recently discovered AAV12 (Schmidt *et al*., 2008). In the case of AAV12, the increased infectivity almost compensates the reduced burst size. To generate the respective *Sf9* cells, the AAV12 *rep* gene instead of that of AAV2 was expressed. In the absence of data on AAV12-derived Rep interaction with the AAV2 ITR, the reduced replication efficiency is not that surprising. Exchange of either *rep* or the RBE may improve burst sizes. All cell lines produced reproducible burst sizes upon successive cell passages, and AAV particle-to-infectivity ratios remained similarly high as those described for 293 cells.

Comparison of scalable rAAV production systems

Production of AAV vectors has long been a challenge. Whereas AAV's high physicochemical stability has allowed the development of sophisticated downstream purification schemes leading to near-homogeneous, stable AAV vector preparations, the upstream scale-up is more demanding. The ideal rAAV production system leads to high vector burst sizes per cell of highly infectious virus stocks. To render a system proficient for production in bioreactors, additional aspects have to be considered: (i) simplicity of scale-up, (ii) modest requirements for cell growth, (iii) efficacy of gene transfer combined with (iv) genetic stability of the components, and (v) flexibility to adapt to an increasing range of AAV serotypes and variants thereof.

The first AAV production systems to be developed consisted of AAV2 producer cell lines of various formats harboring the required components for AAV production to be induced upon adenovirus infection as reviewed by Zolotukhin (2005). Since Rep78 is cell toxic, strict silencing of *rep* is required in the noninduced state. The best-studied producer cell format was generated by extensive multiple-round selection of cell lines with integrated high copy numbers of rAAV and p5-promoter-driven *rep/cap*. *Rep* silencing in the absence of adenovirus infection appears to be mediated by Rep-mediated negative feedback, as is the case in AAV latency. The AAV2 producer cell system has recently been further optimized to yield 5×10^4 to 2×10^5 DNAse-resistant particles per cell (Martin *et al*., 2013). However, new cell lines have to be constructed for every new vector to be produced. It will be seen how readily the system is adaptable to alternative serotypes or novel vectors.

Production of rAAV by plasmid cotransfection of adherent 293 cells (Grimm *et al*., 1998, 2003; Xiao *et al*., 1998) leads to high burst sizes and infectivity rates for virtually all AAV serotypes tested so far. Mammalian 293 cells are robust, and plasmid DNA transfection is a standard technique in research laboratories. The genetic stability of the plasmids and the ease of swapping AAV *rep* and *cap* genes or domains thereof by standard cloning technology have made this system a laboratory standard for rAAV research. Its major limitations are scalability and effectiveness of gene transfer. HEK-293 cells do not grow well in suspension, and plasmid cotransfection is troublesome in suspension cells.

The need for plasmid transfection was overcome when HSV infection-based rAAV production systems were developed. There, AAV's requirement for helper HSV functions is exploited by construction of rHSV strains, one harboring the AAV *rep/cap* cassette, and another harboring the rAAV vector genome (Conway *et al*., 1999; Kang *et al*., 2008). Scalability was achieved by adapting rAAV production to HSV infection of BHK cells grown in suspension. The range of rHSV/AAV recombinants comprises rAAV serotypes 1, 2, 5, 8, and 9 (Clement *et al*., 2009; Thomas *et al*., 2009). Although expression from the integrated *rep* gene modestly inhibits HSV replication (Heilbronn *et al*., 2003), rHSVs are genetically stable and lead to rAAV burst sizes of around 8×10^4 DNAse-resistant particles per cell (Thomas *et al*., 2009).

The insect *Sf9* cell-based rAAV production system, first developed by the Kotin group (Urabe *et al*., 2002; Virag *et al*., 2009), exploits the ease of growth and scalability of *Sf9* cells. *Sf9* cells grow in suspension not only to high densities but also at modest growth requirements. Compared with mammalian cells, simple culture media without FCS and growth at 27°C without need for CO_2 are sufficient. Furthermore, only insect cells offer the possibility to grow rAAVs expressing proteins toxic to mammalian cells (Chen, 2012). Gene transfer by Bac infection *per se* is efficient. However, separate propagation of three Bac strains, Bac-*rep*, Bac-*cap*, and Bac-rAAV, before coinfection at individually optimized MOI ratios reduces effectiveness. Most importantly, Bac-*rep* and Bac-*cap* helpers are genetically unstable. As a consequence, Rep/Cap expression drops upon more than six successive Bac passages (Kohlbrenner *et al*., 2005; Smith *et al*., 2009; Virag *et al*., 2009). The introduction of artificial introns for collinear Rep and Cap expression appears to improve stability, but the necessity for coinfection with three separate Bac strains remains (Chen, 2008). An additional improvement was the combination of *rep* and *cap* into one Bac, thus reducing the number Bac strains to two and extending the number of stable virus passages to seven (Smith *et al*., 2009). The initial three-Bac coinfection system was developed for AAV2, leading to burst sizes of 5×10^4 gp per cell (Urabe *et al*., 2002). AAV serotypes 1, 6, 8, and 9 followed with burst sizes reported between 7×10^3 and 2×10^4 gp per cell (Cecchini *et al*., 2011; Galibert and Merten, 2011).

The here-described most recent development of Bac-based rAAV production systems reduces the number of Bac strains to the one that carries the rAAV backbone. AAV *rep* and *cap* are stably integrated in the genome of the host *Sf9* insect cell but transcriptionally silent. As described before, infection with a single Bac leads to amplification and expression of *rep* and *cap* to levels sufficient for effective rAAV replication and packaging (Aslanidi *et al*., 2009). The resulting burst sizes of up to 5×10^5 benzonase-resistant rAAV genomes per cell exceed those of competitive production systems. The *Sf9-rep/cap* producer cells for AAV1–12 are genetically stable even in the absence of blasticidin, used initially for cell selection. *Sf9-rep/cap* producer cells can be grown and passaged similar to unmodified *Sf9* cells. The OneBac system requires only a single Bac, Bac-rAAV, which can infect over 95% of *Sf9* cells at a typical MOI of 3. Bac-rAAVs constructed for the two- or three-Bac *Sf9* production system can be immediately transferred to the OneBac system, to produce rAAVs with the panel of AAV1–12 *rep/cap* packaging cells. These share the convenience of cell growth and upscaling capabilities of unmodified *Sf9* cells. The major advance of OneBac for rAAV production lies in the combination of the high genetic stability of *Sf9 rep/cap* producer cells, and the simplicity of infection with a single virus. These features, combined with the here-described versatility in the construction of novel AAV serotype-specific *Sf9* cell lines, make the new OneBac system readily applicable for bioreactor-scale rAAV production.

Acknowledgments

The authors thank Jürgen Kleinschmidt and Martin Müller (German Cancer Research Center, Heidelberg, Germany) for the series of mAbs directed against AAV capsids and for pDG/pDP-plasmids, and John Chiorini (National Institutes of Health, Bethesda, MD) and Tadahito Kanda (National Institute of Infectious Diseases, Tokyo, Japan) for plasmids for AAV10, -11, and -12. The authors also thank Kerstin Winter for advice with HPLC-based AAV purification, Kristina von Kietzell for help with FACS, and Catrin Stutika for critical reading of the manuscript (Charité, Berlin, Germany). This project was partially funded by a grant from the German Academic Exchange Service, DAAD (Promos program), and by NIH R01 AI1081961.

Author Disclosure Statement

M.A.-M., N.M., S.Z., and R.H. are inventors of patents related to rAAV technology; S.Z. is inventor in a pending patent on the inducible insect cell-based system for highly efficient production of rAAV vectors (US 20120100606); N.M. and R.H. own equity in a company that is commercializing AAV for gene therapy.

References

Aslanidi, G., Lamb, K., and Zolotukhin, S. (2009). An inducible system for highly efficient production of recombinant adeno-associated virus (rAAV) vectors in insect Sf9 cells. Proc. Natl. Acad. Sci. USA 106, 5059–5064.

Becerra, S.P., Koczot, F., Fabisch, P., *et al.* (1988). Synthesis of adeno-associated virus structural proteins requires both alternative mRNA splicing and alternative initiations from a single transcript. J. Virol. 62, 2745–2754.

Berger, I., Fitzgerald, D.J., and Richmond, T.J. (2004). Baculovirus expression system for heterologous multiprotein complexes. Nat. Biotechnol. 22, 1583–1587.

Cecchini, S., Virag, T., and Kotin, R.M. (2011). Reproducible high yields of recombinant adeno-associated virus produced using invertebrate cells in 0.02- to 200-liter cultures. Hum. Gene Ther. 22, 1021–1030.

Chadeuf, G., Ciron, C., Moullier, P., *et al.* (2005). Evidence for encapsidation of prokaryotic sequences during recombinant adeno-associated virus production and their *in vivo* persistence after vector delivery. Mol. Ther. 12, 744–753.

Chen, H. (2008). Intron splicing-mediated expression of AAV Rep and Cap genes and production of AAV vectors in insect cells. Mol. Ther. 16, 924–930.

Chen, H. (2012). Exploiting the intron-splicing mechanism of insect cells to produce viral vectors harboring toxic genes for suicide gene therapy. Mol. Ther. Nucleic Acids 1, e57.

Clark, K.R., Voulgaropoulou, F., and Johnson, P.R. (1996). A stable cell line carrying adenovirus-inducible rep and cap genes allows for infectivity titration of adeno-associated virus vectors. Gene Ther. 3, 1124–1132.

Clement, N., Knop, D.R., and Byrne, B.J. (2009). Large-scale adeno-associated viral vector production using a herpesvirus-based system enables manufacturing for clinical studies. Hum. Gene Ther. 20, 796–806.

Conway, J., Rhys, C., Zolotukhin, I., *et al.* (1999). High-titer recombinant adeno-associated virus production utilizing a recombinant herpes simplex virus type I vector expressing AAV-2 rep and cap. Gene Ther. 6, 986–993.

Excoffon, K.J., Koerber, J.T., Dickey, D.D., *et al.* (2009). Directed evolution of adeno-associated virus to an infectious respiratory virus. Proc. Natl. Acad. Sci. USA 106, 3865–3870.

Galibert, L., and Merten, O.W. (2011). Latest developments in the large-scale production of adeno-associated virus vectors in insect cells toward the treatment of neuromuscular diseases. J. Invertebr. Pathol. 107 Suppl, S80–S93.

Gao, G.P., Alvira, M.R., Wang, L., *et al.* (2002). Novel adeno-associated viruses from rhesus monkeys as vectors for human gene therapy. Proc. Natl. Acad. Sci. USA 99, 11854–11859.

Gao, G., Alvira, M.R., Somanathan, S., *et al.* (2003). Adeno-associated viruses undergo substantial evolution in primates during natural infections. Proc. Natl. Acad. Sci. USA 100, 6081–6086.

Grimm, D., Kern, A., Rittner, K., *et al.* (1998). Novel tools for production and purification of recombinant adenoassociated virus vectors. Hum. Gene Ther. 9, 2745–2760.

Grimm, D., Kay, M.A., and Kleinschmidt, J.A. (2003). Helper virus-free, optically controllable, and two-plasmid-based production of adeno-associated virus vectors of serotypes 1 to 6. Mol. Ther. 7, 839–850.

Heilbronn, R., Engstler, M., Weger, S., *et al.* (2003). ssDNA-dependent colocalization of adeno-associated virus Rep and herpes simplex virus ICP8 in nuclear replication domains. Nucleic Acids Res. 31, 6206–6213.

Hüser, D., Weger, S., and Heilbronn, R. (2003). Packaging of human chromosome 19-specific adeno-associated virus (AAV) integration sites in AAV virions during AAV wild-type and recombinant AAV vector production. J. Virol. 77, 4881–4887.

Kang, W., Wang, L., Harrell, H., *et al.* (2008). An efficient rHSV-based complementation system for the production of multiple rAAV vector serotypes. Gene Ther. 16, 229–239.

Kastelein, J.J., Ross, C.J., and Hayden, M.R. (2013). From mutation identification to therapy: discovery and origins of the first approved gene therapy in the Western world. Hum. Gene Ther. 24, 472–478.

Kohlbrenner, E., Aslanidi, G., Nash, K., *et al.* (2005). Successful production of pseudotyped rAAV vectors using a modified baculovirus expression system. Mol. Ther. 12, 1217–1225.

Kuck, D., Kern, A., and Kleinschmidt, J.A. (2007). Development of AAV serotype-specific ELISAs using novel monoclonal antibodies. J. Virol. Methods 140, 17–24.

Lock, M., Alvira, M., Vandenberghe, L.H., *et al.* (2010). Rapid, simple, and versatile manufacturing of recombinant adeno-associated viral vectors at scale. Hum. Gene Ther. 21, 1259–1271.

Martin, J., Frederick, A., Luo, Y., *et al.* (2013). Generation and characterization of adeno-associated virus producer cell lines for research and preclinical vector production. Hum. Gene Ther. Methods 24, 253–269.

Mingozzi, F., and High, K.A. (2011). Therapeutic *in vivo* gene transfer for genetic disease using AAV: progress and challenges. Nat. Rev. Genet. 12, 341–355.

Mitchell, M., Nam, H.J., Carter, A., *et al.* (2009). Production, purification and preliminary X-ray crystallographic studies of adeno-associated virus serotype 9. Acta Crystallogr. Sect. F Struct. Biol. Cryst. Commun. 65, 715–718.

Mori, S., Wang, L., Takeuchi, T., *et al.* (2004). Two novel adeno-associated viruses from cynomolgus monkey: pseudotyping characterization of capsid protein. Virology 330, 375–383.

Nathwani, A.C., Tuddenham, E.G., Rangarajan, S., *et al.* (2011). Adenovirus-associated virus vector-mediated gene transfer in hemophilia B. N. Engl. J. Med. 365, 2357–2365.

Nony, P., Chadeuf, G., Tessier, J., *et al.* (2003). Evidence for packaging of rep-cap sequences into adeno-associated virus (AAV) type 2 capsids in the absence of inverted terminal repeats: a model for generation of rep-positive AAV particles. J. Virol. 77, 776–781.

Schmidt, M., Voutetakis, A., Afione, S., *et al.* (2008). Adeno-associated virus type 12 (AAV12): a novel AAV serotype with sialic acid- and heparan sulfate proteoglycan-independent transduction activity. J. Virol. 82, 1399–1406.

Smith, R.H., Levy, J.R., and Kotin, R.M. (2009). A simplified baculovirus-AAV expression vector system coupled with one-step affinity purification yields high-titer rAAV stocks from insect cells. Mol. Ther. 17, 1888–1896.

Sonntag, F., Bleker, S., Leuchs, B., *et al.* (2006). Adeno-associated virus type 2 capsids with externalized VP1/VP2 trafficking domains are generated prior to passage through the cytoplasm and are maintained until uncoating occurs in the nucleus. J. Virol. 80, 11040–11054.

Sonntag, F., Schmidt, K., and Kleinschmidt, J.A. (2010). A viral assembly factor promotes AAV2 capsid formation in the nucleolus. Proc. Natl. Acad. Sci. USA 107, 10220–10225.

Sonntag, F., Kother, K., Schmidt, K., *et al.* (2011). The assembly-activating protein promotes capsid assembly of different adeno-associated virus serotypes. J. Virol. 85, 12686–12697.

Thomas, D.L., Wang, L., Niamke, J., *et al.* (2009). Scalable recombinant adeno-associated virus production using recombinant herpes simplex virus type 1 coinfection of

suspension-adapted mammalian cells. Hum. Gene Ther. 20, 861–870.
Urabe, M., Ding, C., and Kotin, R.M. (2002). Insect cells as a factory to produce adeno-associated virus type 2 vectors. Hum. Gene Ther. 13, 1935–1943.
Urabe, M., Nakakura, T., Xin, K.Q., *et al.* (2006). Scalable generation of high-titer recombinant adeno-associated virus type 5 in insect cells. J. Virol. 80, 1874–1885.
Virag, T., Cecchini, S., and Kotin, R.M. (2009). Producing recombinant adeno-associated virus in foster cells: overcoming production limitations using a baculovirus-insect cell expression strategy. Hum. Gene Ther. 20, 807–817.
Winter, K., von Kietzell, K., Heilbronn, R., *et al.* (2012). Roles of E4orf6 and VA I RNA in adenovirus-mediated stimulation of human parvovirus B19 DNA replication and structural gene expression. J. Virol. 86, 5099–5109.
Wistuba, A., Weger, S., Kern, A., *et al.* (1995). Intermediates of adeno-associated virus type 2 assembly: identification of soluble complexes containing Rep and Cap proteins. J. Virol. 69, 5311–5319.
Wistuba, A., Kern, A., Weger, S., *et al.* (1997). Subcellular compartmentalization of adeno-associated virus type 2 assembly. J. Virol. 71, 1341–1352.
Xiao, X., Li, J., and Samulski, R.J. (1998). Production of high-titer recombinant adeno-associated virus vectors in the absence of helper adenovirus. J. Virol. 72, 2224–2232.
Zolotukhin, S. (2005). Production of recombinant adeno-associated virus vectors. Hum. Gene Ther. 16, 551–557.

Address correspondence to:
Dr. Regine Heilbronn
Institute of Virology
Campus Benjamin Franklin
Charité Universitätsmedizin Berlin
Hindenburgdamm 27
12203 Berlin
Germany

E-mail: regine.heilbronn@charite.de

Received for publication October 1, 2013;
accepted after revision November 29, 2013.

Published online: December 3, 2013.

Supplementary Data

Supplementary Table S1. Primers for Polymerase Chain Reaction Amplification of *rep* and *cap* Genes for Cloning of pIR-VP-hr2-RBE- or pIR-rep78-hr2-RBE-Derived Constructs (Fig. 1A) or for Quantitative Analysis of Recombinant Adeno-Associated Virus Vector Preparations

Primer	*5′-sequence-3′*
AAV3-Fwd	5′-ATTAAAGATCTTGTTAAGACGGCTGCTGACGGTTATC-3′
AAV4-Fwd	5′-AATTAAGGATCCTGTTAAGACGACTGACGGTTACCTTCC-3′
AAV5-Fwd	5′-AATTAAAGATCTTGTTAAGACGTCTTTTGTTGATCACCC-3′
AAV6-Fwd	5′-AATTAAGGATCCTGTTAAGACGGCTGCCGATGGTTATC-3′
AAV7-Fwd	5′-AATTAAGGATCCTGTTAAGACGGCTGCCGATGGTTATCTTC-3′
AAV7-Rev	5′-AATTAAGTCGACTTACAGATTACGGGTGAGG-3′
AAV8-Fwd	5′-AATTAAAGATCTTGTTAAGACGGCTGCCGATGGTTATC-3′
AAV9-Fwd	5′-AATTAAAGATCTTGTTAAGACGGCTGCCGATGGTTATCTTCC-3′
pDP-Rev	5′-AATTAATGATCAGATACATTGATGAGTTTGGAC-3′
AAVrh10-Fwd	5′-GGAGATCTCCTGTCGATTGGCTCGAG-3′
AAVrh10-Rev	5′-GCTCTAGACGAATCTTCGCAGAGACC-3′
AAV11/12-Fwd	5′-AATTAAGGATCCTGTTAAGACGGCTGCTGACGGTTATCTTC-3′
AAV11-Rev	5′-AATTAATCTAGATTACAAATGATTAGTCAAATAAC-3′
AAV12-Rev	5-AATTAATCTAGATTACAAGTGGTGGGTGAGGAAAC-3′
AAV4-Rep-Fwd	5′-AATTAAGCGGCCGCAAAATGTGGTCAGGAGGGTATATAACC-3′
AAV4-Rep-Rev	5′-AATTAATCTAGATTATTGTTCCATGTCACAGTC-3′
AAV12-Rep-Fwd	5′-AATTAAAGATCTGAAGTTTGAACGAGCAGCAG-3′
AAV12-Rep-Rev	5′-AATTAATCTAGATTATTGCTCAAATTGGCAATCGTCC-3′
Bga-1	5′-CTAGAGCTCGCTGATCAGCC-3′
Bga-2	5′-TGTCTTCCCAATCCTCCCCC-3′
Rep-Fwd	5′-GGTGGAGCATGAATTCTACG-3′
Cap1-Rev	5′-TGGTTATACCGCAGGTACGG-3′
Cap2-Rev	5′-CGTAGGCTTTGTCGTGCTCG-3′
Cap8-Rev	5′-CCGCAGGTACGGATTGTCAC-3′

Fwd, forward; Rev, reverse.

2.2 Differential AAV Serotype-Specific Interaction Patterns with Synthetic Heparins and Other Glycans

Authors: Mario Mietzsch, Felix Broecker, Anika Reinhardt, Peter H. Seeberger and Regine Heilbronn

Year: 2014

Journal: Journal of Virology 88; 2991-3003

2.2.1 Contribution to the Publication

For this publication I exploited the previously described OneBac system to produce highly concentrated and purified AAV vectors of the full panel of AAV serotypes. This allowed labeling of AAV vectors with a fluorescent dye for AAV binding studies on glycan arrays (Fig. 1A and 3) as offered by the Consortium for Functional Glycomics, Atlanta, USA. AAV binding to specialized heparin arrays as developed by Prof. Peter Seeberger, Max-Planck Institute for Colloids and Interfaces Potsdam, and Freie Universität Berlin was performed by Felix Broecker and Anika Reinhardt in his lab. They contributed the data and readout of the heparin arrays as presented in Fig. 4A, 5 and 6A. I analyzed the raw data from all arrays to detect differential AAV serotype-specific glycan interaction patterns. The results of these evaluations are shown in Fig. 1 B-D; Fig. 2 and Fig. 4 B of the publication. I also performed the experiments to inhibit AAV transduction, constructed and tested the glycan-binding mutants to confirm the glycan-binding profiles *in vivo*, as displayed in Fig. 6, 7 and 8.

I wrote the first draft of the manuscript, which was revised and finalized by myself and my mentor Prof. Regine Heilbronn.

http://dx.doi.org/10.1128/JVI.03371-13

JVI Journals.ASM.org

Differential Adeno-Associated Virus Serotype-Specific Interaction Patterns with Synthetic Heparins and Other Glycans

Mario Mietzsch,[a] Felix Broecker,[b,c] Anika Reinhardt,[b,c] Peter H. Seeberger,[b,c] Regine Heilbronn[a]

Institute of Virology, Campus Benjamin Franklin, Charité Medical School, Berlin, Germany[a]; Department of Biomolecular Systems, Max-Planck Institute of Colloids and Interfaces, Potsdam, Germany[b]; Institute of Chemistry and Biochemistry, Free University of Berlin, Berlin, Germany[c]

All currently identified primary receptors of adeno-associated virus (AAV) are glycans. Depending on the AAV serotype, these carbohydrates range from heparan sulfate proteoglycans (HSPG), through glycans with terminal α2-3 or α2-6 sialic acids, to terminal galactose moieties. Receptor identification has largely relied on binding to natural compounds, defined glycan-presenting cell lines, or enzyme-mediated glycan modifications. Here, we describe a comparative binding analysis of highly purified, fluorescent-dye-labeled AAV vectors of various serotypes on arrays displaying over 600 different glycans and on a specialized array with natural and synthetic heparins. Few glycans bind AAV specifically in a serotype-dependent manner. Differential glycan binding was detected for the described sialic acid-binding AAV serotypes 1, 6, 5, and 4. The natural heparin binding serotypes AAV2, -3, -6, and -13 displayed differential binding to selected synthetic heparins. AAV7, -8, -rh.10, and -12 did not bind to any of the glycans present on the arrays. For discrimination of AAV serotypes 1 to 6 and 13, minimal binding moieties are identified. This is the first study to differentiate the natural mixed heparin binding AAV serotypes 2, 3, 6, and 13 by differential binding to specific synthetic heparins. Also, sialic acid binding AAVs display differential glycan binding specificities. The findings are relevant for further dissection of AAV host cell interaction. Moreover, the definition of single AAV-discriminating glycan binders opens the possibility for glycan microarray-based discrimination of AAV serotypes in gene therapy.

Adeno-associated viruses (AAVs) represent a family of helper-dependent parvoviruses composed of single-stranded DNA genomes packaged into icosahedral capsids. AAV capsids directly interact with specific host cell receptors. Various AAV serotypes of human and primate origin (AAV1 to AAV13) that differ in the structures of their capsids and display variable cell or tissue tropism have been defined (1). AAV-derived vectors are increasingly used in gene therapy. The differential tropism of various AAV serotypes is ideal for directing the vector to a certain cell type or tissue for gene therapy.

For many AAV serotypes, it has been shown that binding to cell surface glycans is required for infection (2–7). Cell surface glycans are commonly attached to proteins (glycoproteins and proteoglycans) or lipids (sphingolipids) of the cell membrane. These carbohydrates are structurally the most complex building blocks of life. The diversity of mammalian glycan biopolymers is achieved by alternate sequences of 10 different building blocks of monosaccharides, variable glycosidic linkages, and branching and modifications of saccharides. In addition, attachment to different proteins is achieved via asparagine (N-linked glycans) or serine or threonine (O-linked glycans) residues or via lipids (8). Virtually all membrane proteins are glycosylated, but their glycosylation patterns differ in different tissues (9). The biological roles of glycans are diverse and not yet fully understood. They have been associated with a variety of cellular processes, including protein folding (10) and signal transduction (11). In addition, surface-exposed glycans are recognized by various virus families that exploit them as host cell receptors (12).

The first identified receptor for AAV was heparin sulfate proteoglycan (HSPG), described as a primary receptor for prototype AAV2. Competition experiments with soluble heparin and pretreatment of cells with heparinase helped to identify its cell receptor (2). HSPG and the closely related heparin represent mixtures of naturally occurring, polydisperse linear polysaccharides that are composed of alternate units of glucosamine (GlcN) and uronic acid, either a glucuronic acid (GlcA) or an iduronic acid (IdoA). The alternate units are joined by 1 to 4 glycosidic linkages and can be variably modified by sulfates or acetyl groups. Heparin displays a higher degree of sulfation than HSPGs. Heparins are stored in vesicles of mast cells and are released upon stimulation. In contrast, HSPGs are ubiquitously found on cell surfaces, covalently linked to proteoglycan core proteins (13).

HSPG was subsequently confirmed as the primary receptor for AAV3 and AAV13 (3, 7). Furthermore, AAV6 was shown to bind to heparin *in vitro*. However, in contrast to the results with AAV2, AAV3, or AAV13, AAV6 infection *in vivo* was resistant to inhibition by soluble HSPG (14). Other AAV serotypes are heparin insensitive (15). Instead, cell pretreatment with neuraminidases revealed that sialic acids were required for infection with AAV serotype 1, 4, 5, or 6 (4, 5, 16). Sialic acids represent N- or O-substituted derivatives of neuraminic acid, a 9-carbon monosaccharide. The most common sialic acid, *N*-acetyl-neuraminic acid (Neu5Ac), is typically found at terminating branches of *N*-glycans, *O*-glycans, or glycosphingolipids (17). AAV4 was reported to require *O*-linked α2-3 sialic acids for infection, whereas AAV1, AAV5, and AAV6 bound to *N*-linked α2-3 or α2-6 sialic acids (4, 5, 18).

In the present study, we set out to directly compare the glycan binding specificities of AAV serotypes 1 to 8, 10, 12, and 13 using

Received 17 November 2013 **Accepted** 19 December 2013
Published ahead of print 26 December 2013
Editor: M. J. Imperiale
Address correspondence to Regine Heilbronn, regine.heilbronn@charite.de.

doi:10.1128/JVI.03371-13

highly purified fluorescently labeled AAV vectors. Their binding profiles on arrays of synthetic glycans and heparins identified AAV serotype-specific capsid-carbohydrate interactions, allowing AAV capsid differentiation by glycan/heparin binding patterns.

MATERIALS AND METHODS

Cloning and mutagenesis. For the introduction of mutations into the capsid genes of AAV2 and AAV3, the respective cap genes were subcloned from pDG or pDP3rs (19) into pBluescript II SK(+). The capsid gene of AAV13 was mutated directly in the pAAV-13-cap plasmid. Using the QuikChange site-directed mutagenesis protocol, the double-exchange mutation R585A/R588A was introduced into the *cap* gene of AAV2, the point mutation R594A into the *cap* gene of AAV3, and the point mutation K528E into the *cap* gene of AAV13. The DNA sequence-verified *cap* genes were cloned back into pDG or pDP3rs, respectively.

Cell culture. HEK 293- or HeLa-derived C12 cells were cultivated as adherent monolayers at 37°C and 5% CO_2 in Dulbecco's modified Eagle's medium (DMEM) (Gibco) supplemented with 2.5 g/liter glucose, 100 μg/ml streptomycin, 100 U/ml penicillin (PAA), and 10% (vol/vol) fetal calf serum (FCS) (Gibco). Sf9 cell lines for recombinant AAV (rAAV) production expressing Rep and Cap of various serotypes were described previously (20). Sf9 cells were maintained in suspension culture under constant agitation with serum-free Spodopan medium (Pan-Biotech) supplemented with 200 μg/ml streptomycin, 200 U/ml penicillin, and 250 ng/ml amphotericin B (Invitrogen) at 27°C.

rAAV production in 293 cells. HEK 293 cells were seeded at 25 to 33% confluence. The cells were transfected 24 h later with plasmids for AAV *rep*, *cap*, and adenovirus type 5 (Ad5) helper genes and an additional plasmid for the rAAV cassette expressing green fluorescent protein (GFP) under the control of the cytomegalovirus (CMV) promoter (pTR-UF5) using the calcium phosphate cotransfection method as described previously (21). rAAV1, rAAV2, and rAAV3 subtype vectors and mutants derived from them were produced by the two-plasmid transfection method (19) using pDP1, pDG, pDG-R585A-R588A, pDP3, or pDP3-R594A as a helper plasmid. Generation of rAAV13 or the mutant derived from it required triple-plasmid transfections of pTR-UF5, pDGdeltaVP, and pAAV13-cap or pAAV13-cap-K528E, respectively. For the production of rAAV12 vectors, transfection of four plasmids, pTR-UF5, pAAV12-Rep, pAAV12-Cap, and pHelper, was required (15). After 12 h, the culture medium was replaced by medium with 2% FCS. Cells and medium were harvested 72 h after transfection and lysed by three freeze-thaw cycles. The crude lysates were treated with 250 U benzonase (Merck) per ml of lysate at 37°C for 1 h to degrade input and unpackaged AAV DNA before centrifugation at 8,000 × *g* for 30 min to pellet cell debris.

rAAV production in Sf9 cells. Sf9 cell-derived AAV *rep-cap*-expressing cell lines (20, 22) were continuously held in suspension culture within the logarithmic growth phase prior to infection with the recombinant baculovirus Bac-rAAV-GFP (multiplicity of infection [MOI] = 5). The infected cells were incubated for 72 h at 27°C under constant agitation. The cells were pelleted at 2,000 × *g* for 5 min. The cell pellets were resuspended in lysis buffer containing 10 mM Tris-HCl (pH 8.5), 150 mM NaCl, 1 mM $MgCl_2$, and 1% (vol/vol) Triton X-100. Crude lysates from 1-liter cell suspensions were treated with 3,000 U of benzonase (Merck) at 37°C for 1 h to degrade unpackaged AAV DNA and centrifuged at 8,000 × *g* for 30 min.

rAAV purification. rAAV vectors were further purified from the benzonase-treated, cleared freeze-thaw supernatants by one-step AVB Sepharose affinity chromatography using 1-ml prepacked HiTrap columns on an ÄKTA purifier (GE Healthcare) as follows. Freeze-thaw supernatants were diluted 1:1 in 1× phosphate-buffered saline (PBS) supplemented with 1 mM $MgCl_2$ and 2.5 mM KCl (PBS-MK) prior to loading on the column. The loading rate of the sample was set to 0.5 ml/min. Washing of the column was performed with 20 ml of 1× PBS-MK at a flow rate of 1 ml/min. AAV vectors were eluted with 0.1 M sodium acetate, 0.5 M NaCl, pH 2.5, at a flow rate of 1 ml per min and neutralized immediately with 1/10 volume of 1 M Tris-HCl, pH 10. The peak fractions of purified rAAV preparations were dialyzed against 1× PBS-MK using Slide-A-Lyzer dialysis cassettes (molecular weight cutoff [MWCO], 10,000; Thermo Scientific).

Quantification of rAAV vector preparations. Highly purified rAAV vector preparations or rAAV-containing freeze-thaw supernatants were digested with proteinase K (Roth, Germany) to release the vector genomes from the capsids. Aliquots of the vector preparation were incubated in buffer containing 25 mM Tris-HCl (pH 8.5), 10 mM EDTA (pH 8.0), 1% (wt/vol) *N*-lauroyl sarcosinate, 40 μg proteinase K, and 1 μg pBluescript carrier plasmid for 2 h at 56°C. DNA was purified by extraction with phenol-chloroform-isoamyl alcohol (25:24:1) and precipitated with ethanol. The DNAs were analyzed by quantitative Light-Cycler PCR with a Fast Start DNA Master SYBR green kit (Roche) with dilutions depending on the subtype. Primers specific for the bovine growth hormone-derived poly(A) site of the vector backbone were used (forward primer, 5′-CTAG AGCTCGCTGATCAGCC-3′, and reverse primer, 5′-TGTCTTCCCAAT CCTCCCCC-3′).

Fluorescence labeling of rAAV vectors. Highly purified rAAV vectors with a titer of at least 1×10^{13} genomic particles per ml were fluorescently labeled using the DyLight488 Labeling Kit (Pierce) following the manufacturer's protocol. Labeled rAAV vector preparations were dialyzed twice against 1× PBS-MK using Slide-A-Lyzer dialysis cassettes (MWCO, 10,000; Thermo Scientific) to remove unbound dye from the vector preparation. To verify a successful labeling reaction, 10-μl aliquots of the vector preparations were lysed in 2× SDS protein sample buffer for 5 min at 95°C and analyzed on SDS-polyacrylamide gels. The DyLight-labeled AAV capsid bands could be visualized under UV light (data not shown).

Glycan array screening. Fluorophore-labeled rAAV vectors were sent to the Consortium for Functional Glycomics (CFG) for glycan binding analysis on microarrays. The procedure is described in detail on the CFG webpage (http://www.functionalglycomics.org). In brief, up to 611 (version 5.0) or 610 (version 5.1) different glycan structures are printed on microscope glass slides, each available in replicates of six. PBS-MK was used as a binding and wash buffer during this assay. Dried slides are analyzed at the fluorophore-emitting wavelength in a PerkinElmer ScanArray scanner. The spots on the slide are aligned with the help of a grid and biotin control spots using Imagene software. Once aligned, the amount of fluorophore binding to each spot is quantified. The data sets were analyzed by averaging the six replicates after elimination of the two spots with the highest and lowest intensity, respectively. Full data sets are available at the website of the CFG (http://www.functionalglycomics.org/), and the addresses of individual AAV screens are provided in Table 1.

Heparin array screening. Fluorophore-labeled rAAV vectors were analyzed for binding to chemically defined heparins on a glycan array. *N*-Hydroxysuccinimide (NHS)-activated CodeLink slides (SurModics, Inc., Eden Prairie, MN, USA) containing synthetic heparan sulfate (HS)/heparin oligosaccharides and 5-kDa natural heparin were prepared as described previously (23, 24). Briefly, heparin oligosaccharides bearing an aminopentyl linker at the reducing end were procured through a modular chemical synthesis approach. The oligosaccharides were immobilized on NHS-activated slides via their terminal amine groups using a piezoelectric spotting device (S3; Scienion, Berlin, Germany). Heparin oligosaccharides were spotted at concentrations of 1, 0.25, 0.063, and 0.016 mM dissolved in 50 mM phosphate buffer, pH 8.5 (10 spots for each concentration). The microarray slides were incubated in a humid chamber for 24 h to complete the reaction; quenched with 50 mM aminoethanol solution, pH 9, for 1 h at 50°C; washed three times with deionized water; and stored desiccated until use. For binding analyses, the slides were blocked at room temperature for 1 h with 1% (wt/vol) bovine serum albumin (BSA) in PBS-MK, washed three times with PBS-MK, and dried by centrifugation (5 min; 300 × *g*). The slides were incubated at 4°C overnight with purified and fluorescence-labeled rAAV vectors at a concentration of 100 μg/ml in PBS-MK with 0.01% (vol/vol) Tween 20 in a humid chamber. Then, the slides were washed three times with PBS-MK containing 0.1% (vol/vol)

TABLE 1 Web addresses of full data sets of primary AAV screens in the CFG database

AAV serotype[a]	Web address
AAV1	www.functionalglycomics.org/glycomics/HServlet?operation=view&psId=primscreen_5777
AAV2	www.functionalglycomics.org/glycomics/HServlet?operation=view&psId=primscreen_5347
AAV2*	www.functionalglycomics.org/glycomics/HServlet?operation=view&psId=primscreen_4405
AAV3	www.functionalglycomics.org/glycomics/HServlet?operation=view&psId=primscreen_5349
AAV4	www.functionalglycomics.org/glycomics/HServlet?operation=view&psId=primscreen_4406
AAV5	www.functionalglycomics.org/glycomics/HServlet?operation=view&psId=primscreen_5780
AAV6	www.functionalglycomics.org/glycomics/HServlet?operation=view&psId=primscreen_4407
AAV7	www.functionalglycomics.org/glycomics/HServlet?operation=view&psId=primscreen_5350
AAV8	www.functionalglycomics.org/glycomics/HServlet?operation=view&psId=primscreen_5779
AAVrh.10	www.functionalglycomics.org/glycomics/HServlet?operation=view&psId=primscreen_5351
AAV12	www.functionalglycomics.org/glycomics/HServlet?operation=view&psId=primscreen_5778

[a] Glycan array binding of fluorophore-labeled AAV serotypes 1 to 12 was detected directly. Unlabeled AAV2* was detected by MAb A20.

Tween 20, rinsed once with water, and dried by centrifugation. The slides were scanned with a GenePix 4300A microarray scanner (Molecular Devices). Fluorescence was excited at 488 nm, and fluorescence intensities were determined with GenePix Pro 7 software (Molecular Devices). The photomultiplier tube (PMT) voltage was adjusted so that scans were free of saturation signals. The mean fluorescence intensity (MFI) values were exported to Microsoft Excel for further analysis.

Heparin competition assay. HeLa C12 cells were seeded in 24-well plates at 50% confluence and infected 24 h later with adenovirus type 2 for 1 h (MOI = 10). AAV-GFP vectors were incubated with serial dilutions of heparins in a total volume of 50 μl of DMEM at 37°C for 1 h. After aspiration of the adenovirus-containing cell medium, the rAAV vector-heparin mixture was added to the cells and incubated for 1 hour with occasional tilting. To remove nontransduced AAV vectors, the cells were washed twice with PBS. The cells were cultivated for 40 h in medium with 2% FCS, and the proportion of GFP-positive cells was determined by fluorescence-activated cell sorter (FACS) analysis (FACSCalibur; Becton Dickinson) according to the manufacturer's protocol. For each sample, 100,000 cells were counted. Cells that exceeded the cutoff of 40 in the FL1-H channel were regarded as GFP positive.

RESULTS

Generation of fluorescently labeled vectors of various AAV serotypes. For the analysis of AAV capsid-glycan interactions, AAV vectors of serotypes 1 to 8, rh.10, 12, and 13 were produced either in Sf9 cells or in 293 cells. Virus binding to glycan microarrays is typically detected by specific antibodies visualized by fluorophore-labeled secondary antibodies. Direct fluorophore labeling of AAV capsids was expected to yield less nonspecific background signals. The required high AAV titers and extensive virus purification were achieved by AVB-Sepharose affinity chromatography, as described in Materials and Methods. Concentrated AAV preparations exhibiting 1×10^{13} genomic particles (gp) per ml were analyzed by electron microscopy (EM) analysis and on silver gels to confirm AAV purity (data not shown). Unfortunately, AAV9 and AAV11 were refractory to sufficient purification. Therefore, these serotypes were omitted from the analysis. The AAVs were labeled with the fluorescent dye DyLight488, which is conjugated to surface-exposed lysines on the capsids. Their numbers vary among different serotypes. AAV2 capsids expose significantly fewer lysines than capsids from other AAV subtypes. This led to variable labeling efficiencies of individual AAV serotypes. The number of dye molecules per capsid was calculated to range from approximately 10 in the case of AAV2 to up to 30 for other AAV serotypes. Only a small fraction of surface-exposed lysines are tagged; many more unmodified lysines are available for receptor attachment. Side-by-side transduction analysis of labeled and unlabeled AAV vectors showed comparable transduction efficiencies (data not shown).

CFG glycan array screening of various AAV serotypes. The panel of fluorescently labeled AAV vectors was analyzed for binding to the glycan array offered by the CFG. The array is composed of 610 (v5.1) or 611 (v5.0) different natural or synthetic glycan structures, each in replicates of six. The original data sets, including full statistical analysis of all glycan screens, are available online (Table 1) (www.functionalglycomics.org/). Conclusive data for the interaction of AAV capsids with specific glycans on the array were observed for AAV1, AAV4, AAV5, and AAV6 (Fig. 1A).

The capsids of the two closely related AAV serotypes 1 and 6 exhibited binding to the same predominant glycan (number 237) shown in Fig. 1A and B. This glycan displays a terminal α2-3-linked sialic acid (Neu5Ac), which has been described as a receptor for either serotype (5). Our data show that the α2-3-linked sialic acid is not sufficient for AAV1 or -6 binding (Fig. 1B). Of over 70 alternative glycans with terminal α2-3 sialic acids present on the array, only glycan 237 showed significant AAV1/6 binding. The combination of a linked *N*-acetylgalactosamine and an additional β1-4-linked *N*-acetylglucosamine appears to be required. Minor changes of the glycan structure, as displayed in Fig. 1B, led to a reduction in binding efficiency in the range of 1 to 8% of that observed for glycan 237. On the AAV6 screen, glycan 237 was the only glycan binding reproducibly (1,153 ± 40 relative fluorescence units [RFU]). AAV6 showed multiple additional binding signals in the range of 40% of that of glycan 237 (Fig. 1A). They were disregarded, either because of large standard deviations or because of binding to a single monosaccharide (mannose). The relevance of mono- or disaccharide binding is unclear, since CFG binding data have previously shown nonreproducible results with alternative AAV serotypes.

AAV5 has been reported to require either terminal α2-3 or α2-6 sialic acids (4). Here, we show specific binding to glycan 46 and 230, both of which display terminal α2-3 sialic acids (Fig. 1A). AAV5 did not bind to any of over 70 alternative glycans with terminal α2-3 sialic acids or to any of 52 alternative glycans with terminal α2-6 sialic acids. In addition, a terminal α2-3 sialic acid was obviously not sufficient for binding. Linkage to a sulfated galactose in the second position was required, and the galactose moiety could not be replaced by acetylglucosamine (Fig. 1C). Fucosylation of the *N*-acetylglucosamine in the third position was not required but moderately improved AAV5 binding. Furthermore, certain biantennary glycans, with 483 as a prototype, showed interaction with AAV5, though with reduced binding efficiencies (Fig. 2B). Although not sulfated at the galactose in the second position, these glycans confirmed the requirement for ter-

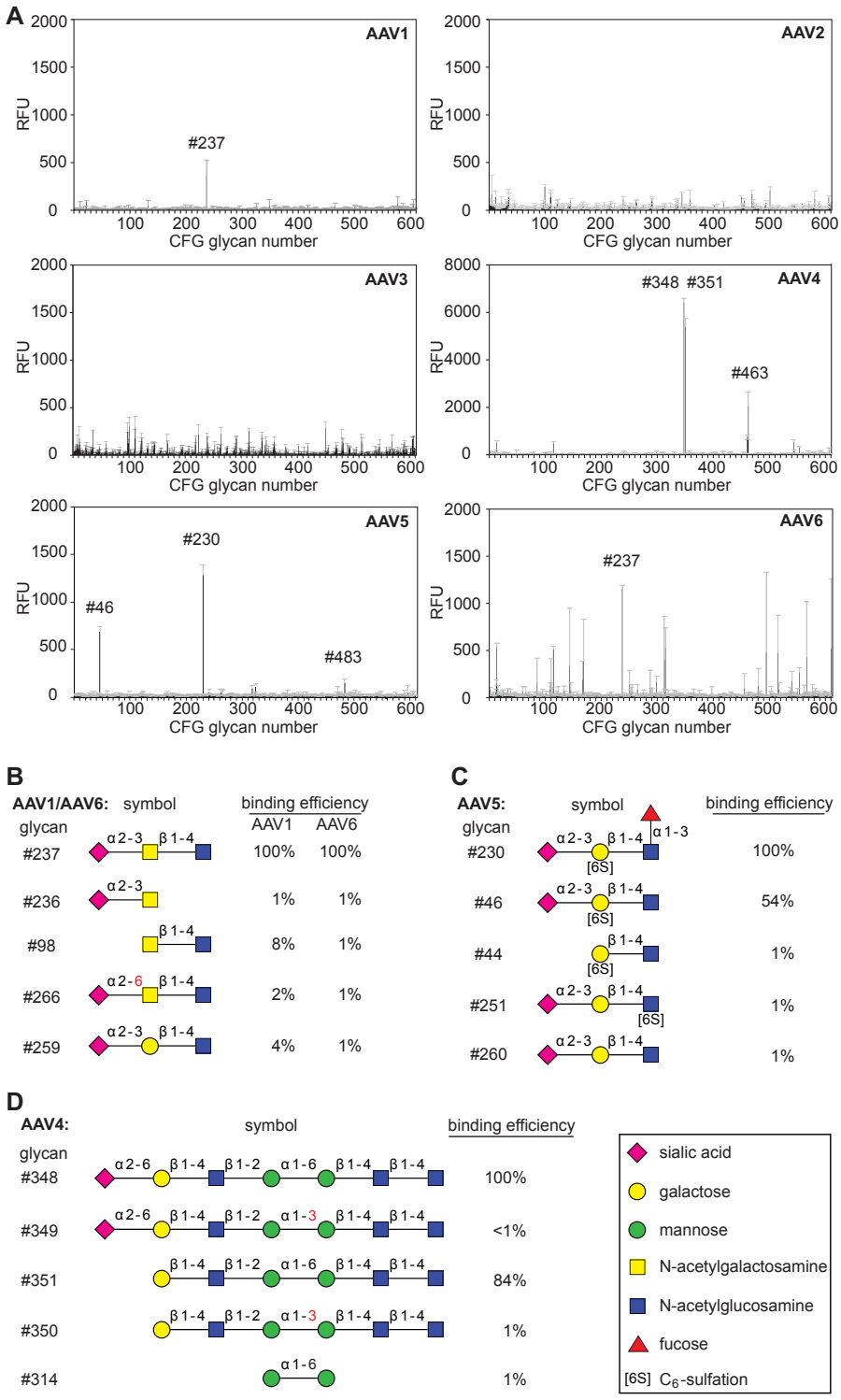

FIG 1 CFG glycan array screening of AAV serotypes 1 to 6. (A) Binding efficiencies of fluorescently labeled AAV1 to -6 vectors on CFG glycan arrays displaying 611 different glycan structures, each in replicates of six. Glycans with significantly higher binding efficiencies are highlighted with the corresponding CFG number. Due to different versions of the CFG glycan screen, the glycan numbers of the AAV6 screen glycan were adapted to the numbering of the newer version (5.1) to facilitate direct comparison to the AAV1 binding profile. Note that the binding signals for glycans 81, 265, and 518 were removed from the AAV2 and -3 screens based on a statement of the CFG that these glycans repeatedly produced nonspecific signals in unrelated glycan arrays performed with the same array batch. (B to D) Glycans that were identified in panel A to interact with the capsids of a particular serotype (42). Shown is a comparison of AAV serotype-dependent binding to families of closely related glycan structures present on the CFG array. Relative binding efficiencies are represented as percentages of that of the most efficiently binding glycan for the depicted AAV serotype. Error bars represent standard deviations.

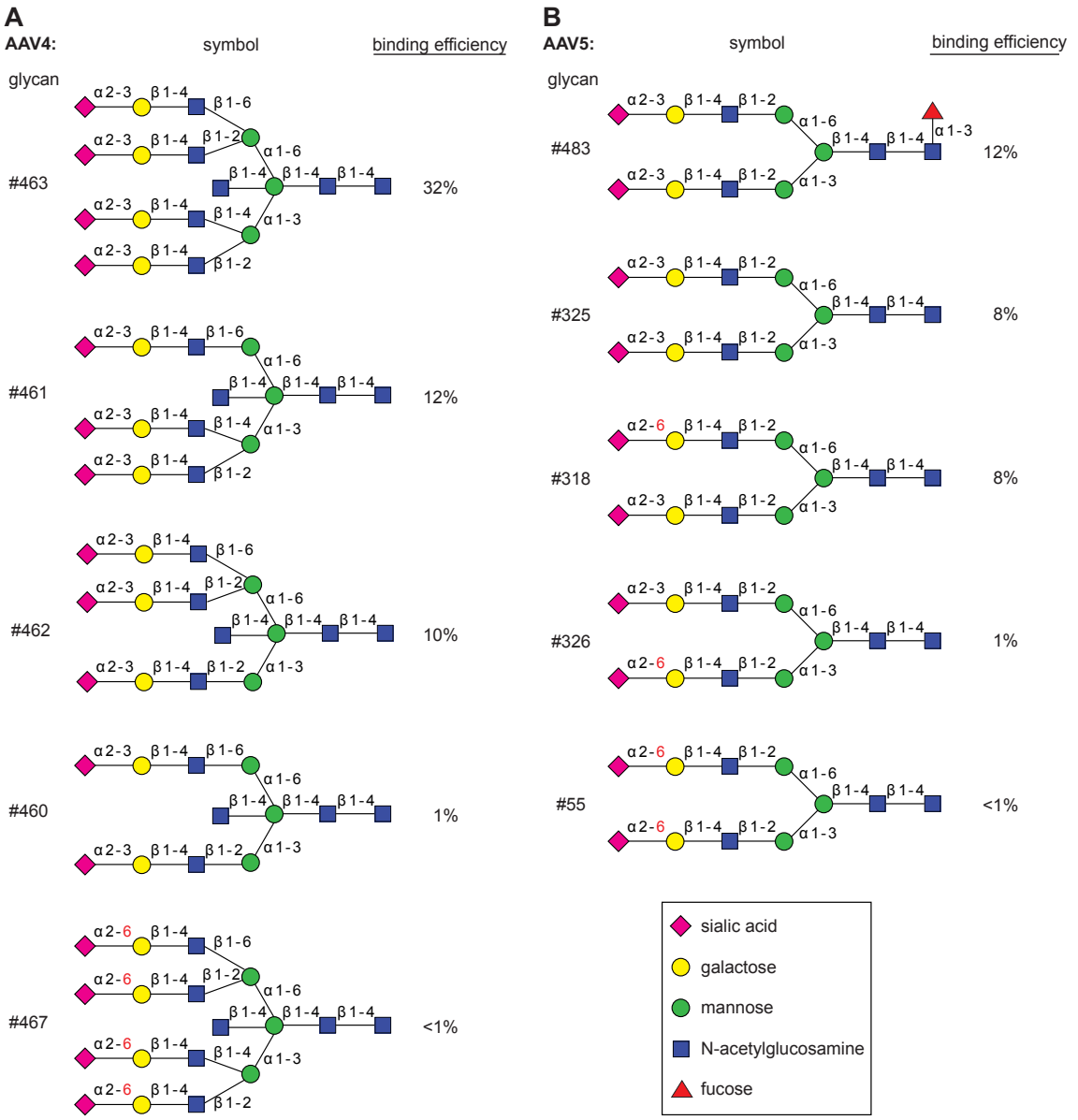

FIG 2 Differential binding of branched glycans with the capsids of AAV4 or AAV5. (A) Branched glycan 463 binding to AAV4 as shown in Fig. 1A compared to closely related glycan structures with reduced binding efficiencies, shown as percentages of that of glycan 348. (B) Branched glycan 483 binding to AAV5 as shown in Fig. 1A compared to closely related glycan structures with reduced binding efficiencies, shown as percentages of that of glycan 230.

minal α2-3 sialic acids. It appears that glycans with terminal α2-3 sialic acids are bound, but only when attached to the mannose α1-3 arm of the biantennary glycan (Fig. 2B). However, an even more complex glycan structure (e.g., glycan 462 of the CFG array) (Fig. 2A) possessed an identical arm with the terminal α2-3 sialic acid but was not bound by AAV5. In summary, the minimal glycan binding structure for AAV5 appears to be composed of a terminal α2-3 sialic acid linked to sulfated galactose, followed by a β1-4-linked *N*-acetylglucosamine.

The glycan array for AAV4 displays the highest and most specific glycan binding pattern of all AAVs analyzed. The predominant binders, glycans 348 and 351, share a backbone of six sugar molecules extended by a terminal α2-6 sialic acid in the case of glycan 348 (Fig. 1A and D). Since the AAV4 binding efficiencies differ only marginally, the presence of the terminal sialic acid appears not to be required. On the other hand, the α1-6 linkage between two internal mannose moieties appears to be essential. Identical glycans with an α1-3 linkage between the two mannose moieties lose AAV4 binding. Two α1-6-linked mannoses alone, however, were not sufficient to bind AAV4. Branched glycan 463 displaying a binding efficiency about one-third that of glycan 348 carries terminal α2-3 sialic acids. Their replacement by α2-6 sialic acids leads to a dramatic drop in AAV4 binding, even below background levels (Fig. 2A). In view of the very clear AAV4 binding profile, it is not obvious how the findings can be reconciled with *O*-linked terminal α2-3 sialic acid being described as a primary receptor for AAV4 (4).

Screening the CFG glycan array using fluorescently labeled

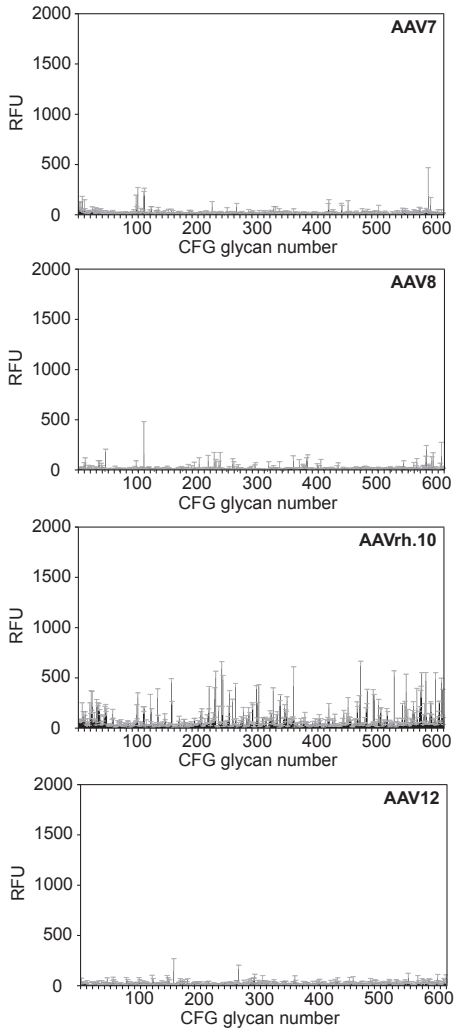

FIG 3 CFG glycan array screens of AAV7, -8, -rh.10, and -12. Shown are binding efficiencies of fluorescently labeled AAV7, -8, -rh.10, and -12 vectors on CFG glycan arrays displaying 611 different glycan structures, each in replicates of six. Note that binding signals for glycans 81, 265, and 518 were removed from the AAV7 and -rh.10 screens, respectively, based on a statement of the CFG that these glycans repeatedly produced nonspecific signals in unrelated glycan arrays performed with the same array batch. Error bars represent standard deviations.

AAV vectors of serotypes 2 and 3 (Fig. 1A), 7, 8, rh.10, or 12 (Fig. 3) did not lead to any significant interaction with a specific glycan. In the case of AAV2, a second screen was performed with unlabeled virus, which was detected by AAV2 capsid-specific monoclonal antibody (MAb) A20 (25). As mentioned above, this procedure markedly increased the background. Nevertheless, the negative results with the directly labeled viral particles were confirmed (Table 1). The lack of specific glycan interaction of the heparin binders AAV2 and AAV3 was expected, since heparins were not present on the CFG array.

Heparin array screening of various AAV serotypes. AAV binding to defined heparin variants was analyzed on a specialized microarray with 13 synthetic single heparins and mixed natural low-molecular-weight heparin (26). All previous AAV heparin binding studies had relied on natural heparins as competitors. Natural heparins represent a mixture of heterogeneous biomolecules. Therefore, the exact composition and structure is unpredictable and varies from batch to batch. Single synthetic heparins offer the opportunity to differentiate the heparin binding specificities of different AAV serotypes, which has not been possible so far. The panel of fluorophore-labeled AAV preparations showed strong and specific heparin binding signals, but only in the cases of AAV2 and AAV3 (Fig. 4). The 2-fold-higher overall binding efficiency of AAV3 compared to AAV2 likely reflects the higher fluorophore-labeling efficiency. AAV6 and AAV13, which had been reported to require HSPG for infection (7), showed weaker binding. No binding to any of the heparins was detected for the other AAV serotypes (Fig. 4A and 5). These findings reflect previous observations that the majority of AAV serotypes were unable to bind to natural heparin.

AAV2 efficiently bound to natural heparin 14 and two synthetic heparins, 1 and 7. These oligosaccharides have similar sequences but differ in length (Fig. 4B). Binding to these compounds is even more efficient than binding to mixed natural heparin. The same heparins are bound by AAV3, but in addition, AAV3 binds to heparin 5 (Fig. 4). Heparin 5 is a hexasaccharide that, in contrast to 1 and 7, is not 6-*O*-sulfated on glucosamine. The data suggest that AAV2 binds to heparins containing glucosamines that are both *N*- and 6-*O*-sulfated (Fig. 4B). Obviously, 6-*O*-sulfation of heparin is not necessary for AAV3 binding. Instead, heparins with *N*-sulfated glucosamines alternating with 2-*O*-sulfated iduronic acids are bound (Fig. 4B).

AAV6 is a special case, since it binds efficiently to α2-3-linked sialic acid containing glycan 237, as shown above. AAV6 was shown previously to weakly bind to natural heparin *in vivo* (14). On the heparin array, AAV6 did not bind to natural heparin 14 but showed weak binding signals to heparins 3 and 8 (Fig. 4A). The two heparins are related, as they are sulfated only on glucosamine but not on iduronic acid, and differ in chain length (Fig. 4B). More highly sulfated heparins, as well as singly sulfated heparins (number 6; 2-*O*-sulfation on iduronic acid), were not bound by AAV6.

AAV13, also called VR-942 (7), bound best to natural heparin 14 (Fig. 4A). The array contained heparins only up to a maximum concentration of 0.25 mM, whereas arrays with heparins up to 1 mM had been used for all other AAV serotypes. Comparing the binding intensities of all AAVs at 0.25 mM heparin showed that the efficiency of AAV13 binding to natural heparin 14 is in the range of that seen for AAV2 and AAV3 (data not shown). In addition, AAV13 showed enhanced binding to heparin 2. Heparin 2 is a hexasaccharide composed of acetylated, 6-*O*-sulfated glucosamines and 2-*O*-sulfated iduronic acids.

Binding efficiencies to variant heparins by wild-type or mutant capsids of AAV2 or AAV3. To validate that the AAV2 or -3 capsid structures defined as binding sites for natural heparin also mediate binding to synthetic heparin variants, AAV2 (R585A/R588A) and AAV3 (R594A) capsid mutants that had been shown previously to be deficient for binding to natural heparin were generated (27, 28). As anticipated, fluorophore-labeled AAV2 or AAV3 capsid mutants were unable to bind to any of the specific heparins (Fig. 6A). Surprisingly, the AAV3 interaction with low-molecular-weight heparin 14 was not impaired. The interaction of AAV capsids and heparin was analyzed at increasing heparin concentrations, leading to saturation curves typical for receptor-ligand interactions (Fig. 6B). The apparently lower saturation levels of AAV2 and AAV3 binding to natural heparin 14 further empha-

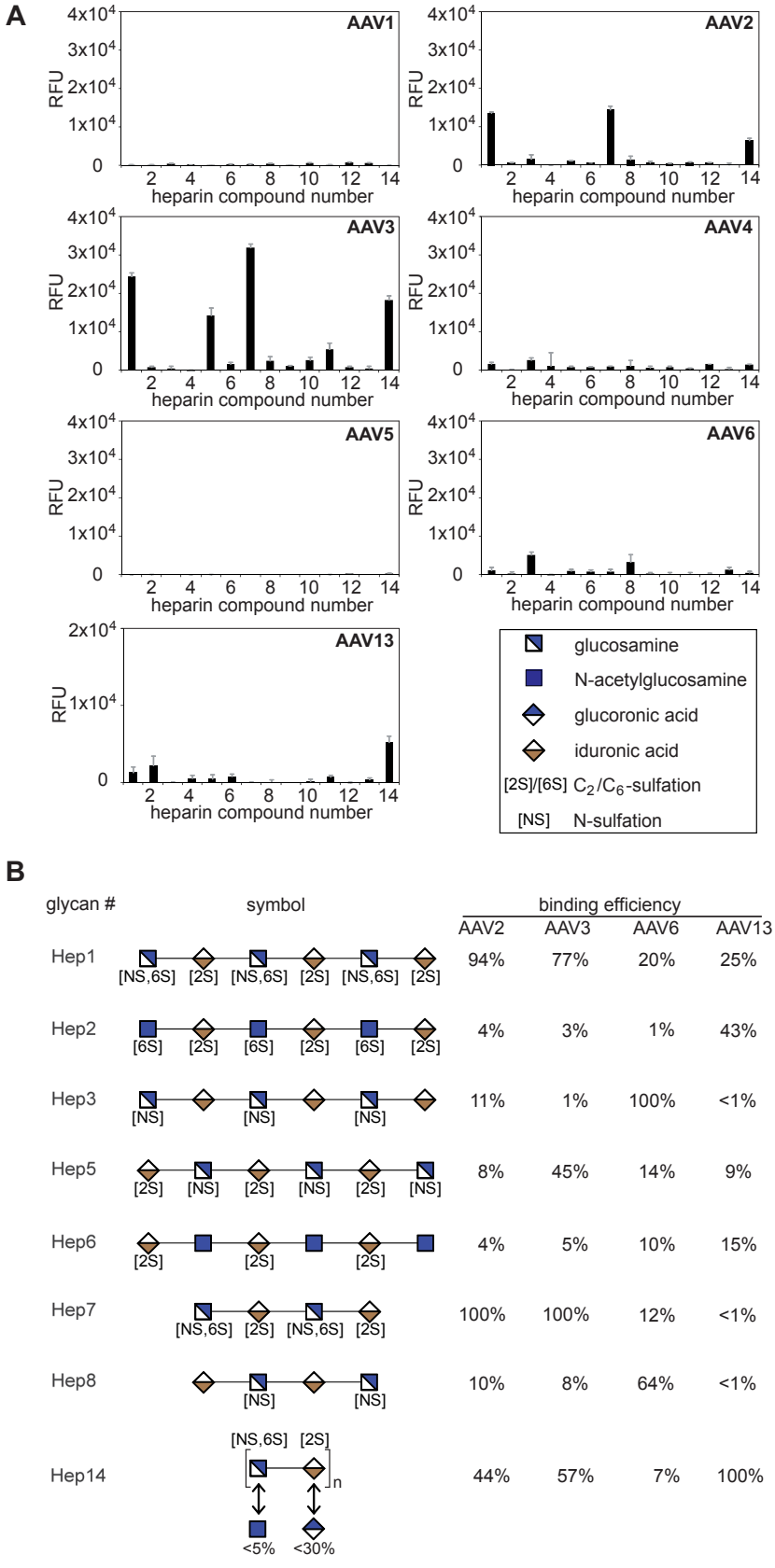

FIG 4 Heparin array screening of AAV serotypes 1 to 6 and 13. (A) Binding efficiencies of fluorescently labeled AAV1 to -6 and -13 vectors on heparin arrays displaying 13 different synthetic heparin structures and low-molecular-weight natural heparin 14, each in replicates of 10. Note that the binding signals of AAV13 were obtained from arrays displaying lower concentrations (0.25 mM) of the various heparin variants in contrast to all other AAV serotypes (1 mM). The error bars represent standard deviations. (B) Heparins that were identified in panel A to interact with the capsids of a particular serotype (42). Shown is a comparison of AAV serotype-dependent binding to related glycan structures present on the heparin array. Relative binding efficiencies are represented as percentages of that of the most efficiently binding glycan for the depicted AAV serotype.

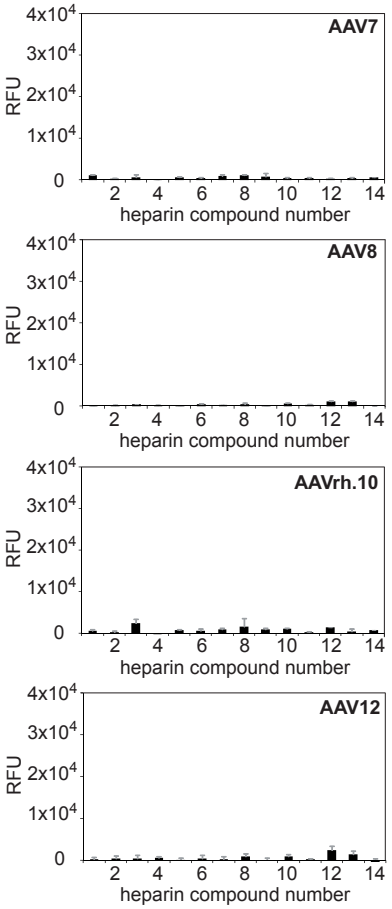

FIG 5 Heparin array screens of AAV7, -8, -rh.10, and -12. Shown are binding efficiencies of fluorescently labeled AAV7, -8, -rh.10, and -12 vectors on heparin arrays displaying 13 different synthetic heparin structures and low-molecular-weight natural heparin 14, each in replicates of 10. The error bars represent standard deviations.

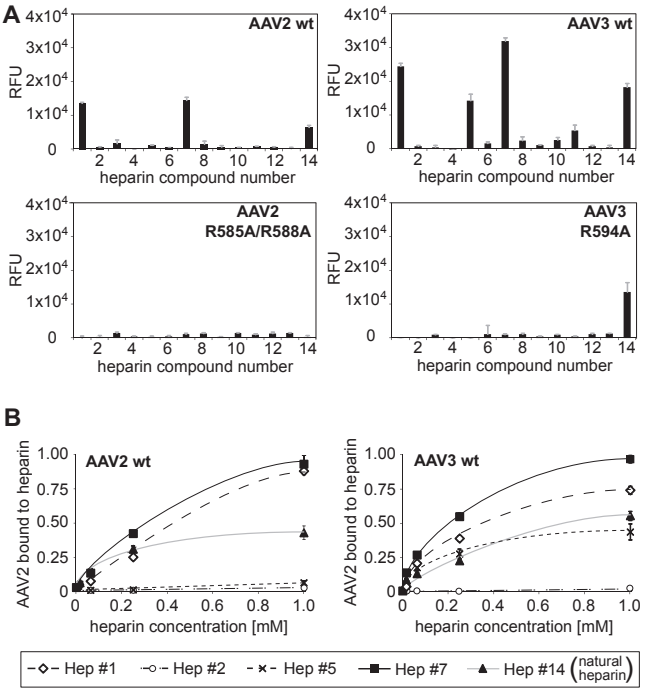

FIG 6 Specificities of AAV2 and -3 capsid binding to heparins. (A) Binding efficiencies of fluorescently labeled AAV2(R585A/R588A) and AAV3(R594A) vectors on heparin arrays displaying 13 different single synthetic heparin structures and low-molecular-weight natural heparin 14, each in replicates of 10. (B) Concentration-dependent binding of wild-type AAV2 and AAV3 to selected heparins. Heparins on arrays were present at increasing concentrations, 16 μM, 64 μM, 250 μM, and 1 mM, each in replicates of 10. The error bars represent standard deviations.

size the high-affinity binding of AAV2 and AAV3 to the synthetic heparins 1 and 7.

In vivo inhibition of AAV infection by natural and synthetic heparins. To allow competition with heparin-like cell surface receptors on the target cell line, AAV infection neutralization assays were performed in the presence of soluble heparin. Increasing concentrations of heparin were preincubated with AAV before infection of C12 cells, as outlined in Materials and Methods. Heparin-dependent inhibition of AAV infection can be monitored by the expression of GFP as a transgene. The percentage of GFP-positive cells was determined by FACS analysis and served as a readout for AAV infection efficiency (Fig. 7A). The infection efficiency of wild-type AAV in the absence of heparin was arbitrarily set to 1.0. Infection by AAV2 and AAV13 was inhibited by more than 99% in the presence of increasing concentrations of heparin (Fig. 7B and C). The infectivity of the AAV2 and -13 heparin binding mutants was severely reduced and was unresponsive to increasing heparin concentrations (Fig. 7A, B, and C). AAV3 infection could not be fully blocked by heparin; approximately 20 to 30% of the initial infectivity remained at the highest heparin concentration of 1 mg/ml ($P < 0.001$) (Fig. 7D). The AAV3 heparin binding mutant was unresponsive to increasing heparin concentrations. Compared to wild-type (wt) AAV3, the mutant's infectivity was reduced to 50% in the absence of soluble heparin (Fig. 7D). The only partial neutralization of AAV3 by heparin may be taken as an indication of an alternative AAV3 entry mechanism, presumably by coreceptors, as described previously (29–31). As expected, AAV serotypes 1, 6, and rh.10 were resistant to increasing concentrations of natural heparin (Fig. 7E), as anticipated from the lack of binding to natural heparin on the array (Fig. 4A).

The synthetic heparins were available only in limiting amounts, allowing competition assays up to a maximum concentration of 100 μg/ml. At this concentration, AAV2 had shown a clear inhibition by natural low-molecular-weight heparin 14 (Fig. 7B), and this subtype was therefore chosen to test neutralization by synthetic heparin 7, as described above. The results showed that synthetic heparin 7, in contrast to heparin 14, did not neutralize AAV infection (Fig. 8A). Since heparin 7 binding to AAV2 capsids on the array was more efficient than binding to natural heparin, we wondered whether components absent in synthetic heparin were needed for neutralization of AAV infection. To test this hypothesis, samples of natural heparin at concentrations of 1 μg/ml or 10 μg/ml were spiked with 10 μg/ml synthetic heparin 7 each during preincubation with AAV2 prior to infection. As shown in Fig. 8B, the addition of heparin 7 was unable to significantly enhance AAV neutralization by natural heparin. Heparin 7 is a rather short oligosaccharide. Although *in vitro* binding of pure heparin 7 to AAV2 is very efficient (Fig. 4B), a longer chain length may be required *in vivo* for AAV neutralization.

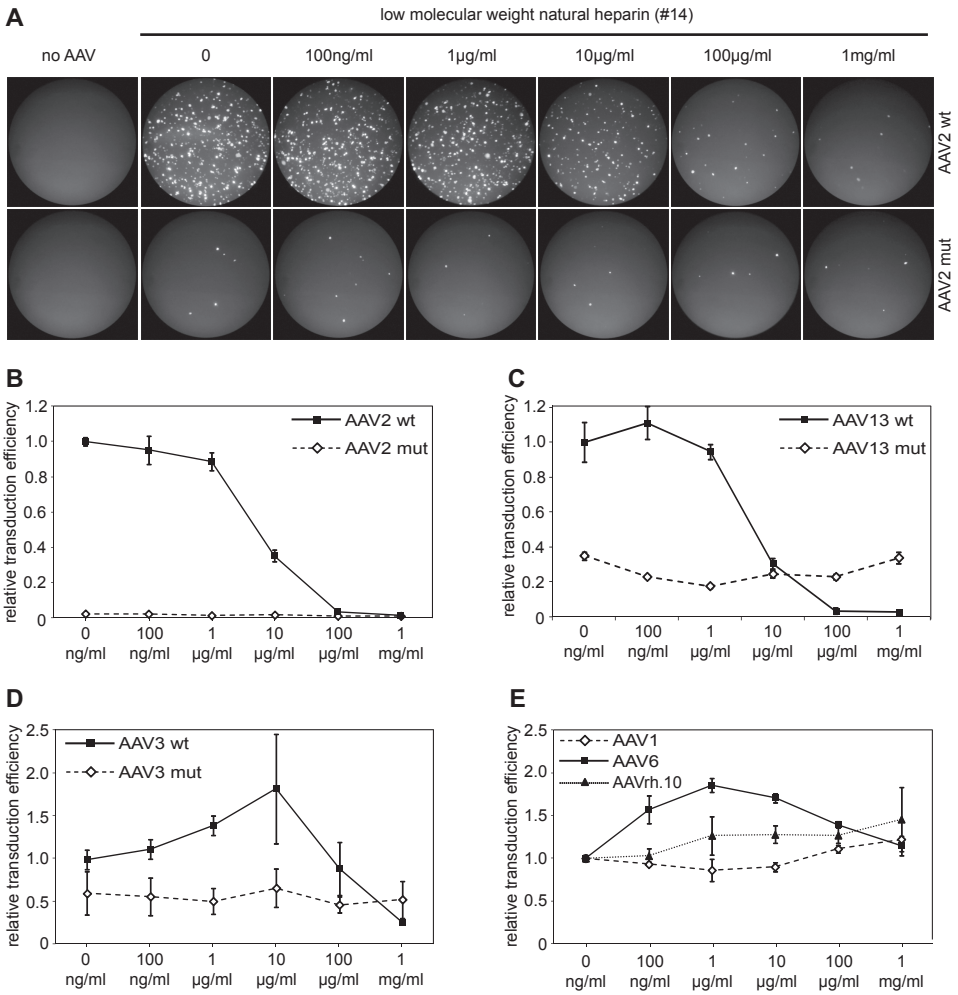

FIG 7 In vivo AAV infection and competition by low-molecular-weight natural heparin. (A) GFP fluorescence of C12 cells infected with AAV2 wt or heparin binding site mutant AAV2(R585A/R588A) GFP vectors. AAV infection was performed in the presence of increasing concentrations of low-molecular-weight heparin as indicated. (B to E) Quantitative analysis ($n = 3$) of infection efficiencies of the indicated AAV serotypes or capsid variants derived from them in the presence of increasing concentrations of low-molecular-weight heparin. The error bars represent standard deviations.

DISCUSSION

Various AAV serotypes differ in the structure of the exposed capsid surfaces (1) that represent the determinants for glycan binding and cell and tissue tropism (32). The primary receptors of eight AAV serotypes have been identified so far (2–7), and they can be assigned to three groups preferentially binding to (i) HSPG (AAV2, AAV3, AAV6, and AAV13), (ii) sialic acid (AAV1, AAV4, AAV5, and AAV6), and (iii) terminal galactose (AAV9). This is the first report to differentiate the HSPG-binding serotypes AAV2, AAV3, AAV6, and AAV13 by their affinities to specific synthetic heparin oligosaccharides. In addition, we further specify the exact nature of glycans bound by sialic acid binding AAVs. Thus, minimal structural glycan requirements could be defined for AAV1, AAV2, AAV3, AAV4, AAV5, AAV6, and AAV13, as summarized in Fig. 9.

Glycan receptor specificities of AAV1 and AAV6. AAV1 and AAV6 capsids differ by only 6 amino acids. Therefore, it is not surprising that the most prominent glycan recognized is the same. The minimal best binding structure, glycan 237, is composed of a terminal α2-3 sialic acid linked to *N*-acetylgalactosamine, followed by a β1-4-linked *N*-acetylglucosamine (Fig. 9). Binding to this glycan has been shown previously for AAV1 empty capsids using an earlier version of the CFG glycan array (5). This previous AAV1 screen was detected by antibodies, indicating that the fluorescent tag did not affect glycan binding specificity. Variants either displaying terminal α2-6 sialic acid or lacking a terminal sialic acid do not bind to either AAV1 or AAV6. Although we cannot exclude the possibility that particular glycans are missing on the array, we did not find evidence for α2-6 sialic acid-containing glycans as the AAV1/6 receptor. In addition, the minimal glycan structure we propose is more complex than previously postulated. Replacement of the middle *N*-acetylgalactosamine by galactose abolishes AAV binding (Fig. 1B). Although *N*-acetylglucosamine appears to be necessary (Fig. 1B), it cannot be determined whether alternative saccharides in this position would also allow binding to AAV1 or AAV6. The required glycan variants are not available on the array. Only AAV6 showed additional, weak interactions to specific heparin compounds, which were low sulfated, with a single *N*-sulfation (Fig. 4B). Natural heparins display a higher degree of sulfation (2.3 to 2.8 sulfates/disaccharide) than HSPG (0.6 to 1.5 sulfates/disaccharide)

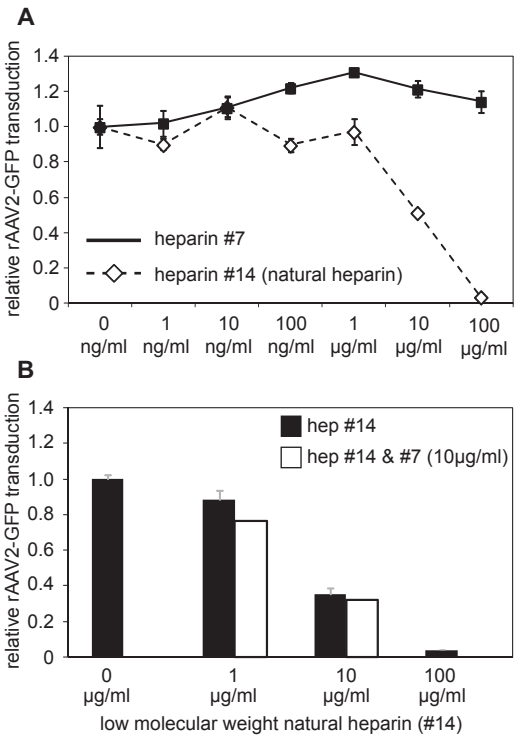

FIG 8 In vivo AAV infection and competition by synthetic heparin. (A) Quantitative analysis of AAV infection of AAV2 vectors in the presence of increasing concentrations of low-molecular-weight natural heparin 14 or synthetic heparin 7. The assay was performed as described in the legend to Fig. 4. (B) AAV2 infection in the presence of increasing concentrations of low-molecular-weight natural heparin 14, either alone or in the presence of 10 μg/ml synthetic heparin (hep) 7. The error bars represent standard deviations.

(13). This difference may explain why competition experiments using natural heparin and AAV6 were not successful in our study (Fig. 7E), as well as in a previous report (14).

Glycan receptor specificity of AAV5. The current notion is that AAV5 capsids bind to both *N*-linked α2-3 and α2-6 sialic acids (4). Here, we confirm that AAV5 capsids recognize glycans with terminal α2-3 sialic acids, but only when they are linked to a sulfated galactose (Fig. 1C and 9). Although the structure is very similar to the one identified for AAV1 and AAV6, no cross-binding was detected. Multiple additional screens with AAV5 empty capsids deposited in the CFG database detected either by capsid-attached fluorophores or by AAV5 antibodies (ADK5) confirm the described binding pattern. All identified branched glycans share the common structure of *N*-glycans (33, 34). AAV5 did not bind to any of the available glycans that exclusively carry α2-6 sialic acid linkages. The lack of evidence for α2-6 sialic acid binding is difficult to reconcile with the description of the AAV5 receptor that has been identified by the use of α2-6-specific sialidases and glycan-expressing cell lines (4).

Glycan receptor specificity of AAV4. The highest binding efficiency of AAV4, more than 100-fold above background, was observed for two linear glycans that share two internal mannose moieties linked by an α1-6 glycosidic bond. Variations of this connectivity were not tolerated (Fig. 1D). The two α1-6-linked mannose moieties alone, however, were not sufficient for AAV4 binding. Only a few more extended variations of the identified linear glycans are present on the CFG array, so the minimal binding structure could not be narrowed down any further. Therefore, glycan 351, which contains two mannose moieties but is devoid of sialic acids, emerged as the minimal best binder for AAV4 (Fig. 9). This finding is surprising in view of the *O*-linked terminal α2-3 sialic acids described previously as an AAV4 receptor (4). Although AAV4 binds to certain branched glycans displaying terminal α2-3 sialic acids, they more closely resemble *N*-glycans, rather than *O*-glycans. Recently, critical amino acids on the outer surface of the AAV4 capsid were characterized (35). Replacement of positively charged lysines by negatively charged glutamic acids dramatically reduced the *in vivo* AAV4 transduction efficiency of the heart and lung, but not of the liver (35). Sialic acids are negatively charged due to a carboxyl group that can interact with positively charged lysines, but not with negatively charged amino acids. Transductions with the described AAV4 mutants resulted in efficiencies comparable to those of AAV4 wild-type vectors after sialidase treatment of the target cells. This may be taken as evidence that the mutated amino acids are involved in sialic acid binding. Since infection of the liver remained largely unaffected, even in the presence of sialidases (35), an additional sialic acid-independent and as yet unidentified cell receptor appears to exist. The identified glycan 348-glycan 351 pair represents a good candidate for an alternative AAV4 cell receptor.

Glycan receptor specificities of AAV2, AAV3, and AAV13. AAV2 and AAV3 have long been known to bind to HSPG, which serves as a primary host cell receptor. HSPGs are ubiquitous on mammalian cell membranes. However, there is considerable structural heterogeneity in terms of chain length, modifications, extent of sulfation, and epimerization within the heparan sulfate molecule (36). This is the first report to demonstrate binding of particular AAVs to chemically distinct synthetic heparins. The heparin binding array shows that both AAV2 and AAV3 bind to 6-*O*- and *N*-sulfated heparan sulfate, whereas AAV3 also binds to 2-*O*- and *N*-sulfated heparan sulfate. AAV13, although closely related to AAV3 (93% identity of the capsids) (7), differs in heparin binding properties. It binds to acetylated 6-*O*- and 2-*O*-sulfated heparins (Fig. 9). The variations in heparin binding specificities appear to reflect reported structural variations of AAV capsids and the relative positions of amino acids found to be critical for heparin binding (7, 37). A recent publication using chemically modified natural heparin further supports the notion that AAV2 binds to 6-*O*- and *N*-sulfated HSPGs (38), and the loss of function of the well-studied AAV2 heparin binding site mutant (R585A/R588A) shows that HSPG binding is critical for cell entry (28). In contrast to the situation with AAV2, transduction with AAV3 was only partially inhibited by soluble heparins. In addition, the heparin binding-deficient AAV3 capsid mutant R594 had retained some infectivity in the presence of heparin (Fig. 7D). Additional AAV3 capsid-exposed amino acids may mediate binding to alternative glycan variants present in mixed natural heparin 14, but not on the CFG glycan array or on the specialized heparin array.

The only synthetic glycan available in sufficient quantities for *in vivo* competition assays was synthetic heparin 7. Although synthetic heparin 7 was bound by AAV2 more efficiently than natural heparin 14, *in vivo* competition assays were unsuccessful. Heparin 7 is a tetrasaccharide of 1.3 kDa that is considerably shorter than natural low-molecular-mass heparin, with a mean mass of 5 kDa, translating into a 14-mer glycosaminoglycan. Previously pub-

AAV serotype	Glycan specificity (symbol nomenclature)	Glycan specificity (text nomenclature)
AAV1	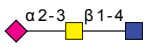	Neu5Acα2-3GalNAcβ1-4GlcNAc
AAV2	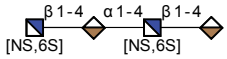	6-O- and N-sulfated heparin
AAV3	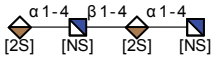	2-O- and N-sulfated heparin
AAV4	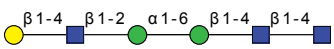	Galβ1-4GlcNAcβ1-2Manα1-6Manβ 1-4GlcNAcβ1-4GlcNAc
AAV5	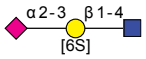	Neu5Acα2-3(6S)Galβ1-4GlcNAc
AAV6	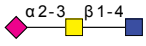	Neu5Acα2-3GalNAcβ1-4GlcNAc
	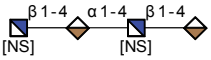	N-sulfated heparin
AAV13	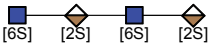	Acetylated, 2/6-O- sulfated heparin

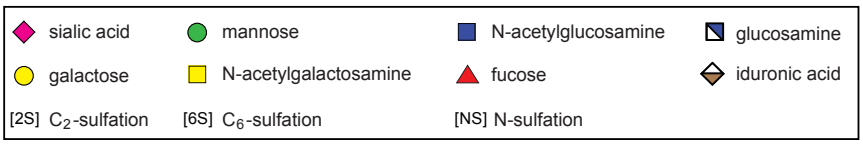

FIG 9 Discriminating minimal glycan structures bound by AAV serotypes 1 to 6 and 13. Definitions of the minimal glycan structure selected to allow discrimination of AAV serotypes 1, 2, 3, 4, 5, 6, and 13 are specified. Glycan structures are displayed in symbol nomenclature and in text nomenclature.

lished competition assays with short, size-fractionated heparins have shown only marginal inhibitory effects on AAV2 infection efficiencies (29). This is in line with the recent claim that a chain length of at least 13 would be needed to make full contact with the positively charged amino acids at the 3-fold symmetry axis on the capsid surface of AAV2 (38). The lack of AAV2 neutralization by heparin 7 could also be explained by lower affinity of AAV for pure synthetic heparins than for mixed natural heparin (Fig. 6B). In this case, AAV binding to heparin 7 might be outcompeted by components of cell culture medium and fetal calf serum or by higher-affinity cell surface-bound HSPG molecules.

Glycan receptor specificities of AAV serotypes 7 to 12. For AAV serotypes 7 to 12, no primary receptor has been described, except for AAV9, where glycans with terminal galactoses were reported (6). Unfortunately, neither the CFG glycan array, with 611 different glycans, nor the heparin array revealed potential interaction partners for any of these serotypes. Since glycans can form an infinite variety of structures, the most likely explanation is that appropriate ligands were not present on the arrays. It will be interesting to see whether updated glycan arrays will detect receptor candidates for these AAV serotypes.

Implications and applications of the identified glycan receptor binding specificity. HSPGs and sialic acids are present on the surface of almost every human cell, yet variant AAV serotypes display distinct cell- and tissue-specific targeting profiles. Their differentiation may have immediate implications for successful AAV infection. The currently best-examined viral-protein–glycan interaction is that of influenza virus hemagglutinin interacting with sialic acids on the cell surface. Human influenza virus strains bind to terminal α2-6 sialic acids linked to galactose, which primarily reside in the human upper respiratory tract, whereas avian influenza virus strains preferentially bind to α2-3 sialic acids linked to galactose. These types of glycans are prevalent in the intestinal mucosa of birds and the lower respiratory tract of humans (39). The variant cell receptor distribution determines the host and pathogenicity profiles of variant influenza virus strains. A comparable description of cell surface determinants would help to further define the targeting profiles of the increasing repertoire of AAV serotypes and their variants. This seems especially relevant in view of the increasing success of AAV vectors in human gene therapy. Research to characterize the glycomes of specific cell types and tissues (e.g., the CFG glycan-profiling program) is in progress. Most of the analyses were done by mass spectrometry, which cannot determine linkages in glycan structures. Our study demonstrates the importance of specific linkages between glycan moieties for binding to AAV capsids. Since these variations may determine if a cell can be infected, alternative methods, like nuclear magnetic resonance spectroscopy, are necessary for full characterization of

the cell glycome (40). Further identification of the preferred binding structures for particular AAV variants may improve gene delivery, as shown recently for enhanced AAV9 cell transduction by prior modification of glycan target cell receptors (41).

ACKNOWLEDGMENTS

We thank John Chiorini (National Institutes of Health, Bethesda, MD, USA) for AAV plasmids and Stefan Weger and Catrin Stutika (Charité, Berlin, Germany) for critical readings of the manuscript.

Generous financial support was provided by the German academic exchange service DAAD (PROMOS) and the Max-Planck Society. A.R. thanks the Studienstiftung des Deutschen Volkes for a doctoral fellowship.

REFERENCES

1. **Agbandje-McKenna M, Kleinschmidt J.** 2011. AAV capsid structure and cell interactions. Methods Mol. Biol. **807:**47–92. http://dx.doi.org/10.1007/978-1-61779-370-7_3.
2. **Summerford C, Samulski RJ.** 1998. Membrane-associated heparan sulfate proteoglycan is a receptor for adeno-associated virus type 2 virions. J. Virol. **72:**1438–1445.
3. **Handa A, Muramatsu S, Qiu J, Mizukami H, Brown KE.** 2000. Adeno-associated virus (AAV)-3-based vectors transduce haematopoietic cells not susceptible to transduction with AAV-2-based vectors. J. Gen. Virol. **81:**2077–2084. http://vir.sgmjournals.org/content/81/8/2077.long.
4. **Kaludov N, Brown KE, Walters RW, Zabner J, Chiorini JA.** 2001. Adeno-associated virus serotype 4 (AAV4) and AAV5 both require sialic acid binding for hemagglutination and efficient transduction but differ in sialic acid linkage specificity. J. Virol. **75:**6884–6893. http://dx.doi.org/10.1128/JVI.75.15.6884-6893.2001.
5. **Wu Z, Miller E, Agbandje-McKenna M, Samulski RJ.** 2006. Alpha2,3 and alpha2,6 N-linked sialic acids facilitate efficient binding and transduction by adeno-associated virus types 1 and 6. J. Virol. **80:**9093–9103. http://dx.doi.org/10.1128/JVI.00895-06.
6. **Bell CL, Vandenberghe LH, Bell P, Limberis MP, Gao GP, Van Vliet K, Agbandje-McKenna M, Wilson JM.** 2011. The AAV9 receptor and its modification to improve in vivo lung gene transfer in mice. J. Clin. Invest. **121:**2427–2435. http://dx.doi.org/10.1172/JCI57367.
7. **Schmidt M, Govindasamy L, Afione S, Kaludov N, Agbandje-McKenna M, Chiorini JA.** 2008. Molecular characterization of the heparin-dependent transduction domain on the capsid of a novel adeno-associated virus isolate, AAV(VR-942). J. Virol. **82:**8911–8916. http://dx.doi.org/10.1128/JVI.00672-08.
8. **Bertozzi CR, Rabuka D.** 2009. Structural basis of glycan diversity, p 23–36. *In* Varki A, Cummings RD, Esko JD, Freeze HH, Stanley P, Bertozzi CR, Hart GW, Etzler ME (ed), Essentials of glycobiology, 2nd ed. Cold Spring Harbor Press, Cold Spring Harbor, NY.
9. **Benallal M, Anner BM.** 1994. Identification of organ-specific glycosylation of a membrane protein in two tissues using lectins. Experientia **50:**664–668. http://dx.doi.org/10.1007/BF01952869.
10. **Molinari M.** 2007. N-glycan structure dictates extension of protein folding or onset of disposal. Nat. Chem. Biol. **3:**313–320. http://dx.doi.org/10.1038/nchembio880.
11. **Zhao YY, Takahashi M, Gu JG, Miyoshi E, Matsumoto A, Kitazume S, Taniguchi N.** 2008. Functional roles of N-glycans in cell signaling and cell adhesion in cancer. Cancer Sci. **99:**1304–1310. http://dx.doi.org/10.1111/j.1349-7006.2008.00839.x.
12. **Nizet V, Esko JD.** 2009. Bacterial and viral infections, p 537–552. *In* Varki A, Cummings RD, Esko JD, Freeze HH, Stanley P, Bertozzi CR, Hart GW, Etzler ME (ed), Essentials of glycobiology, 2nd ed. Cold Spring Harbor Press, Cold Spring Harbor, NY.
13. **Dreyfuss JL, Regatieri CV, Jarrouge TR, Cavalheiro RP, Sampaio LO, Nader HB.** 2009. Heparan sulfate proteoglycans: structure, protein interactions and cell signaling. Ann. Acad. Bras. Cienc. **81:**409–429. http://dx.doi.org/10.1590/S0001-37652009000300007.
14. **Halbert CL, Allen JM, Miller AD.** 2001. Adeno-associated virus type 6 (AAV6) vectors mediate efficient transduction of airway epithelial cells in mouse lungs compared to that of AAV2 vectors. J. Virol. **75:**6615–6624. http://dx.doi.org/10.1128/JVI.75.14.6615-6624.2001.
15. **Schmidt M, Voutetakis A, Afione S, Zheng C, Mandikian D, Chiorini JA.** 2008. Adeno-associated virus type 12 (AAV12): a novel AAV serotype with sialic acid- and heparan sulfate proteoglycan-independent transduction activity. J. Virol. **82:**1399–1406. http://dx.doi.org/10.1128/JVI.02012-07.
16. **Walters RW, Yi SM, Keshavjee S, Brown KE, Welsh MJ, Chiorini JA, Zabner J.** 2001. Binding of adeno-associated virus type 5 to 2,3-linked sialic acid is required for gene transfer. J. Biol. Chem. **276:**20610–20616. http://dx.doi.org/10.1074/jbc.M101559200.
17. **Varki A, Schauer R.** 2009. Sialic acids, p 199–218. *In* Varki A, Cummings RD, Esko JD, Freeze HH, Stanley P, Bertozzi CR, Hart GW, Etzler ME (ed), Essentials of glycobiology, 2nd ed. Cold Spring Harbor Press, Cold Spring Harbor, NY.
18. **Walters RW, Pilewski JM, Chiorini JA, Zabner J.** 2002. Secreted and transmembrane mucins inhibit gene transfer with AAV4 more efficiently than AAV5. J. Biol. Chem. **277:**23709–23713. http://dx.doi.org/10.1074/jbc.M200292200.
19. **Grimm D, Kay MA, Kleinschmidt JA.** 2003. Helper virus-free, optically controllable, and two-plasmid-based production of adeno-associated virus vectors of serotypes 1 to 6. Mol. Ther. **7:**839–850. http://dx.doi.org/10.1016/S1525-0016(03)00095-9.
20. **Aslanidi G, Lamb K, Zolotukhin S.** 2009. An inducible system for highly efficient production of recombinant adeno-associated virus (rAAV) vectors in insect Sf9 cells. Proc. Natl. Acad. Sci. U. S. A. **106:**5059–5064. http://dx.doi.org/10.1073/pnas.0810614106.
21. **Winter K, von Kietzell K, Heilbronn R, Pozzuto T, Fechner H, Weger S.** 2012. Roles of E4orf6 and VA I RNA in adenovirus-mediated stimulation of human parvovirus B19 DNA replication and structural gene expression. J. Virol. **86:**5099–5109. http://dx.doi.org/10.1128/JVI.06991-11.
22. **Mietzsch M, Grasse S, Zurawski C, Weger S, Bennett A, Agbandje-McKenna M, Muzyczka N, Zolotukhin S, Heilbronn R.** OneBac: platform for scalable and high-titer production of AAV serotype 1–12 vectors for gene therapy. Hum. Gene Ther. http://dx.doi.org/10.1089/hum.2013.184.
23. **Noti C, de Paz JL, Polito L, Seeberger PH.** 2006. Preparation and use of microarrays containing synthetic heparin oligosaccharides for the rapid analysis of heparin-protein interactions. Chemistry **12:**8664–8686. http://dx.doi.org/10.1002/chem.200601103.
24. **de Paz JL, Spillmann D, Seeberger PH.** 2006. Microarrays of heparin oligosaccharides obtained by nitrous acid depolymerization of isolated heparin. Chem. Commun. **29:**3116–3118. http://dx.doi.org/10.1039/B605318A.
25. **Wistuba A, Kern A, Weger S, Grimm D, Kleinschmidt JA.** 1997. Subcellular compartmentalization of adeno-associated virus type 2 assembly. J. Virol. **71:**1341–1352.
26. **Yin J, Seeberger PH.** 2010. Applications of heparin and heparan sulfate microarrays. Methods Enzymol. **478:**197–218. http://dx.doi.org/10.1016/S0076-6879(10)78009-5.
27. **Lerch TF, Chapman MS.** 2012. Identification of the heparin binding site on adeno-associated virus serotype 3B (AAV-3B). Virology **423:**6–13. http://dx.doi.org/10.1016/j.virol.2011.10.007.
28. **Opie SR, Warrington KH, Jr, Agbandje-McKenna M, Zolotukhin S, Muzyczka N.** 2003. Identification of amino acid residues in the capsid proteins of adeno-associated virus type 2 that contribute to heparan sulfate proteoglycan binding. J. Virol. **77:**6995–7006. http://dx.doi.org/10.1128/JVI.77.12.6995-7006.2003.
29. **Messina EL, Nienaber J, Daneshmand M, Villamizar N, Samulski J, Milano C, Bowles DE.** 2012. Adeno-associated viral vectors based on serotype 3b use components of the fibroblast growth factor receptor signaling complex for efficient transduction. Hum. Gene Ther. **23:**1031–1042. http://dx.doi.org/10.1089/hum.2012.066.
30. **Blackburn SD, Steadman RA, Johnson FB.** 2006. Attachment of adeno-associated virus type 3H to fibroblast growth factor receptor 1. Arch. Virol. **151:**617–623. http://dx.doi.org/10.1007/s00705-005-0650-6.
31. **Ling C, Lu Y, Kalsi JK, Jayandharan GR, Li B, Ma W, Cheng B, Gee SW, McGoogan KE, Govindasamy L, Zhong L, Agbandje-McKenna M, Srivastava A.** 2010. Human hepatocyte growth factor receptor is a cellular coreceptor for adeno-associated virus serotype 3. Hum. Gene Ther. **21:**1741–1747. http://dx.doi.org/10.1089/hum.2010.075.
32. **Zincarelli C, Soltys S, Rengo G, Rabinowitz JE.** 2008. Analysis of AAV serotypes 1–9 mediated gene expression and tropism in mice after systemic injection. Mol. Ther. **16:**1073–1080. http://dx.doi.org/10.1038/mt.2008.76.
33. **Stanley P, Cummings RD.** 2009. Structures common to different glycans, p 175–198. *In* Varki A, Cummings RD, Esko JD, Freeze HH, Stanley P, Bertozzi CR, Hart GW, Etzler ME (ed), Essentials of glycobiology, 2nd ed. Cold Spring Harbor Press, Cold Spring Harbor, NY.
34. **Stanley P, Schachter H, Taniguchi N.** 2009. N-glycans, p 101–114. *In* Varki A, Cummings RD, Esko JD, Freeze HH, Stanley P, Bertozzi CR, Hart

GW, Etzler ME (ed), Essentials of glycobiology, 2nd ed. Cold Spring Harbor Press, Cold Spring Harbor, NY.
35. **Shen S, Troupes AN, Pulicherla N, Asokan A.** 2013. Multiple roles for sialylated glycans in determining the cardiopulmonary tropism of adeno-associated virus 4. J. Virol. **87:**13206–13213. http://dx.doi.org/10.1128/JVI.02109-13.
36. **Bishop JR, Schuksz M, Esko JD.** 2007. Heparan sulphate proteoglycans fine-tune mammalian physiology. Nature **446:**1030–1037. http://dx.doi.org/10.1038/nature05817.
37. **Lerch TF, Xie Q, Chapman MS.** 2010. The structure of adeno-associated virus serotype 3B (AAV-3B): insights into receptor binding and immune evasion. Virology **403:**26–36. http://dx.doi.org/10.1016/j.virol.2010.03.027.
38. **Zhang F, Aguilera J, Beaudet JM, Xie Q, Lerch TF, Davulcu O, Colon W, Chapman MS, Linhardt RJ.** 2013. Characterization of interactions between heparin/glycosaminoglycan and adeno-associated virus. Biochemistry **52:**6275–6285. http://dx.doi.org/10.1021/bi4008676.
39. **Esko JD, Sharon N.** 2009. Microbial lectins: hemagglutinins, adhesins, and toxins, p 489–500. *In* Varki A, Cummings RD, Esko JD, Freeze HH, Stanley P, Bertozzi CR, Hart GW, Etzler ME (ed), Essentials of glycobiology, 2nd ed. Cold Spring Harbor Press, Cold Spring Harbor, NY.
40. **Brisson JR, Vinogradov E, McNally DJ, Khieu NH, Schoenhofen IC, Logan SM, Jarrell H.** 2010. The application of NMR spectroscopy to functional glycomics. Methods Mol. Biol. **600:**155–173. http://dx.doi.org/10.1007/978-1-60761-454-8_11.
41. **Shen S, Bryant KD, Brown SM, Randell SH, Asokan A.** 2011. Terminal N-linked galactose is the primary receptor for adeno-associated virus 9. J. Biol. Chem. **286:**13532–13540. http://dx.doi.org/10.1074/jbc.M110.210922.
42. **Harvey DJ, Merry AH, Royle L, Campbell MP, Dwek RA, Rudd PM.** 2009. Proposal for a standard system for drawing structural diagrams of N- and O-linked carbohydrates and related compounds. Proteomics **9:**3796–3801. http://dx.doi.org/10.1002/pmic.200900096.

2.3 Arcuate NPY Controls Sympathetic Output and BAT Function via a Relay of Tyrosine Hydroxylase Neurons in the PVN

Authors: Yan-Chuan Shi, Jackie Lau, Zhou Lin, Hui Zhang, Lei Zhai, Guenther Sperk, Regine Heilbronn, Mario Mietzsch, Stefan Weger, Xu-Feng Huang, Ronaldo F. Enriquez, Paul A. Baldock, Lei Zhang, Amanda Sainsbury, Herbert Herzog and Shu Lin

Year: 2013

Journal: Cell Metabolism 17; 236-48

2.3.1 Contribution to the Publication

This publication evolved from the cooperation of my mentor Prof. Heilbronn with Prof Herbert Herzog at the Garvan Institute of Medical Research in Sydney, Australia. The study analyzed the role of Neuropeptide Y (NPY), a 36 amino acid neurotransmitter, for the development of obesity. As indispensable tool for local and persistent NPY expression in the hypothalamus of the CNS, AAV vectors for NPY expression were required that allowed stereotactic injection into sites within the hypothalamus of NPY wild type or knockout mice.

During my diploma thesis I constructed a miniaturized, self complementary scAAV vector with a truncated CBA promoter, a codon-optimized NPY gene, a post-transcriptional regulatory element (WPRE) and a polyA site. The vector backbone was packaged as a self-complementary AAV2 vector and highly purified by HPLC column affinity chromatography to yield concentrated scAAV2 stocks. Functionality of NPY expression from the AAV vectors was verified in cell culture.

As a side project during my thesis, an additional AAV-NPY vector construct was generated with the NPY gene in reverse-complementary orientation embedded within a FLEX element. The corresponding AAV2 vector was packaged and purified as described above. The flipping of the NPY gene in presence of Cre-recombinase was confirmed in cell culture. In transgenic mice expressing the Cre-recombinase under control of the endogenous NPY promoter, NPY expression from AAV vectors after flipping of the NPY gene is only achieved in cells that naturally express NPY.

The AAV-NPY vectors were used by the group of Prof. Herzog for most experiments shown in this publication (Fig. 1B/C, 2, 3 4A/B/C/E/F, 5A/B/C/D, 7C/D/E/F and S1).

http://dx.doi.org/10.1016/j.cmet.2013.01.006

2.4 DNA-Binding Activity of Adeno-Associated Virus Rep Is Required for Inverted Terminal Repeat-Dependent Complex Formation with Herpes Simplex Virus ICP8

Authors: Martin Alex, Stefan Weger, Mario Mietzsch, Heiko Slanina, Toni Cathomen and Regine Heilbronn

Year: 2012

Journal: Journal of Virology 86; 2859-63

2.4.1 Contribution to the Publication

This publication is based on the doctoral dissertation of Martin Alex with the title "Die Bedeutung von Rep78 und ICP8 bei der Initiation der DNA-Replikation des Adeno-assoziierten Virus durch Herpes Simplex Virus" which he submitted to the Charité in May 2010. For subsequent publication of the study, additional experiments with another mutant Rep protein were required. To complement the existing data, I generated a Rep78 mutant with retained DNA-binding and helicase-activity, but deficient endonuclease activity. I characterized its *in vitro* interaction with the herpes simplex virus (HSV) single-stranded DNA binding protein ICP8 on ssDNA and dsDNA AAV genomes in comparison to existing Rep protein mutants as presented in Fig. 1C. Additionally, I analyzed the Rep/ICP8 interaction in the presence of isolated single or double-stranded AAV-ITR-DNA for a panel of existing Rep mutants (Fig. 1E). The results extended the existing model of the initiation of AAV DNA replication (Fig. 2F) in the presence of HSV as the helper virus.

For the publication I contributed the above-mentioned figures, their description and interpretation.

http://dx.doi.org/10.1128/JVI.06364-11

JVI
Journals.ASM.org

DNA-Binding Activity of Adeno-Associated Virus Rep Is Required for Inverted Terminal Repeat-Dependent Complex Formation with Herpes Simplex Virus ICP8

Martin Alex,[a]* Stefan Weger,[a] Mario Mietzsch,[a] Heiko Slanina,[a]* Toni Cathomen,[a,b] and Regine Heilbronn[a]

Institute of Virology, Campus Benjamin Franklin, Charité—Medical School, Berlin, Germany,[a] and Institute of Experimental Hematology, Hannover Medical School, Hannover, Germany[b]

Herpes simplex virus (HSV) helper functions for (AAV) replication comprise HSV ICP8 and helicase-primase UL5/UL52/UL8. Here we show that N-terminal amino acids of AAV Rep78 that contact the Rep-binding site within the AAV inverted terminal repeat (ITR) are required for ternary-complex formation with infected-cell protein 8 (ICP8) on AAV single-strand DNA (ssDNA) *in vitro* and for colocalization in nuclear replication domains *in vivo*. Our data suggest that HSV-dependent AAV replication is initiated by Rep contacting the AAV ITR and by cooperative binding of ICP8 on AAV ssDNA.

A subset of six out of seven herpes simplex virus (HSV)-encoded replication functions was shown to provide helper activity for productive replication of adeno-associated virus (AAV). Four of these, the single-strand-DNA (ssDNA)-binding protein infected-cell protein 8 (ICP8) (UL29) and the heterotrimeric helicase-primase complex UL5/UL8/UL52, constitute the minimal four-protein complex of helper functions for AAV DNA replication (32). Further analysis showed that the helicase UL5 and the primase UL52 are primarily needed as structural components of replicative structures, able to recruit AAV Rep and the AAV genome for the initiation of AAV DNA replication (10, 27).

AAV type 2 contains a 4.7-kb linear single-stranded DNA genome flanked by 145-bp inverted terminal repeats (ITR), which comprise the origins of replication where AAV Rep78 and its C-terminal variant Rep68 bind to the Rep-binding site (RBS). By means of its ATP-dependent helicase activity, Rep unwinds the ITR, and its endonuclease activity leads to nicking of the adjacent terminal resolution site (3, 5, 14, 28). The role of Rep78/68 as *ori*-binding proteins and initiators of AAV DNA replication was analyzed previously using HSV as a helper virus. In coinfection experiments, Rep78 was found to colocalize to HSV ICP8 in nuclear replication compartments in a manner dependent on ITR-flanked single-stranded AAV genomes. Furthermore, direct AAV ssDNA-dependent interaction of purified ICP8 and Rep78 was shown *in vitro* (10). ICP8 displays high-affinity, cooperative binding to ssDNA (1, 7, 20). Rep78/68 also displays some ssDNA-binding activity (16, 19, 36) but preferentially binds to the double-stranded RBS within the hairpin-shaped AAV ITR (12). We have shown before that ssDNA devoid of AAV ITRs displayed severely reduced ternary-complex formation with wild-type Rep78/68 and ICP8 (10).

In this study, we aimed to identify the Rep domain(s) (Fig. 1A and B) responsible for the interaction with ICP8 on the AAV genome. Ternary-complex formation between Rep78, HSV ICP8, and AAV DNA was analyzed by *in vitro* pulldown assays with purified glutathione *S*-transferase (GST)-tagged ICP8 and *in vitro*-translated ^{35}S-labeled Rep proteins as described before (10). Plasmid-excised, full-length AAV wild-type genomes were gel purified and either used directly as linear dsDNA templates or heat denatured to adopt ssDNA conformation. Subsequent snap-cooling on ice ensured reassociation of the hairpin-shaped ITRs flanking the single-stranded AAV genome (9). Rep78 and ICP8 interact to a low degree in the absence of DNA (Fig. 1C; Fig. 1D, lane 3) without enhancement upon addition of double-stranded full-length AAV DNA (Fig. 1D, lane 5). In contrast, single-stranded AAV genomes significantly enhanced the interaction between Rep78 and ICP8 up to 10-fold (Fig. 1C; Fig. 1D, lane 7).

In order to delineate the domain(s) involved in ternary-complex formation, a series of Rep mutants (Fig. 1B) were assessed. As shown in Fig. 1C, ssDNA-dependent complex formation was maintained with the single-amino-acid exchange mutant RepK340H. RepK340H is impaired in ATP-binding precluding DNA helicase activity *in vitro* (3, 4, 35) and AAV DNA replication *in vivo* (2, 17). The ability of RepK340H to bind to the hairpin-structured AAV ITR (4, 23, 24, 33) and its site-specific endonuclease activity are retained (5). Likewise, Rep78 mutants with deletions of the C terminus encompassing the nuclear localization signal (M1/481) retained the ability to interact with ICP8 and AAV ssDNA *in vitro* (Fig. 1C). In contrast, N-terminal-deletion mutants of Rep, shown to be replication negative *in vivo* (13, 17), were entirely deficient for ternary-complex formation *in vitro* (Fig. 1C, Rep52 and Met172). The N terminus of Rep78/68 comprises the DNA-binding domain that mediates site-specific binding to the RBS within the AAV ITR and also the domain for endonuclease activity (Fig. 1A). In addition, endonuclease requires binding to the RBS to exert its activity (5). To differentiate between the two activities, the exclusively endonuclease-deficient mutant RepY156F (5) was generated, which proved to retain

Received 20 September 2011 **Accepted** 16 December 2011
Published ahead of print 28 December 2011
Address correspondence to Regine Heilbronn, regine.heilbronn@charite.de.
* Present address: Martin Alex, Medical Clinic for Oncology and Hematology, CCM, Charité Medical School, Berlin, Germany; Heiko Slanina, Institute of Hygiene and Microbiology, University of Würzburg, Germany.
M.A. and S.W. contributed equally to this article.

doi:10.1128/JVI.06364-11

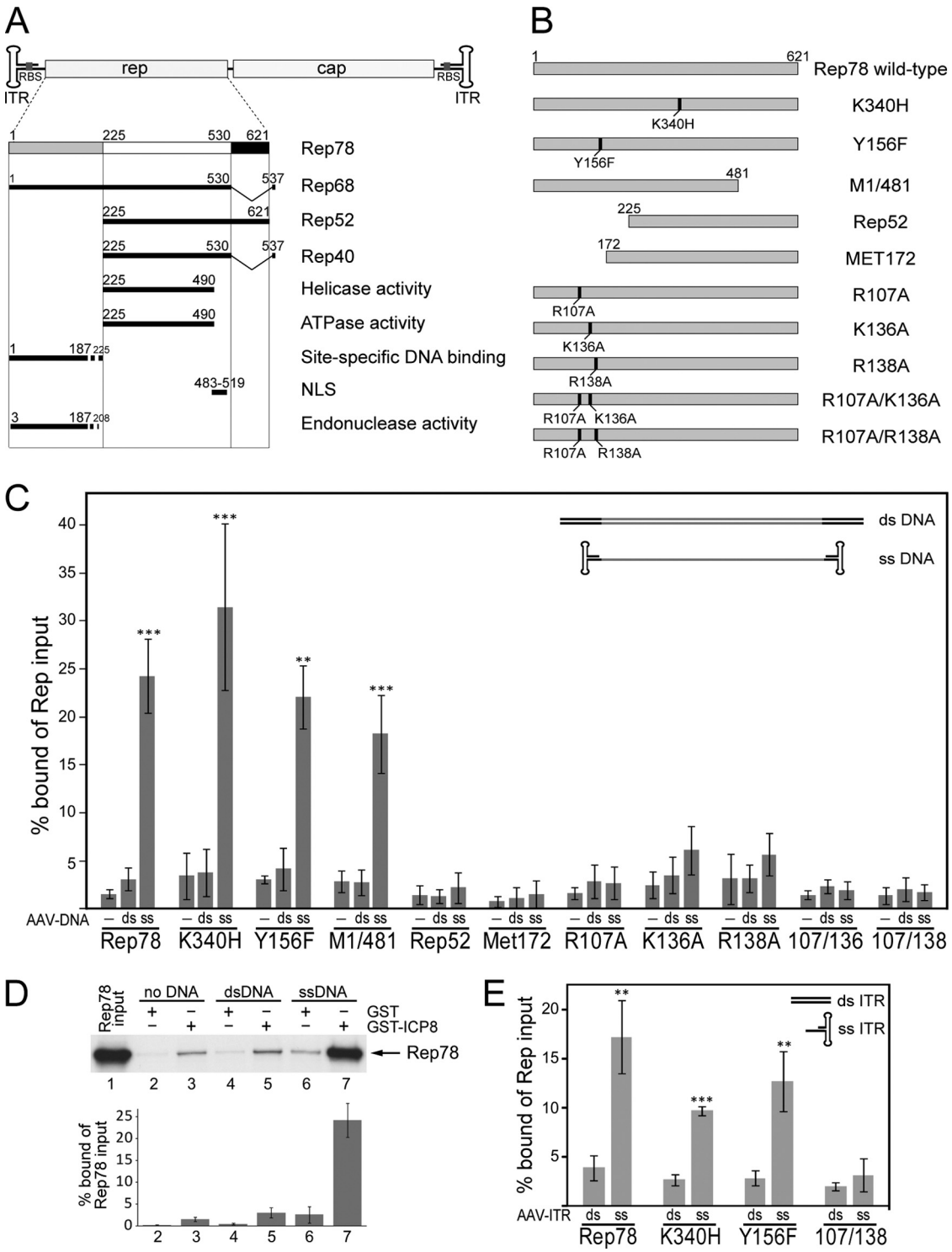

FIG 1 Rep78 domains involved in AAV ssDNA-dependent interaction with HSV ICP8. (A) Individual domains of Rep78 are shown as rectangles. The N terminus unique to Rep78 and Rep68 (amino acids 1 to 225) is gray, the central region common to all four Rep proteins is white, and the C terminus specific to Rep78 and Rep52 derived from unspliced mRNAs is black. Domains involved in functional activities are represented by solid black lines. Approximate amino acid positions are shown as boundary marks as compiled from the literature. The respective references are given in the text. (B) Plasmid constructs for Rep78 and mutants thereof. The mutated amino acids and the amino acid positions are indicated. (C) AAV DNA-dependent interaction of AAV Rep78 with HSV ICP8 was analyzed by *in vitro* GST pulldown assays. *In vitro*-translated ^{35}S-labeled Rep78 and its mutants were incubated with GST-ICP8. Assays were performed either in the absence of DNA, in the presence of double-stranded wild-type AAV-2 DNA, or in the presence of heat-denatured, single-stranded wild-type AAV-2 DNA. Bound Rep proteins were analyzed by autoradiography in sodium dodecyl sulfate-polyacrylamide gel electrophoresis (SDS-PAGE) gels. The results of phosphorimager quantifications in three to five independent experiments are given as means ± standard deviations. Significances were calculated for ssDNA versus dsDNA by Student's *t* test. Significance levels are indicated as follows: ***, $P < 0.001$; **, $P < 0.01$; *, $P < 0.05$. (D) Representative autoradiogram and results of five independent *in vitro* pulldown experiments either with GST alone or with wild-type Rep78, performed as described for panel C. The lane labeled "Rep78input" was loaded with 50% of the amount of Rep included in the binding assay. (E) Results of an experiment performed as described for panel C with AAV plasmid-excised dsITR or hairpin-structured ssITR (nt 1 to 181).

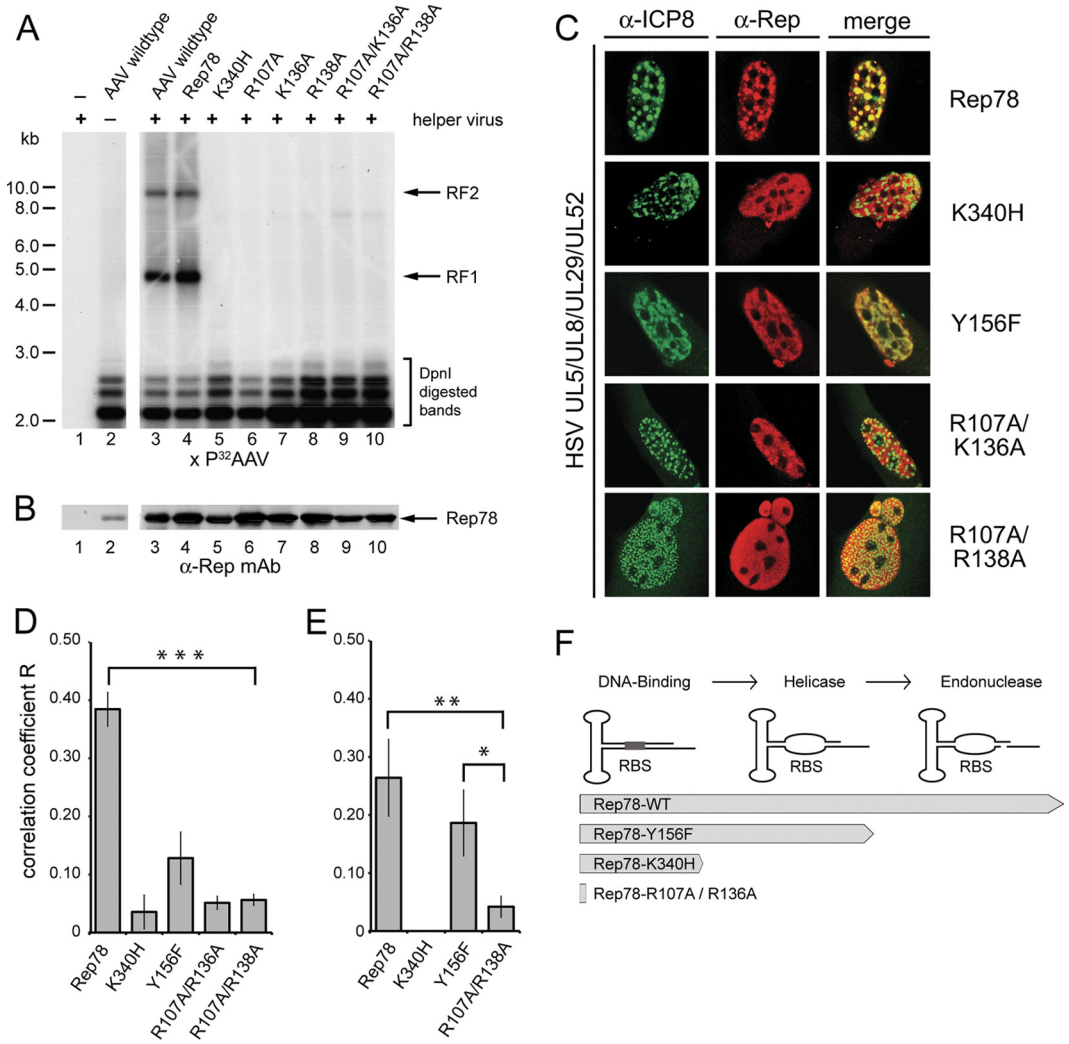

FIG 2 *In vivo* analysis of AAV DNA-dependent nuclear colocalization of Rep78 mutants and ICP8. (A) Analysis of AAV DNA replication by Rep78 and mutants thereof. HeLa cells were transfected with AAV-2 constructs expressing Rep78 or mutants thereof, as described in the text (data not shown for RepY156F). Sixteen hours later, cells were infected with helper virus (Ad-2) and were harvested 24 h postinfection. Low-molecular-weight DNA was prepared by Hirt extraction and digested with DpnI. Equal amounts of DNA were separated on agarose gels, and Southern blots were hybridized with a ^{32}P-labeled DNA probe spanning the AAV cap. Replicated AAV DNA was visualized by autoradiography. RF1 and RF2, monomeric and dimeric replicative forms. Similar results were obtained with helper HSV (data not shown). (B) Rep expression was analyzed by Western blot analysis of cell extracts processed in parallel to the Southern blot in panel A. Rep expression was detected by the anti-Rep monoclonal antibody 303.9. (C) AAV DNA-dependent nuclear colocalization of Rep78 and ICP8. BHK cells grown on coverslips were cotransfected with AAV plasmids expressing Flag-tagged Rep78 wild-type protein or mutants, together with plasmids for the minimal set of HSV helper genes, the primase/helicase complex UL5/UL8/UL52 and the ssDNA binding protein ICP8 (UL29). Cells were fixed and permeabilized by formaldehyde-Triton treatment 40 h later and stained with antibodies against HSV ICP8 and the Flag tag of AAV Rep, followed by fluorophore-labeled secondary antibodies, as described previously (27). Cells were analyzed by confocal microscopy with a Zeiss LSM 510 microscope. The images represent cross sections of 0.8 μm. Anti-ICP8 reactivity is displayed in green, while anti-Flag (Rep) reactivity yields red. Merged foci (yellow) indicate colocalization. (D) Quantification of AAV DNA-dependent nuclear colocalization of Rep78 and ICP8 displayed in panel C. To determine the extent of colocalization, the correlation coefficient (R) of green (ICP8) and red (Rep) fluorescence above a fixed background value was determined with the help of the Zeiss LSM 510 software for a total of 15 cells for each individual construct, and values are means ± standard errors of the means (*, $P < 0.05$; **, $P < 0.01$; ***, $P < 0.001$). (E) Quantification of colocalization of Rep78 and ICP8 in U2OS cells transduced with a monomeric rAAV subtype 2 vector at an MOI of 1×10^4 genomic particles/cell as a source of AAV ssDNA. Cells had been transfected with plasmids expressing Rep and the minimal HSV helper genes. Colocalization was quantified in six individual cells per construct, as described for panel D. (F) The initial steps of Rep-dependent initiation of AAV DNA replication at the AAV ITR are displayed in consecutive order: DNA binding of Rep to the RBS followed by Rep-dependent helicase activity, leading to ssDNA strands, followed by the Rep-dependent endonuclease step. The degree to which Rep78wt and the mutants support these activities are indicated by arrows.

ternary-complex formation (Fig. 1C). Rep mutants with exclusive ITR-binding defects were designed as follows. Based on crystal structure analysis of the N terminus of AAV-5 Rep78 bound to the RBS of the AAV-5 ITR (12), the critical amino acids of AAV-2 Rep78 that contact the ITR were aligned to positions R107, R136, and R138 (11, 12). These amino acid positions were mutated individually or in combination, as shown in Fig. 1B. In pulldown assays, all R-to-A exchanges at position 107 (R107A, R107A/K136A, and R107A/R138A) led to a complete loss and the mutations K136A and R138A to a severe reduction in ternary-complex

formation (Fig. 1C). To further narrow down the presumed site of interaction, the experiment was repeated with the isolated AAV ITR (nucleotides [nt] 1 to 181) in a double-stranded conformation, or a hairpin-structured, partially single-stranded conformation (Fig. 1E). Similar to the entire AAV-2 genome, Rep78wt, RepK340H, and RepY156F retained the capacity for ssDNA-dependent complex formation with ICP8, whereas the RBS binding-deficient mutant RepR107A/R138A lost this activity. Together, these data show that the ability of Rep78 to directly contact the AAV ITR is required for ternary-complex formation with ICP8.

To analyze whether *in vitro* ternary-complex formation is reflected *in vivo* by the ability of AAV-Rep and HSV-ICP8 to colocalize in nuclear replication domains, their distribution was analyzed by confocal microscopy. We had previously demonstrated colocalization of Rep and ICP8 upon coinfection of wild-type AAV and HSV (10) and upon cotransfection of plasmids coding for wild-type AAV-2 and for the minimal set of HSV helper proteins, consisting of ICP8 and the helicase-primase complex UL5/UL8/UL52 (27). Full-length AAV-2 plasmids were generated that expressed Flag-tagged versions of Rep78wt, RepK340H, RepY156F, or N-terminal amino acid exchange mutants. In the presence of helper virus, the plasmids mediated comparable Rep expression but, with the exception of Rep78wt, had lost DNA replication properties (Fig. 2A and B). Subcellular localization of Rep and ICP8 was quantified by confocal microscopy 40 h after cotransfection of expression plasmids for Rep and the four HSV helper functions as described before (27). When transfected alone, Rep and all mutants thereof displayed a homogenous nuclear distribution pattern (data not shown). In the presence of HSV replication proteins, Rep78wt followed the punctate distribution pattern of HSV replication foci and colocalized to ICP8 (Fig. 2C and D), as described before (27). In contrast, the DNA binding-deficient mutants RepR107A/K136A and RepR107A/R138A hardly ever colocalized to ICP8 above threshold levels (Fig. 2C and D). The helicase-deficient mutant RepK340H, despite its ability to form the ternary complex *in vitro*, never colocalized to ICP8, whereas the helicase-proficient mutant RepY156F occasionally colocalized to ICP8 in HSV replication foci (Fig. 2C and D).

To test *in vivo* colocalization on authentic AAV ssDNA, U2OS cells were infected with recombinant AAV (rAAV) vectors at a multiplicity of infection (MOI) of 1×10^4 genomic particles/cell after cotransfection with plasmids for Rep and the four HSV helper genes. The data displayed in Fig. 2E confirmed the drop in colocalization to ICP8 of the N-terminal mutant RepR107A/R136A compared to that of Rep78wt ($P < 0.01$). In contrast, RepY156F showed a high and significant degree of colocalization to ICP8 ($P < 0.05$) just slightly below that of Rep78wt, whereas RepK340H never colocalized with either plasmid- or virus-derived AAV template DNA (Fig. 2D and E). Although both RepK340H and RepY156F can bind to the AAV ITR, only RepY156F unwinds it to expose ssDNA (5), but it cannot proceed with DNA replication due to its endonuclease defect (Fig. 2F). Obviously, the unwound AAV ITR exposes sufficient ssDNA for ICP8 binding. RepK340H, which is entirely defective in ITR unwinding only *in vitro*, binds to ssDNA templates (Fig. 1) but is unable to generate ssDNA for *in vivo* ternary-complex formation.

In summary, colocalization of Rep and ICP8 in nuclear replication domains depends on the ability of Rep to bind and unwind the AAV ITR, generating ssDNA regions. The *in vitro* data show that neither helicase nor endonuclease activities of Rep are needed as such for ternary-complex formation as long as AAV ssDNA is present. In addition, the reduced *in vivo* colocalization of ICP8 and certain Rep78 mutants likely reflects their inability to support AAV DNA replication to generate and amplify sufficient AAV ssDNA templates (Fig. 2F).

HSV ICP8 is characterized by highly cooperative and DNA sequence-independent ssDNA-binding (21) with an apparent binding constant (K_α) for monomeric ICP8 on ssDNA in the range of $1 \times 10^7\ M^{-1}$ (1, 7, 20). Electron microscopy confirmed the highly cooperative but unspecific nature of ICP8 binding to ssDNA (18, 25) whereas Rep molecules on the AAV ssDNA genome bind exclusively to the hairpin-shaped ITR that contains the RBS (14, 15, 34, 37). For Rep78/68 DNA-binding affinities to the isolated RBS of up to $8 \times 10^{10}\ M^{-1}$ were calculated (3, 8, 22), while Rep68 also binds to unrelated ssDNA (16), though with a lower binding affinity, around $2 \times 10^8\ M^{-1}$ (19, 36). Obviously, the affinity of Rep for the AAV ITR is roughly 2 orders of magnitude higher than its affinity for ssDNA. These data, taken together with the above findings, suggest that Rep78/68 serves as the driving force for ternary-complex formation by binding to the RBS within the ITR. Due to the high degree of cooperativity, ICP8 quickly covers available ssDNA regions. We cannot say at present whether the two processes are coupled or take place independently. Rep domains interacting with heterologous proteins have been exclusively mapped to the C terminus (6, 8, 26, 29–31), and the ICP8 domain for interactions with heterologous proteins was described as separate from that engaged in cooperative ssDNA binding (21). In an alternative scenario, formation of the ternary complex could therefore be initiated by protein-protein interaction of ICP8 and Rep with subsequent binding to the AAV genome. Our data extend previous evidence that Rep78 serves as origin-binding protein on the AAV ITR (27). In analogy to the HSV *ori*-binding protein (UL9), AAV Rep78 binds and unwinds the AAV ITR and recruits ICP8, the HSV helicase-primase complex, and additional replication factors to initiate AAV DNA replication.

ACKNOWLEDGMENTS

We thank E. Hammer for experienced technical help, J. Richter for expert confocal microscopy service, and C. Stutika for critical reading of the manuscript.

The initial phase of the study was supported by grants from the Deutsche Forschungsgemeinschaft, DFG-SFB506.

REFERENCES

1. **Boehmer PE, Craigie MC, Stow ND, Lehman IR.** 1994. Association of origin binding protein and single strand DNA-binding protein, ICP8, during herpes simplex virus type 1 DNA replication in vivo. J. Biol. Chem. **269**:29329–29334.
2. **Chejanovsky N, Carter BJ.** 1990. Mutation of a consensus purine nucleotide binding site in the adeno-associated virus *rep* gene generates a dominant negative phenotype for DNA replication. J. Virol. **64**:1764–1770.
3. **Chiorini JA, et al.** 1994. Sequence requirements for stable binding and function of Rep68 on the adeno-associated virus type 2 inverted terminal repeats. J. Virol. **68**:7448–7457.
4. **Davis MD, Wonderling RS, Walker SL, Owens RA.** 1999. Analysis of the effects of charge cluster mutations in adeno-associated virus Rep68 protein in vitro. J. Virol. **73**:2084–2093.
5. **Davis MD, Wu J, Owens RA.** 2000. Mutational analysis of adeno-associated virus type 2 Rep68 protein endonuclease activity on partially single-stranded substrates. J. Virol. **74**:2936–2942.
6. **Di Pasquale G, Stacey SN.** 1998. Adeno-associated virus Rep78 protein interacts with protein kinase A and its homolog PRKX and inhibits CREB-dependent transcriptional activation. J. Virol. **72**:7916–7925.

7. **Dudas KC, Ruyechan WT.** 1998. Identification of a region of the herpes simplex virus single-stranded DNA-binding protein involved in cooperative binding. J. Virol. **72**:257–265.
8. **Han SI, et al.** 2004. Rep68 protein of adeno-associated virus type 2 interacts with 14-3-3 proteins depending on phosphorylation at serine 535. Virology **320**:144–155.
9. **Heilbronn R, Bürkle A, Stephan S, zur Hausen H.** 1990. The adeno-associated virus *rep* gene suppresses herpes simplex virus-induced DNA-amplification. J. Virol. **64**:3012–3018.
10. **Heilbronn R, et al.** 2003. ssDNA-dependent colocalization of adeno-associated virus Rep and herpes simplex virus ICP8 in nuclear replication domains. Nucleic Acids Res. **31**:6206–6213.
11. **Hickman AB, Ronning DR, Kotin RM, Dyda F.** 2002. Structural unity among viral origin binding proteins: crystal structure of the nuclease domain of adeno-associated virus Rep. Mol. Cell **10**:327–337.
12. **Hickman AB, Ronning DR, Perez ZN, Kotin RM, Dyda F.** 2004. The nuclease domain of adeno-associated virus rep coordinates replication initiation using two distinct DNA recognition interfaces. Mol. Cell **13**: 403–414.
13. **Hörer M, et al.** 1995. Mutational analysis of adeno-associated virus Rep. protein-mediated inhibition of heterologous and homologous promoters. J. Virol. **69**:5485–5496.
14. **Im D-S, Muzyczka N.** 1990. The AAV origin-binding protein Rep68 is an ATP-dependent site-specific endonuclease with helicase activity. Cell **61**: 447–457.
15. **Im D-S, Muzyczka N.** 1989. Factors that bind to adeno-associated virus terminal repeats. J. Virol. **63**:3095–3104.
16. **Im D-S, Muzyczka N.** 1992. Partial purification of adeno-associated virus Rep78, Rep52, and Rep40 and their biochemical characterization. J. Virol. **66**:1119–1128.
17. **Kleinschmidt JA, Möhler M, Weindler F, Heilbronn R.** 1995. Sequence elements of the adeno-associated virus *rep*-gene required for suppression of herpes-simplex virus induced DNA amplification. Virology **206**:254–262.
18. **Makhov AM, Boehmer PE, Lehman IR, Griffith JD.** 1996. Visualization of the unwinding of long DNA chains by the herpes simplex virus type 1 UL9 protein and ICP8. J. Mol. Biol. **258**:789–799.
19. **Mansilla-Soto J, et al.** 2009. DNA structure modulates the oligomerization properties of the AAV initiator protein Rep68. PLoS Pathog. **5**:e1000513.
20. **Mapelli M, Mühleisen M, Persico G, van der Zandt H, Tucker PA.** 2000. The 60-residue C-terminal region of the single-stranded DNA binding protein of herpes simplex virus type 1 is required for cooperative DNA binding. J. Virol. **74**:8812–8822.
21. **Mapelli M, Panjikar S, Tucker PA.** 2005. The crystal structure of the herpes simplex virus 1 ssDNA-binding protein suggests the structural basis for flexible, cooperative single-stranded DNA binding. J. Biol. Chem. **280**:2990–2997.
22. **McCarty DM, Ryan JH, Zolotukhin S, Zhou X, Muzyczka N.** 1994. Interaction of the adeno-associated virus Rep protein with a sequence within the A palindrome of the viral terminal repeat. J. Virol. **68**:4998–5006.
23. **Owens RA, Trempe JP, Chejanovsky N, Carter BJ.** 1991. Adeno-associated virus rep proteins produced in insect and mammalian expression systems: wild-type and dominant-negative mutant proteins bind to the viral replication origin. Virology **184**:14–22.
24. **Owens RA, Weitzman MD, Kyöstiö SRM, Carter BJ.** 1993. Identification of a DNA-binding domain in the amino terminus of adeno-associated virus Rep proteins. J. Virol. **67**:997–1005.
25. **Ruyechan WT, Weir AC.** 1984. Interaction with nucleic acids and stimulation of the viral DNA polymerase by the herpes simplex virus type 1 major DNA-binding protein. J. Virol. **52**:727–733.
26. **Schmidt M, Chiorini JA, Afione S, Kotin R.** 2002. Adeno-associated virus type 2 Rep78 inhibition of PKA and PRKX: fine mapping and analysis of mechanism. J. Virol. **76**:1033–1042.
27. **Slanina H, Weger S, Stow ND, Kuhrs A, Heilbronn R.** 2006. Role of the herpes simplex virus helicase-primase complex during adeno-associated virus DNA replication. J. Virol. **80**:5241–5250.
28. **Snyder RO, et al.** 1993. Features of the adeno-associated virus origin involved in substrate recognition by the viral Rep protein. J. Virol. **67**: 6096–6104.
29. **Weger S, Hammer E, Heilbronn R.** 2004. SUMO-1 modification regulates the protein stability of the large regulatory protein Rep78 of adeno associated virus type 2 (AAV-2). Virology **330**:284–294.
30. **Weger S, Hammer E, Heilbronn R.** 2002. Topors, a p53 and topoisomerase I binding protein, interacts with the adeno-associated virus (AAV-2) Rep78/68 proteins and enhances AAV-2 gene expression. J. Gen. Virol. **83**:511–516.
31. **Weger S, Wendland M, Kleinschmidt J, Heilbronn R.** 1999. The adeno-associated virus type 2 regulatory proteins Rep78/Rep68 interact with the transcriptional coactivator PC4. J. Virol. **73**:260–269.
32. **Weindler FW, Heilbronn R.** 1991. A subset of herpes simplex virus replication genes provides helper functions for productive adeno-associated virus replication. J. Virol. **65**:2476–2483.
33. **Weitzman MD, Kyöstiö SRM, Carter BJ, Owens RA.** 1996. Interaction of wild-type and mutant adeno-associated virus (AAV) Rep proteins on AAV hairpin DNA. J. Virol. **70**:2440–2448.
34. **Weitzman MD, Kyöstiö SRM, Kotin RM, Owens RA.** 1994. Adeno-associated virus (AAV) Rep. proteins mediate complex formation between AAV DNA and its integration site in human DNA. Proc. Natl. Acad. Sci. U. S. A. **91**:5808–5812.
35. **Wonderling RS, Kyostio SR, Owens RA.** 1995. A maltose-binding protein/adeno-associated virus Rep68 fusion protein has DNA-RNA helicase and ATPase activities. J. Virol. **69**:3542–3548.
36. **Yoon-Robarts M, et al.** 2004. Residues within the B′ motif are critical for DNA binding by the superfamily 3 helicase Rep40 of adeno-associated virus type 2. J. Biol. Chem. **279**:50472–50481.
37. **Young SM, Jr., McCarty DM, Degtyareva N, Samulski RJ.** 2000. Roles of adeno-associated virus Rep. protein and human chromosome 19 in site-specific recombination. J. Virol. **74**:3953–3966.

3 Discussion

Gene therapy with AAV vectors is becoming increasingly successful in clinical trials. The major impediment to progress with increasing patient numbers constitutes the availability of AAV vectors in sufficient quantities. While rAAV production in adherent 293 cells is mostly sufficient for pre-clinical trials with mice or other small-animal models, its limits in scalability hamper broader application in humans. In a recently published gene therapy trial for the treatment of hemophilia B with six participants [93] $2x10^{15}$ AAV vectors (genomic particles) were produced in a total of 432 10-stack culture chambers [124]. The amount of AAV vectors needed for a single treatment of six patients was produced in ~275 m^2 of cell monolayer, equaling the size of a tennis court.

Alternative AAV production systems have been developed which are appropriate for the growth in bioreactors. Suspension culture-adapted rAAV vector production induced by infection with either adenovirus, baculovirus or herpesvirus have been described [125]. Glybera®, the first human gene therapy to become commercially available [94], represents a rAAV1 vector that is produced by one of the most advanced technologies: triple infection of *Sf*9 cells with three recombinant baculovirus (Bac) strains to deliver the required components.

3.1 Scalable AAV Vector Production in Insect Cells

The three Bac system has been shown to produce high-titer rAAV preparations. However, the requirement of three different baculoviruses reduces the effectiveness of this production system. In the present thesis the scalable OneBac *Sf*9-based rAAV productions system, previously described for AAV1 and AAV2 by Aslanidi *et al.* [103] was used as starting point to adapt it for the full range of available AAV serotypes 1-12. The newly generated cell lines for AAV production allowed stable, high-titer rAAV production with higher per cell burst sizes than HEK 293 cells. Additionally, the infectivity and structural integrity of AAV vectors produced in these cell lines were mostly comparable to the vectors derived from HEK 293 cells, the only system offering easy access to an extended range of AAV serotypes so far. Compared to other scalable rAAV production systems, which are based on the infection of mammalian cells by adenovirus or herpes virus, insect cell culture offers the advantage of very modest growth requirements, neither bovine fetal calf serum (FCS) nor supplementation of CO_2 are needed. Insect cells can easily be cultured in bioreactors up to a volume of 200 liter and higher [126]. Furthermore, rAAV production in insect *Sf*9 cells by infection with recombinant baculoviruses represents the only scalable system that allows vector generation in the absence of a human pathogen. The original *Sf*9 cell-based rAAV production system required the coinfection of three different recombinant baculoviruses for the

transfer of AAV *rep* and *cap* genes and the desired transgene cassette in the rAAV producer cells [101]. This production method has been shown to efficiently generate AAV vectors. Unfortunately, the genetic instability of recombinant baculoviruses leads to the accumulation of baculoviruses lacking the transgene after 5-6 virus passages [127], which limits the efficiency of large-scale rAAV production. Especially, the separate propagation of three individual inherently unstable recombinant baculovirus strains, Bac-*rep*, Bac-*cap*, and Bac-rAAV, reduces the effectiveness of the three Bac rAAV production system. Last but not least, a carefully balanced testing of optimal multiplicities of infection (MOI) is required to ensure that a high percentage of the cells are infected with at least one copy of each baculovirus strain to be productive.

To overcome this limitation, the number of coinfecting baculoviruses needed for AAV production should be reduced down to one. This can be achieved either by the construction of a recombinant baculovirus providing *rep*, *cap* and the rAAV cassette in one Bac or by the generation of stable *rep*/*cap* expressing *Sf*9 cell lines, so that only one baculovirus carrying the AAV vector genome is needed as described by Aslanidi *et al.* [103]. The construction of recombinant baculoviruses with three different genetic elements is not trivial and genetic stability of the recombinant baculovirus genome with large insertions may even be more critical. Moreover, such baculoviruses lack flexibility since they have to be reconstructed anew once rAAV-transgenes or serotype capsids have to be changed. Stable *rep*/*cap* expressing cell lines are more versatile and were therefore chosen for AAV production as described here. The generated cell lines harboring *cap* genes of different AAV serotypes offer similar convenience of cell growth and upscaling capabilities as unmodified *Sf*9 cells. For the generation of AAV vectors, baculovirus strains containing the desired rAAV cassette can be applied to any cell line. Thereby the transgene can be easily packaged into capsids of the AAV serotype of choice. Furthermore, the Bac-rAAVs constructed for the original three baculovirus rAAV production method are compatible with the OneBac system and require no further adaptations. The production of rAAV vectors like Glybera® which is currently produced by the three baculovirus system could be dramatically facilitated.

3.2 AAV Purification

At the beginning of my thesis the most advanced technique for AAV vectors purification constituted of iodixanol gradient ultracentrifugation followed by affinity chromatography either on heparin agarose columns in case of heparin-binding AAV serotypes or on anion-exchange columns for all other AAV serotypes [128,129]. For the planned glycan interaction studies highly concentrated and absolutely pure AAV preparations were required and the available protocols for AAV purification were critical in this respect. Anion-exchange purification is based on the net charge of proteins, which don’t exclude contaminating proteins of similar charge and may reduce

the degree of AAV purity. Heparin columns on the other hand bind heparin-binding proteins, which could severely compromise the analysis of the glycan interaction. A newly available affinity chromatography technique (AVB sepharose) was therefore chosen, which is based on single chain antibodies specific for AAV capsids. This method was originally described by the supplier to support purification of the AAV serotypes 1, 2, 3 and 5 but was shown here to be applicable to almost all AAV serotypes except AAV9 and AAV11. Direct comparison of AAV2 vectors purified by heparin agarose or with AVB sepharose revealed even higher AAV yields with the new technique. In a comparative analysis the AAV vectors from either purification protocol showed similar infectivity levels (unpublished data).

3.3 AAV – Glycan Interaction

For the analysis of the glycan binding characteristics of AAV, AVB-purified AAV vectors were labeled with a fluorescent dye which allows the detection of the vectors bound to glycan arrays. These vectors were incubated either on glycan arrays of the Consortium for Functional Glycomics (CFG) or on specialized heparin arrays developed by the group of Peter H. Seeberger (Max-Planck Institute of Colloids and Interfaces, Potsdam) [130]. The results of these analyses showed differential glycan binding capacities for the AAV serotypes 1-6 and 13 whereas no glycan binding partner could be found for the remaining AAV serotypes. These serotypes (AAV7-12) need to be analyzed on updated glycan arrays with alternative glycan structures to identify appropriate ligands.

According to the previous criteria of the receptors for specific AAVs, some serotypes, e.g. AAV1, AAV4, AAV5 and AAV6, should have bound to fifty or seventy different glycan structures on the CFG glycan array. However, only few defined glycan structures showed efficient binding to AAV capsids. Interestingly, the variant AAV serotypes with previously described similar receptors binding characteristics (chapter 1.1.5) bound to chemically divergent glycan structures.

Differential and discriminating AAV glycan binding characteristics could be exploited for several applications in AAV gene therapy. As soon as the full glycome of a chosen cell type is determined a prediction of the ideal AAV serotype for AAV vectored gene transfer may become possible. Furthermore, external modifications (e.g. by enzymes) of the cell surface glycan composition may help to enhance cell transduction efficiencies. An example for this possibility represents a recent study in which mice were pretreated with neuraminidase leading to an increased efficiency of rAAV9 vector delivery [89]. Moreover, the selective glycan binding properties of the different AAV serotypes may be exploited for diagnostic approaches to differentiate AAV serotypes. Thereby the purity and the identity of the AAV vector capsids may be analyzed in rAAV batches produced in bioreactors.

3.4 Application of AAV Vectors for Genetic Studies

AAV vectors are increasingly applied in gene therapy, especially for the treatment of monogenetic disorders. Alternatively, AAV vectors can also be utilized for basic genetic research. Traditionally, the functions of genes are studied using genetically modified mouse models such as knockin or knockout mice, which may lead to changes in a mouse's developmental phenotype. However, the modified genes affect cells throughout the entire body. Multiple functions of a gene may therefore cause interfering phenotypes. Furthermore, some gene knockouts are developmentally lethal, which makes the determination of a gene's function difficult.

By local injection of AAV vectors a desired gene can be overexpressed in a cell-type or tissue-specific manner. Alternatively, the expression of a protein can also be repressed in case of packaged siRNA/miRNA-cassettes. Thereby the function of a gene of a defined tissue and its effects on the whole organism can be characterized.

In the present thesis AAV vectors have been developed for a collaboration project to analyze the role of NPY for the development of obesity. For this study in mice, self-complementary rAAV2-NPY vectors were generated, which allow the immediate expression of NPY in neurons. Due to the reduced packaging capacity of scAAV vectors a truncated CBA promoter was generated and cloned upstream of the NPY gene. Whereas in cell culture (transduction of 293 cells) only the NPY precursor of 97 amino acids was detectable, the precursor was successfully processed to the 36 amino acid neurotransmitter in neurons *in vivo* (unpublished data). These AAV-NPY vectors were injected stereotactically close to the arcuate nucleus of the hypothalamus of wild type and NPY knockout mice confirming not only the role of NPY as appetite stimulant but also providing evidence for a role of NPY for the reduction of energy expenditure. AAV vector-induced NPY expression induced long-lasting expression over months, as required for extended periods of animal observation. Preceding studies had injected recombinant NPY whose half-life *in vivo* is too short for a long-term functional read-out [131]. Furthermore, the vector-encoded transgene is properly processed by the cell transcription/translation machinery, thereby mimicking the natural expression and processing system, e.g. release of the neurotransmitter from the cell only upon a certain stimulus.

Despite precise stereotactic injection and usage of cell-type-specific AAV serotypes the transgene may also be delivered to other cells at the site of the injection. Especially in the CNS with neurotransmitter-secreting neurons embedded in astrocytes and neuroglia, unintentional AAV vector-mediated expression of neurotransmitter in the "wrong" cell type may impair the analysis of their function. To circumvent this problem Cre recombinase (Cre)-dependent FLEX elements have been developed [132]. Genetic elements embedded within the FLEX cassette were shown to be

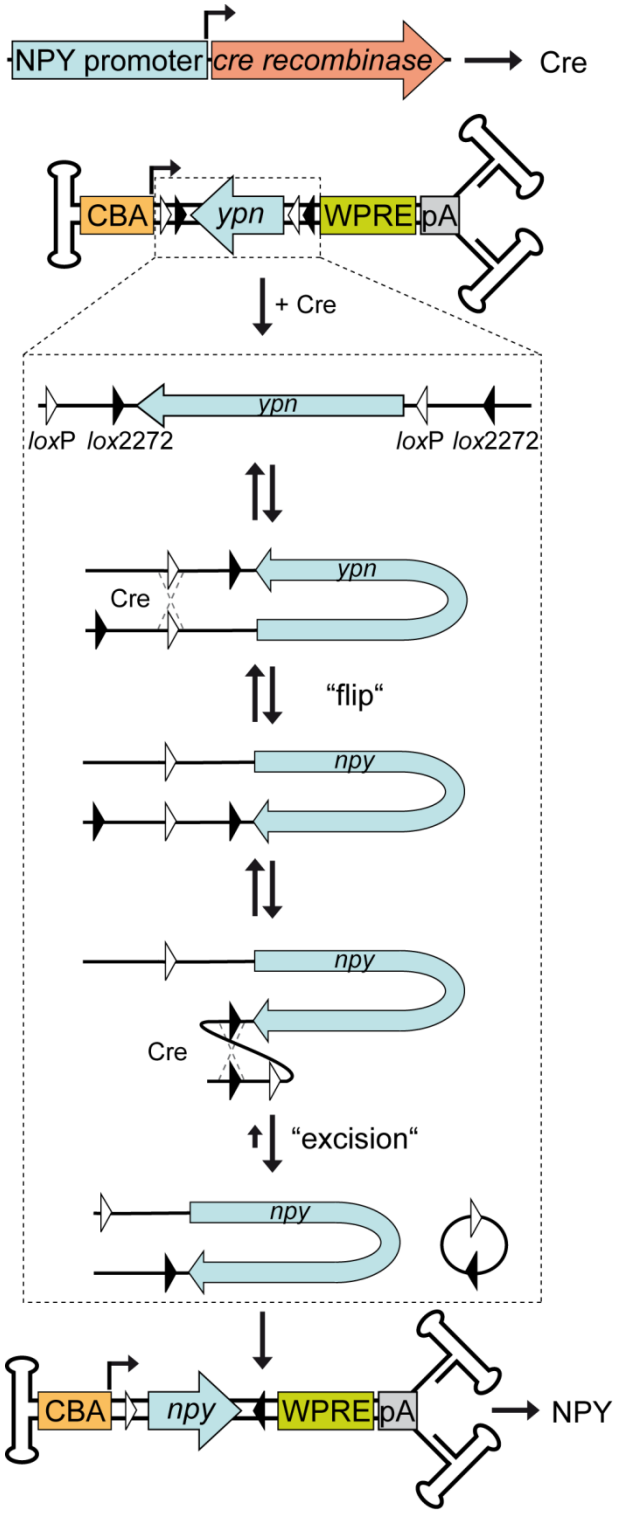

Fig. 10 Flip-Excision (FLEX) Mechanism of AAV-FLEX-NPY Expression Cassettes: AAV vectors injected in transgenic mice (NPY:*cre*) only lead to expression of NPY in neurons with an active NPY promoter. In these neurons Cre-recombinase is expressed which catalyzed the inversion of the NPY-ORF. CBA = CBA promoter, WPRE = Woodchuck post-transcriptional regulatory element, pA = polyA signal

inverted in the presence of Cre recombinase (Fig. 10). The inversion occurs in two steps. Binding of Cre to either pair of homologous lox recognition sites results in a recombination of these sites and the "flipping" of embedded DNA sequences. In the second step Cre catalyzes the recombination between the other pair of lox recognition sites leading to the excision of a small genetic element containing two lox recognition sites. After the excision of these recognition sites the resulting DNA construct is stable since the excision is a product-favored reaction. In this thesis AAV vectors with an inverted NPY-ORF embedded in a FLEX element were constructed (Fig. 10). The functionality of the FLEX-NPY cassette was verified in cell culture by cotransfection of a Cre-expressing plasmid (unpublished data). For *in vivo* delivery of the AAV-NPY-FLEX vectors transgenic mice were used with the *cre* gene under the control of the endogenous NPY promoter. In these mice expression of vectored NPY was restricted to neurons which allow expression of NPY in wild type mice. Non-NPY-expressing nearby neurons transduced by AAV-NPY-FLEX vectors will fail to produce Cre required for vectored NPY expression.

3.5 Viral Helper Factors for the Initiation of AAV Replication

No matter which production system is used for the generation of AAV vectors helper factors are necessary for the initiation of the AAV DNA replication. As shown in this thesis unwinding of the DNA through the Rep helicase activity after binding to the RBS recruits HSV ICP8 which binds to single stranded DNA. Similarly, the adenoviral E2A single stranded DNA binding protein was shown to be necessary for AAV replication [24]. While adenoviruses mostly promote AAV replication indirectly, HSV can directly enhance AAV replication by its replication machinery [29]. For baculoviruses, especially the best-characterized baculovirus, *Autographa californica* multicapsid nucleopolyhedrovirus (AcMNPV), the helper factors necessary for AAV replication have not yet been described. Similar to herpesviruses, baculoviruses have a large dsDNA genome of approximately 134 kb and encode their own replication machinery [133]. One could speculate that the Ac-ssDNA-binding protein encoded by the lef3 gene [134] is responsible for ssDNA-binding to the single-stranded AAV genome similar to adenovirus E2A or the HSV ICP8 protein. Furthermore, a direct promotion of AAV DNA replication could involve the Ac-DNA polymerase [135] and Ac-helicase similar to comparable enzymes of the HSV DNA polymerase complex (UL30/UL42) and the helicase/primase complex (UL5/UL8/UL52). Additional evidence comes from biochemical studies which have shown that the Ac-DNA polymerase is closely related to the DNA polymerases from herpes- and poxviruses [136]. The transactivation of the AAV promoters as shown for adenoviral E1A or HSV ICP0 could be mediated by the Ac-transactivator proteins IE-0 and/or IE-1 [137]. For IE-1 binding to the AAV2 p19-promoter has already been demonstrated [103]. Whether a transactivating effect of IE-1 on the AAV promoters exists has not been analyzed so far.

To test the hypothetical baculovirus helper factors isolated genes could be cotransfected in cells similar to the approaches that have previously led to the identification and characterization of the HSV helper proteins [30]. In a first step the ssDNA-binding protein from AcMNPV could be expressed *in vitro* and the colocalization to Rep proteins in presence of ssAAV genomes could be analyzed similar as presented in our publication.

The identification of the helper factors from baculovirus would be of help to improve the genetic stability of the inherently unstable recombinant baculoviruses. Critical and possibly unnecessary Bac genes not required for AAV replication and baculovirus propagation in cell culture could be deleted. Initial experiments in this direction, deleting chitinase and cathepsin protease genes, which are only necessary for dissemination of progeny virions in insects, had positive effects for the expression of recombinant proteins [138].

4 Summary

Gene therapy based on adeno-associated virus (AAV) vectors becomes a very promising option for the treatment of monogenetic disorders. For broad clinical application of AAV vectors efficient and economical production methods are required to keep pace with the rapidly increasing demand. In this thesis, a scalable rAAV production system was developed with individual stable insect *Sf*9 cell lines harboring the AAV1–12 *rep* and *cap* genes. Upon infection with a single baculovirus carrying the rAAV vector genome stable, high-titer rAAV production is induced for an AAV serotype of choice. AAV vectors generated by these cell lines reached higher per cell burst sizes with infectivities similar to vectors produced by the current gold standard, plasmid transfection of HEK 293 cells.

For transgene delivery of AAV vectors of variant serotypes to the target cells binding of the capsids to a specific receptor on the host cell is required. The capsids of different AAV serotypes have been shown to use variable cell surface glycans as their primary receptors. In this thesis the analysis of highly-purified, fluorescence-labeled AAV capsids to hundreds of synthetic glycan structures or heparins on microarrays led to the identification of specific glycans which bound to AAV capsids in a serotype-dependent manner. Furthermore, the natural heparin binding AAV serotypes 2, 3, 6, and 13 were shown for the first time to bind to different chemical-defined, synthetic heparins. Through comparative analysis of binding and non-binding glycans the minimal binding structure for various AAV serotypes could be determined thereby extending the existing definition of the host cell receptors.

For a neurobiological collaboration project AAV vectors for the expression of neuropeptide Y (NPY) have been generated in this thesis. These vectors were used in genetic studies investigating the role of NPY for the development of obesity in mice. Stereotactic injections into the hypothalamus of wild type and NPY knock-out mice confirmed not only the function of NPY as an appetite stimulant but also gave evidence for a role of NPY in the reduction of energy expenditure.

In addition to baculovirus-infected insect cells AAV vectors can also be produced in mammalian cells by infection of herpesviruses (HSV). In this process the HSV-encoded replication machinery is required for AAV DNA replication. The AAV replication is initiated by the formation of a ternary complex of AAV Rep78 and HSV-ICP8 at the single-stranded AAV DNA genome. Studies with different AAV Rep mutants demonstrated that an intact DNA binding domain of Rep78 is necessary for the formation of the ternary complex. With the results a model was developed, suggesting that HSV-dependent AAV replication is most probably initiated by Rep binding to the AAV ITR followed by cooperative binding of ICP8 on the single-stranded AAV DNA.

5 Zusammenfassung

Rekombinante Adeno-assoziierte Virus Vektoren (rAAV) werden mit zunehmendem Erfolg in gentherapeutischen Studien für die Behandlung von monogenetischen Krankheiten eingesetzt. Für die breite klinische Anwendung sind effiziente Produktionsmethoden notwendig, um den schnell-wachsenden Bedarf zu decken. In dieser Arbeit wird die Entwicklung eines skalierbaren rAAV Produktionssystems für die Herstellung von AAV Vektoren der Serotypen 1 bis 12 beschrieben, das auf stabilen Insektenzelllinien basiert. Die AAV Vektorproduktion des gewünschten AAV Serotyps wird durch Infektion der entsprechenden Zelllinie mit Baculoviren induziert. Die Ausbeute produzierter AAV Vektoren erreichen höhere Titer bei ähnlicher Infektiosität im Vergleich zu Vektoren, die mit dem bisherigen Goldstandard, aber nur begrenzt skalierbaren Produktionssystem in HEK 293 Zellen hergestellt wurden.

Für den Transfer des Fremdgens in die Zielzelle müssen AAV Vektoren verschiedener Serotypen an ihre spezifischen Zellrezeptoren binden. Die AAV Serotypen benutzen dabei unterschiedliche Glykanstrukturen auf der Zelloberfläche. Mit Hilfe von Glykan- und Heparin-Mikroarrays wurde die Interaktion der AAV Kapside mit hunderten Glykanen bzw. Heparinen untersucht. Dabei konnten differentielle Glykanstrukturen identifiziert werden, die Serotyp-spezifisch an die AAV Kapside binden. Erstmals gelang die differentielle Bindung von AAV Serotypen an einzelne chemisch definierte Heparine zu zeigen, die gleichermaßen an natürliche Heparingemische binden. Durch den Vergleich der AAV Bindungseigenschaften an unterschiedliche Glykane konnten die Rezeptorspezifitäten unterschiedlicher AAV Serotypen weiter differenziert werden.

Für ein neurobiologisches Kooperationsprojekt wurden AAV Vektoren für die Expression von Neuropeptid Y (NPY) generiert. Diese wurden für die Untersuchung der NPY-Funktionen im zentralen Nervensystem bei der Entstehung von Fettleibigkeit eingesetzt. Durch stereotaktische Injektion der AAV Vektoren in den Hypothalamus von Wildtyp bzw. NPY-Knockout Mäusen konnte neben der bereits bekannten Appetit-stimulierenden Wirkung eine weitere Funktion bei der Regulierung des Energieverbrauchs identifiziert werden.

Neben der Produktion in Baculovirus-infizierten Insektenzellen können AAV Vektoren auch mithilfe von Herpesviren (HSV) in Säugerzellen produziert werden. Dabei wird der HSV-kodierte Replikationskomplex für die AAV Replikation benötigt. Die AAV Replikation wird initiiert durch die Bildung eines ternären Komplexes aus AAV Rep78 und HSV-ICP8 mit dem AAV ssDNA Genom. Durch Generierung verschiedener Rep-Mutanten konnte demonstriert werden, dass eine intakte DNA-Bindungsdomäne von Rep Voraussetzung für diese Komplexbildung ist. Die Ergebnisse wurden in einem Modell für die HSV-abhängige AAV Replikation zusammengefasst, das die initiale Bindung von Rep an die AAV ITRs und die anschließende kooperative Bindung von ICP8 an die einzelsträngige AAV DNA umfasst.

6 References

1. Atchinson RW, Casto BC, Hammon WMCD (1965) Adenovirus-associated defective virus particles. Science 194: 754-756.
2. Hoggan MD, Blacklow NR, Rowe WP (1966) Studies of small DNA viruses found in various adenovirus preparations: physical, biological, and immunological characteristics. Proc Natl Acad Sci U S A 55: 1467-1474.
3. Casto BC, Atchison RW, Hammon WM (1967) Studies on the relationship between adeno-associated virus type I (AAV-1) and adenoviruses. I. Replication of AAV-1 in certain cell cultures and its effect on helper adenovirus. Virology 32: 52-59.
4. Buller RM, Janik JE, Sebring ED, Rose JA (1981) Herpes simplex virus types 1 and 2 completely help adenovirus-associated virus replication. J Virol 40: 241-247.
5. McPherson RA, Rosenthal LJ, Rose JA (1985) Human cytomegalovirus completely helps adeno-associated virus replication. Virology 147: 217-222.
6. Boutin S, Monteilhet V, Veron P, Leborgne C, Benveniste O, et al. (2010) Prevalence of serum IgG and neutralizing factors against adeno-associated virus (AAV) types 1, 2, 5, 6, 8, and 9 in the healthy population: implications for gene therapy using AAV vectors. Hum Gene Ther 21: 704-712.
7. Srivastava A, Lusby EW, Berns KI (1983) Nucleotide sequence and organization of the adeno-associated virus 2 genome. J Virol 45: 555-564.
8. Hauswirth WW, Berns KI (1977) Origin and termination of adeno-associated virus DNA replication. Virology 78: 488-499.
9. King JA, Dubielzig R, Grimm D, Kleinschmidt JA (2001) DNA helicase-mediated packaging of adeno-associated virus type 2 genomes into preformed capsids. EMBO J 20: 3282-3291.
10. Im DS, Muzyczka N (1989) Factors that bind to adeno-associated virus terminal repeats. J Virol 63: 3095-3104.
11. Lusby EW, Berns KI (1982) Mapping of the 5' termini of two adeno-associated virus 2 RNAs in the left half of the genome. J Virol 41: 518-526.
12. Green MR, Roeder RG (1980) Definition of a novel promoter for the major adenovirus-associated virus mRNA. Cell 22: 231-242.
13. Becerra SP, Koczot F, Fabisch P, Rose JA (1988) Synthesis of adeno-associated virus structural proteins requires both alternative mRNA splicing and alternative initiations from a single transcript. J Virol 62: 2745-2754.
14. Mouw MB, Pintel DJ (2000) Adeno-associated virus RNAs appear in a temporal order and their splicing is stimulated during coinfection with adenovirus. J Virol 74: 9878-9888.
15. Trempe JP, Carter BJ (1988) Alternate mRNA splicing is required for synthesis of adeno-associated virus VP1 capsid protein. J Virol 62: 3356-3363.
16. McPherson RA, Rose JA (1983) Structural proteins of adenovirus-associated virus: subspecies and their relatedness. J Virol 46: 523-529.
17. Sonntag F, Schmidt K, Kleinschmidt JA (2010) A viral assembly factor promotes AAV2 capsid formation in the nucleolus. Proceedings of the National Academy of Sciences of the United States of America 107: 10220-10225.
18. Kotin RM, Siniscalco M, Samulski RJ, Zhu XD, Hunter L, et al. (1990) Site-specific integration by adeno-associated virus. Proc Natl Acad Sci U S A 87: 2211-2215.
19. Schnepp BC, Jensen RL, Chen CL, Johnson PR, Clark KR (2005) Characterization of adeno-associated virus genomes isolated from human tissues. J Virol 79: 14793-14803.
20. Pereira DJ, McCarty DM, Muzyczka N (1997) The adeno-associated virus (AAV) Rep protein acts as both a repressor and an activator to regulate AAV transcription during a productive infection. J Virol 71: 1079-1088.
21. Linden RM, Winocour E, Berns KI (1996) The recombination signals for adeno-associated virus site-specific integration. Proc Natl Acad Sci U S A 93: 7966-7972.
22. Hüser D, Gogol-Döring A, Lutter T, Weger S, Winter K, et al. (2010) Integration preferences of wildtype AAV-2 for consensus rep-binding sites at numerous loci in the human genome. PLoS Pathog 6: e1000985.
23. Chang LS, Shi Y, Shenk T (1989) Adeno-associated virus P5 promoter contains an adenovirus E1A-inducible element and a binding site for the major late transcription factor. J Virol 63: 3479-3488.
24. Ward P, Dean FB, O'Donnell ME, Berns KI (1998) Role of the adenovirus DNA-binding protein in in vitro adeno-associated virus DNA replication. J Virol 72: 420-427.

25. Weitzman MD, Fisher KJ, Wilson JM (1996) Recruitment of wild-type and recombinant adeno-associated virus into adenovirus replication centers. J Virol 70: 1845-1854.
26. Nayak R, Pintel DJ (2007) Adeno-associated viruses can induce phosphorylation of eIF2alpha via PKR activation, which can be overcome by helper adenovirus type 5 virus-associated RNA. J Virol 81: 11908-11916.
27. Schwartz RA, Palacios JA, Cassell GD, Adam S, Giacca M, et al. (2007) The Mre11/Rad50/Nbs1 complex limits adeno-associated virus transduction and replication. J Virol 81: 12936-12945.
28. Xiao X, Li J, Samulski RJ (1998) Production of high-titer recombinant adeno-associated virus vectors in the absence of helper adenovirus. J Virol 72: 2224-2232.
29. Alazard-Dany N, Nicolas A, Ploquin A, Strasser R, Greco A, et al. (2009) Definition of herpes simplex virus type 1 helper activities for adeno-associated virus early replication events. PLoS Pathog 5: e1000340.
30. Weindler FW, Heilbronn R (1991) A subset of herpes simplex virus replication genes provides helper functions for productive adeno-associated virus replication. J Virol 65: 2476-2483.
31. Heilbronn R, Engstler M, Weger S, Krahn A, Schetter C, et al. (2003) ssDNA-dependent colocalization of adeno-associated virus Rep and herpes simplex virus ICP8 in nuclear replication domains. Nucleic Acids Res 31: 6206-6213.
32. Ward P, Elias P, Linden RM (2003) Rescue of the adeno-associated virus genome from a plasmid vector: evidence for rescue by replication. J Virol 77: 11480-11490.
33. Im D-S, Muzyczka N (1990) The AAV origin-binding protein Rep68 is an ATP-dependent site-specific endonuclease with helicase activity. Cell 61: 447-457.
34. Brister JR, Muzyczka N (2000) Mechanism of Rep-mediated adeno-associated virus origin nicking. J Virol 74: 7762-7771.
35. Boehmer PE, Lehman IR (1993) Herpes simplex virus type 1 ICP8: helix-destabilizing properties. J Virol 67: 711-715.
36. Bush M, Yager DR, Gao M, Weisshart K, Marcy AI, et al. (1991) Correct intranuclear localization of herpes simplex virus DNA polymerase requires the viral ICP8 DNA-binding protein. J Virol 65: 1082-1089.
37. de Bruyn Kops A, Knipe DM (1988) Formation of DNA replication structures in herpes virus-infected cells requires a viral DNA binding protein. Cell 55: 857-868.
38. Taylor TJ, Knipe DM (2004) Proteomics of herpes simplex virus replication compartments: association of cellular DNA replication, repair, recombination, and chromatin remodeling proteins with ICP8. J Virol 78: 5856-5866.
39. McCarty DM, Monahan PE, Samulski RJ (2001) Self-complementary recombinant adeno-associated virus (scAAV) vectors promote efficient transduction independently of DNA synthesis. Gene Ther 8: 1248-1254.
40. Agbandje-McKenna M, Kleinschmidt J (2011) AAV capsid structure and cell interactions. Methods Mol Biol 807: 47-92.
41. Lerch TF, Xie Q, Chapman MS (2010) The structure of adeno-associated virus serotype 3B (AAV-3B): insights into receptor binding and immune evasion. Virology 403: 26-36.
42. O'Donnell J, Taylor KA, Chapman MS (2009) Adeno-associated virus-2 and its primary cellular receptor--Cryo-EM structure of a heparin complex. Virology 385: 434-443.
43. Xie Q, Bu W, Bhatia S, Hare J, Somasundaram T, et al. (2002) The atomic structure of adeno-associated virus (AAV-2), a vector for human gene therapy. Proc Natl Acad Sci U S A 99: 10405-10410.
44. Raupp C, Naumer M, Muller OJ, Gurda BL, Agbandje-McKenna M, et al. (2012) The threefold protrusions of adeno-associated virus type 8 are involved in cell surface targeting as well as postattachment processing. J Virol 86: 9396-9408.
45. Gurda BL, DiMattia MA, Miller EB, Bennett A, McKenna R, et al. (2013) Capsid antibodies to different adeno-associated virus serotypes bind common regions. J Virol 87: 9111-9124.
46. Kronenberg S, Bottcher B, von der Lieth CW, Bleker S, Kleinschmidt JA (2005) A conformational change in the adeno-associated virus type 2 capsid leads to the exposure of hidden VP1 N termini. J Virol 79: 5296-5303.
47. Girod A, Wobus CE, Zadori Z, Ried M, Leike K, et al. (2002) The VP1 capsid protein of adeno-associated virus type 2 is carrying a phospholipase A2 domain required for virus infectivity. J Gen Virol 83: 973-978.
48. Grieger JC, Snowdy S, Samulski RJ (2006) Separate basic region motifs within the adeno-associated virus capsid proteins are essential for infectivity and assembly. J Virol 80: 5199-5210.
49. Kashiwakura Y, Tamayose K, Iwabuchi K, Hirai Y, Shimada T, et al. (2005) Hepatocyte growth factor receptor is a coreceptor for adeno-associated virus type 2 infection. J Virol 79: 609-614.

50. Di Pasquale G, Davidson BL, Stein CS, Martins I, Scudiero D, et al. (2003) Identification of PDGFR as a receptor for AAV-5 transduction. Nat Med 9: 1306-1312.
51. Summerford C, Bartlett JS, Samulski RJ (1999) AlphaVbeta5 integrin: a co-receptor for adeno-associated virus type 2 infection [see comments]. Nat Med 5: 78-82.
52. Akache B, Grimm D, Pandey K, Yant SR, Xu H, et al. (2006) The 37/67-kilodalton laminin receptor is a receptor for adeno-associated virus serotypes 8, 2, 3, and 9. J Virol 80: 9831-9836.
53. Qing K, Mah C, Hansen J, Zhou S, Dwarki V, et al. (1999) Human fibroblast growth factor receptor 1 is a co-receptor for infection by adeno-associated virus 2 Nat Med 5: 71-77.
54. Bartlett JS, Wilcher R, Samulski RJ (2000) Infectious entry pathway of adeno-associated virus and adeno-associated virus vectors. J Virol 74: 2777-2785.
55. Nonnenmacher M, Weber T (2011) Adeno-associated virus 2 infection requires endocytosis through the CLIC/GEEC pathway. Cell Host Microbe 10: 563-576.
56. Xiao PJ, Samulski RJ (2012) Cytoplasmic trafficking, endosomal escape, and perinuclear accumulation of adeno-associated virus type 2 particles are facilitated by microtubule network. J Virol 86: 10462-10473.
57. Nam HJ, Gurda BL, McKenna R, Potter M, Byrne B, et al. (2011) Structural studies of adeno-associated virus serotype 8 capsid transitions associated with endosomal trafficking. J Virol 85: 11791-11799.
58. Stahnke S, Lux K, Uhrig S, Kreppel F, Hosel M, et al. (2011) Intrinsic phospholipase A2 activity of adeno-associated virus is involved in endosomal escape of incoming particles. Virology 409: 77-83.
59. Sonntag F, Bleker S, Leuchs B, Fischer R, Kleinschmidt JA (2006) Adeno-associated virus type 2 capsids with externalized VP1/VP2 trafficking domains are generated prior to passage through the cytoplasm and are maintained until uncoating occurs in the nucleus. Journal of virology 80: 11040-11054.
60. Wu Z, Miller E, Agbandje-McKenna M, Samulski RJ (2006) Alpha2,3 and alpha2,6 N-linked sialic acids facilitate efficient binding and transduction by adeno-associated virus types 1 and 6. J Virol 80: 9093-9103.
61. Miller EB, Gurda-Whitaker B, Govindasamy L, McKenna R, Zolotukhin S, et al. (2006) Production, purification and preliminary X-ray crystallographic studies of adeno-associated virus serotype 1. Acta Crystallogr Sect F Struct Biol Cryst Commun 62: 1271-1274.
62. Nonnenmacher M, Weber T (2012) Intracellular transport of recombinant adeno-associated virus vectors. Gene Ther 19: 649-658.
63. Summerford C, Samulski RJ (1998) Membrane-associated heparan sulfate proteoglycan is a receptor for adeno-associated virus type 2 virions. J Virol 72: 1438-1445.
64. Kern A, Schmidt K, Leder C, Muller OJ, Wobus CE, et al. (2003) Identification of a heparin-binding motif on adeno-associated virus type 2 capsids. J Virol 77: 11072-11081.
65. Opie SR, Warrington KH, Jr., Agbandje-McKenna M, Zolotukhin S, Muzyczka N (2003) Identification of amino acid residues in the capsid proteins of adeno-associated virus type 2 that contribute to heparan sulfate proteoglycan binding. J Virol 77: 6995-7006.
66. Muramatsu S, Mizukami H, Young NS, Brown KE (1996) Nucleotide sequencing and generation of an infectious clone of adeno-associated virus 3. Virology 221: 208-217.
67. Rutledge EA, Halbert CL, Russell DW (1998) Infectious clones and vectors derived from adeno-associated virus (AAV) serotypes other than AAV type 2. Journal of Virology 72: 309-319.
68. Handa A, Muramatsu S, Qiu J, Mizukami H, Brown KE (2000) Adeno-associated virus (AAV)-3-based vectors transduce haematopoietic cells not susceptible to transduction with AAV-2-based vectors. J Gen Virol 81: 2077-2084.
69. Lerch TF, Chapman MS (2012) Identification of the heparin binding site on adeno-associated virus serotype 3B (AAV-3B). Virology 423: 6-13.
70. Messina EL, Nienaber J, Daneshmand M, Villamizar N, Samulski J, et al. (2012) Adeno-associated viral vectors based on serotype 3b use components of the fibroblast growth factor receptor signaling complex for efficient transduction. Hum Gene Ther 23: 1031-1042.
71. Chao H, Liu Y, Rabinowitz J, Li C, Samulski RJ, et al. (2000) Several log increase in therapeutic transgene delivery by distinct adeno-associated viral serotype vectors. Mol Ther 2: 619-623.
72. Glushakova LG, Lisankie MJ, Eruslanov EB, Ojano-Dirain C, Zolotukhin I, et al. (2009) AAV3-mediated transfer and expression of the pyruvate dehydrogenase E1 alpha subunit gene causes metabolic remodeling and apoptosis of human liver cancer cells. Mol Genet Metab 98: 289-299.
73. Kaludov N, Brown KE, Walters RW, Zabner J, Chiorini JA (2001) Adeno-associated virus serotype 4 (AAV4) and AAV5 both require sialic acid binding for hemagglutination and efficient transduction but differ in sialic acid linkage specificity. J Virol 75: 6884-6893.

74. Shen S, Troupes AN, Pulicherla N, Asokan A (2013) Multiple roles for sialylated glycans in determining the cardiopulmonary tropism of adeno-associated virus 4. J Virol 87: 13206-13213.
75. Davidson BL, Stein CS, Heth JA, Martins I, Kotin RM, et al. (2000) Recombinant adeno-associated virus type 2, 4, and 5 vectors: transduction of variant cell types and regions in the mammalian central nervous system. Proc Natl Acad Sci U S A 97: 3428-3432.
76. Weber M, Rabinowitz J, Provost N, Conrath H, Folliot S, et al. (2003) Recombinant adeno-associated virus serotype 4 mediates unique and exclusive long-term transduction of retinal pigmented epithelium in rat, dog, and nonhuman primate after subretinal delivery. Mol Ther 7: 774-781.
77. Farris KD, Pintel DJ (2010) Adeno-associated virus type 5 utilizes alternative translation initiation to encode a small Rep40-like protein. Journal of virology 84: 1193-1197.
78. Govindasamy L, Dimattia MA, Gurda BL, Halder S, McKenna R, et al. (2013) Structural insights into adeno-associated virus serotype 5. J Virol 87: 11187-11199.
79. Yan Z, Lei-Butters DC, Keiser NW, Engelhardt JF (2013) Distinct transduction difference between adeno-associated virus type 1 and type 6 vectors in human polarized airway epithelia. Gene Ther 20: 328-337.
80. Miyake K, Miyake N, Yamazaki Y, Shimada T, Hirai Y (2012) Serotype-independent method of recombinant adeno-associated virus (AAV) vector production and purification. J Nippon Med Sch 79: 394-402.
81. Wu Z, Asokan A, Grieger JC, Govindasamy L, Agbandje-McKenna M, et al. (2006) Single amino acid changes can influence titer, heparin binding, and tissue tropism in different adeno-associated virus serotypes. J Virol 80: 11393-11397.
82. Ng R, Govindasamy L, Gurda BL, McKenna R, Kozyreva OG, et al. (2010) Structural characterization of the dual glycan binding adeno-associated virus serotype 6. J Virol 84: 12945-12957.
83. Halbert CL, Allen JM, Miller AD (2001) Adeno-associated virus type 6 (AAV6) vectors mediate efficient transduction of airway epithelial cells in mouse lungs compared to that of AAV2 vectors. J Virol 75: 6615-6624.
84. Mori S, Wang L, Takeuchi T, Kanda T (2004) Two novel adeno-associated viruses from cynomolgus monkey: pseudotyping characterization of capsid protein. Virology 330: 375-383.
85. Schmidt M, Voutetakis A, Afione S, Zheng C, Mandikian D, et al. (2008) Adeno-associated virus type 12 (AAV12): a novel AAV serotype with sialic acid- and heparan sulfate proteoglycan-independent transduction activity. J Virol 82: 1399-1406.
86. Bell CL, Vandenberghe LH, Bell P, Limberis MP, Gao GP, et al. (2011) The AAV9 receptor and its modification to improve in vivo lung gene transfer in mice. J Clin Invest 121: 2427-2435.
87. Gao GP, Alvira MR, Wang L, Calcedo R, Johnston J, et al. (2002) Novel adeno-associated viruses from rhesus monkeys as vectors for human gene therapy. Proc Natl Acad Sci U S A 99: 11854-11859.
88. Gao G, Vandenberghe LH, Alvira MR, Lu Y, Calcedo R, et al. (2004) Clades of Adeno-associated viruses are widely disseminated in human tissues. J Virol 78: 6381-6388.
89. Shen S, Bryant KD, Brown SM, Randell SH, Asokan A (2011) Terminal N-linked galactose is the primary receptor for adeno-associated virus 9. J Biol Chem 286: 13532-13540.
90. Foust KD, Nurre E, Montgomery CL, Hernandez A, Chan CM, et al. (2009) Intravascular AAV9 preferentially targets neonatal neurons and adult astrocytes. Nat Biotechnol 27: 59-65.
91. Schmidt M, Govindasamy L, Afione S, Kaludov N, Agbandje-McKenna M, et al. (2008) Molecular characterization of the heparin-dependent transduction domain on the capsid of a novel adeno-associated virus isolate, AAV(VR-942). J Virol 82: 8911-8916.
92. Mingozzi F, High KA (2011) Therapeutic in vivo gene transfer for genetic disease using AAV: progress and challenges. Nat Rev Genet 12: 341-355.
93. Nathwani AC, Tuddenham EG, Rangarajan S, Rosales C, McIntosh J, et al. (2011) Adenovirus-associated virus vector-mediated gene transfer in hemophilia B. N Engl J Med 365: 2357-2365.
94. Kastelein JJ, Ross CJ, Hayden MR (2013) From mutation identification to therapy: discovery and origins of the first approved gene therapy in the Western world. Hum Gene Ther 24: 472-478.
95. Heilbronn R, Weger S (2010) Viral vectors for gene transfer: current status of gene therapeutics. Handb Exp Pharmacol: 143-170.
96. Schnepp BC, Clark KR, Klemanski DL, Pacak CA, Johnson PR (2003) Genetic fate of recombinant adeno-associated virus vector genomes in muscle. J Virol 77: 3495-3504.
97. Smith RH (2008) Adeno-associated virus integration: virus versus vector. Gene Ther 15: 817-822.
98. Gray JT, Zolotukhin S (2011) Design and construction of functional AAV vectors. Methods Mol Biol 807: 25-46.
99. Grimm D, Kay MA, Kleinschmidt JA (2003) Helper virus-free, optically controllable, and two-plasmid-based production of adeno-associated virus vectors of serotypes 1 to 6. Mol Ther 7: 839-850.

100. Ruffing M, Zentgraf H, Kleinschmidt JA (1992) Assembly of viruslike particles by recombinant structural proteins of adeno-associated virus type 2 in insect cells. J Virol 66: 6922-6930.
101. Urabe M, Ding C, Kotin RM (2002) Insect cells as a factory to produce adeno-associated virus type 2 vectors. Hum Gene Ther 13: 1935-1943.
102. Smith RH, Levy JR, Kotin RM (2009) A simplified baculovirus-AAV expression vector system coupled with one-step affinity purification yields high-titer rAAV stocks from insect cells. Mol Ther 17: 1888-1896.
103. Aslanidi G, Lamb K, Zolotukhin S (2009) An inducible system for highly efficient production of recombinant adeno-associated virus (rAAV) vectors in insect Sf9 cells. Proc Natl Acad Sci U S A 106: 5059-5064.
104. Dwek RA (1996) Glycobiology: Toward Understanding the Function of Sugars. Chem Rev 96: 683-720.
105. Marino K, Bones J, Kattla JJ, Rudd PM (2010) A systematic approach to protein glycosylation analysis: a path through the maze. Nat Chem Biol 6: 713-723.
106. Berg JMT, J.L.; Stryer, L. (2002) Biochemistry. 5th edition.
107. Bertozzi CR, Rabuka D (2009) Structural Basis of Glycan Diversity. In: Varki A, Cummings RD, Esko JD, Freeze HH, Stanley P et al., editors. Essentials of Glycobiology. 2nd ed. Cold Spring Harbor (NY).
108. Benallal M, Anner BM (1994) Identification of organ-specific glycosylation of a membrane protein in two tissues using lectins. Experientia 50: 664-668.
109. Hart GW, West CM (2009) Nucleocytoplasmic Glycosylation. In: Varki A, Cummings RD, Esko JD, Freeze HH, Stanley P et al., editors. Essentials of Glycobiology. 2nd ed. Cold Spring Harbor (NY).
110. Esko JD, Kimata K, Lindahl U (2009) Proteoglycans and Sulfated Glycosaminoglycans. In: Varki A, Cummings RD, Esko JD, Freeze HH, Stanley P et al., editors. Essentials of Glycobiology. 2nd ed. Cold Spring Harbor (NY).
111. Harvey DJ, Merry AH, Royle L, Campbell MP, Dwek RA, et al. (2009) Proposal for a standard system for drawing structural diagrams of N- and O-linked carbohydrates and related compounds. Proteomics 9: 3796-3801.
112. Varki A, Lowe JB (2009) Biological Roles of Glycans. In: Varki A, Cummings RD, Esko JD, Freeze HH, Stanley P et al., editors. Essentials of Glycobiology. 2nd ed. Cold Spring Harbor (NY).
113. Molinari M (2007) N-glycan structure dictates extension of protein folding or onset of disposal. Nat Chem Biol 3: 313-320.
114. Zhao YY, Takahashi M, Gu JG, Miyoshi E, Matsumoto A, et al. (2008) Functional roles of N-glycans in cell signaling and cell adhesion in cancer. Cancer Sci 99: 1304-1310.
115. Nizet V, Esko JD (2009) Bacterial and Viral Infections. In: Varki A, Cummings RD, Esko JD, Freeze HH, Stanley P et al., editors. Essentials of Glycobiology. 2nd ed. Cold Spring Harbor (NY).
116. Esko JD, Sharon N (2009) Microbial Lectins: Hemagglutinins, Adhesins, and Toxins. In: Varki A, Cummings RD, Esko JD, Freeze HH, Stanley P et al., editors. Essentials of Glycobiology. 2nd ed. Cold Spring Harbor (NY).
117. Wang B, Brand-Miller J (2003) The role and potential of sialic acid in human nutrition. Eur J Clin Nutr 57: 1351-1369.
118. Varki A, Schauer R (2009) Sialic Acids. In: Varki A, Cummings RD, Esko JD, Freeze HH, Stanley P et al., editors. Essentials of Glycobiology. 2nd ed. Cold Spring Harbor (NY).
119. Dreyfuss JL, Regatieri CV, Jarrouge TR, Cavalheiro RP, Sampaio LO, et al. (2009) Heparan sulfate proteoglycans: structure, protein interactions and cell signaling. An Acad Bras Cienc 81: 409-429.
120. Kreuger J, Prydz K, Pettersson RF, Lindahl U, Salmivirta M (1999) Characterization of fibroblast growth factor 1 binding heparan sulfate domain. Glycobiology 9: 723-729.
121. Nader HB, Chavante SF, dos-Santos EA, Oliveira TW, de-Paiva JF, et al. (1999) Heparan sulfates and heparins: similar compounds performing the same functions in vertebrates and invertebrates? Braz J Med Biol Res 32: 529-538.
122. Bertozzi CR, Sasisekharan R (2009) Glycomics. In: Varki A, Cummings RD, Esko JD, Freeze HH, Stanley P et al., editors. Essentials of Glycobiology. 2nd ed. Cold Spring Harbor (NY).
123. Rillahan CD, Paulson JC (2011) Glycan microarrays for decoding the glycome. Annu Rev Biochem 80: 797-823.
124. Allay JA, Sleep S, Long S, Tillman DM, Clark R, et al. (2011) Good manufacturing practice production of self-complementary serotype 8 adeno-associated viral vector for a hemophilia B clinical trial. Hum Gene Ther 22: 595-604.
125. Wang L, Blouin V, Brument N, Bello-Roufai M, Francois A (2011) Production and purification of recombinant adeno-associated vectors. Methods Mol Biol 807: 361-404.

126. Cecchini S, Virag T, Kotin RM (2011) Reproducible high yields of recombinant adeno-associated virus produced using invertebrate cells in 0.02- to 200-liter cultures. Hum Gene Ther 22: 1021-1030.
127. Kohlbrenner E, Aslanidi G, Nash K, Shklyaev S, Campbell-Thompson M, et al. (2005) Successful production of pseudotyped rAAV vectors using a modified baculovirus expression system. Mol Ther 12: 1217-1225.
128. Zolotukhin S, Byrne BJ, Mason E, Zolotukhin I, Potter M, et al. (1999) Recombinant adeno-associated virus purification using novel methods improves infectious titer and yield. Gene Ther 6: 973-985.
129. Zolotukhin S, Potter M, Zolotukhin I, Sakai Y, Loiler S, et al. (2002) Production and purification of serotype 1, 2, and 5 recombinant adeno-associated viral vectors. Methods 28: 158-167.
130. Yin J, Seeberger PH (2010) Applications of heparin and heparan sulfate microarrays. Methods Enzymol 478: 197-218.
131. Stanley BG, Leibowitz SF (1985) Neuropeptide Y injected in the paraventricular hypothalamus: a powerful stimulant of feeding behavior. Proc Natl Acad Sci U S A 82: 3940-3943.
132. Atasoy D, Aponte Y, Su HH, Sternson SM (2008) A FLEX switch targets Channelrhodopsin-2 to multiple cell types for imaging and long-range circuit mapping. J Neurosci 28: 7025-7030.
133. Evans JT, Rosenblatt GS, Leisy DJ, Rohrmann GF (1999) Characterization of the interaction between the baculovirus ssDNA-binding protein (LEF-3) and putative helicase (P143). J Gen Virol 80 (Pt 2): 493-500.
134. Hang X, Dong W, Guarino LA (1995) The lef-3 gene of Autographa californica nuclear polyhedrosis virus encodes a single-stranded DNA-binding protein. J Virol 69: 3924-3928.
135. Feng G, Thumbi DK, de Jong J, Hodgson JJ, Arif BM, et al. (2012) Selection and characterization of Autographa californica multiple nucleopolyhedrovirus DNA polymerase mutations. J Virol 86: 13576-13588.
136. Hang X, Guarino LA (1999) Purification of Autographa californica nucleopolyhedrovirus DNA polymerase from infected insect cells. J Gen Virol 80 (Pt 9): 2519-2526.
137. Dai X, Willis LG, Huijskens I, Palli SR, Theilmann DA (2004) The acidic activation domains of the baculovirus transactivators IE1 and IE0 are functional for transcriptional activation in both insect and mammalian cells. J Gen Virol 85: 573-582.
138. Kaba SA, Salcedo AM, Wafula PO, Vlak JM, van Oers MM (2004) Development of a chitinase and v-cathepsin negative bacmid for improved integrity of secreted recombinant proteins. J Virol Methods 122: 113-118.

7 Conference Presentations

7.1 Talks

Mario Mietzsch, Dilip Verma, Ramon Tasan, Stefan Weger, Günther Sperk and Regine Heilbronn; "Development of scAAV Vectors for Expression of Neuropeptide Y Variants for different NPY Receptor Subtypes and Functional Analysis in NPY Knock-out Mice"; Workshop on Viral Vectors & Gene Therapy, Cologne, Germany, 2009

Mario Mietzsch and Regine Heilbronn; "Glycan-Binding Profiles for the differentiation of AAV Vectors for Gene Therapy"; 6th Glycan Forum, Berlin, Germany, 2012

Mario Mietzsch, Sergei Zolotukhin and Regine Heilbronn; "AAV Serotype-Specific Capsid Differentiation by Glycan-Binding Profiles"; 14th International Parvovirus Workshop, Ithaca, USA, 2012

7.2 Poster Presentations

Mario Mietzsch and Regine Heilbronn; "Glycan-Binding Profiles for the differentiation of AAV Vectors for Gene Therapy"; 6th Glycan Forum, Berlin, Germany, 2012

8 Curriculum vitae

For privacy reasons the curriculum vitae is not included in the electronic version.